QUANTIFYING TROPICAL FOREST BIOMASS

Tyas Mutiara Basuki

Examining committee:

Prof. Dr. Ing. Wouter Verhoef	University of Twente, The Netherlands
Prof. Dr. Martin van Maarseveen	University of Twente, The Netherlands
Prof. Dr. Frans Bonger	WageningenUniversity, The Netherlands
Prof. Dr. Petter Pilesjö	Lund University, Sweden

ITC dissertation number 208
ITC, P.O. Box 217, 7500 AE Enschede, The Netherlands

ISBN 978-90-6164-332-6
Cover designed by Tyas Mutiara Basuki
Printed by ITC Printing Department

UNIVERSITY OF TWENTE.

FACULTY OF GEO-INFORMATION SCIENCE AND EARTH OBSERVATION

QUANTIFYING TROPICAL FOREST BIOMASS

DISSERTATION

to obtain
the degree of doctor at the University of Twente,
on the authority of the rector magnificus,
prof.dr. H. Brinksma,
on account of the decision of the graduation committee,
to be publicly defended
on Thursday, May 24, 2012 at 16.45 hrs

by
Tyas Mutiara Basuki

born in Nganjuk, Indonesia
on December 20, 1958

This thesis is approved by
Prof. Dr Andrew K. Skidmore, promotor
Dr. Yousif A. Hussin, assistant promotor
Dr. Iris van Duren, assistant promotor

Acknowledgements

Alhamdulillah, without your blessing this work would never have been realized. This thesis would not have been possible without the help from others. I cannot mention everyone separately; nevertheless, I would like to convey my appreciation and thanks to all of you who helped me during my PhD research.

My full appreciation and sincerest thanks go to my promotor Prof. Andrew K. Skidmore. Andrew, your encouragement, support, and scientific guidance during my PhD research were invaluable and your constructive comments greatly improved my research and scientific writing. My gratitude also goes to Dr. Yousif A Hussin, my co-promotor, your guidance, your moral support and your patience during my research, I will never forget. I would like to express my acknowledgement to Dr. Iris van Duren as my assistant promotor. Iris, your constructive comments on the thesis were invaluable and thank you for the Dutch translation. To Dr. Patrick E. van Laake, my previous supervisor, many thanks for your scientific guidance and moral support during the time of your supervision.

This work is supported by a grant from the Netherlands Fellowship Programme (NFP) administered by the Netherlands Organization for International Cooperation in Higher Education (NUFFIC). My appreciation and gratitude go NUFFIC and ITC providing me the chance to conduct PhD research. I would like to thank the former and current research coordinators of ITC, Prof. Martin Hale and Dr. Paul van Dijk, who always listened to me whenever I had difficulties.

I am very grateful to the Director of Forest Research and Development Agency and Watershed Management Technology Centre, Indonesia, who gave me permission to do a PhD. For Dr. Hadi Pasaribu and Ir. Nugroho Priyono MSc, thank you very much for recommending I continue my studies.

Willem Nieuwenhuis and Gerard Reinink, my appreciation and sincere thanks, both of you always had time for me when I needed technical assistance. Special thanks to Esther Hondebrink and Ms. Loes Colenbrander for their administrative assistance during my studies at ITC. Theresa van den Boogaard and Marie-Chantal Metz, thank you for your help during my stay in Enschede. Carla Gerritsen and Nina, thank you for helping me get the literature I needed. I would like to say thank to Benno and Job for finalizing this thesis. To Eva

Skidmore, thank you very much for editing my English and for a very nice gathering at the summer barbeque.

It was very nice to have scientific and lively discussions during my study at ITC. Very special thanks go to Claudia Pittiglio and her family, Dr. Feliz Bektas and Yin Xiu for their warm relationship, the dinners, lunches, and coffee breaks were unforgettable. To Adrie, Maitreyi, Dr. Yali Si, Laura, Mariela, and Ha, thanks very much for sharing knowledge and life with me. It was wonderful to spend time during coffee breaks and discuss with Dr. Jamshid Farifteh, Emmanuel Owusu, Dr. Chudamani Joshi, Dr. Moses A. Cho, Dr. Peter Minang, and Dr. Nicky Knox.

Many thanks to my colleagues Eko, Ragil, Nining, Wisnu, Agus Sugianto, as well as Dr. Endang Savitri, and all of you in Forestry Research Institute of Solo, Indonesia. I will not be able to mention each of you here separately. My gratitude also goes to bapak Bambang Tri Sasongko, MSc in IPB, Bogor, bapak Kartiko, MSc in UNS and bapak Syaiful Anwar, MSi in UNSIRI, Surakarta. Special thanks go to bapak Ir. Dody Hendrika, mas Kirno, pak Pangut, and all staff of PT. Hutan Sanggam Labanan Lestari and PT. Puji Sempurna Raharja concessionaires who helped me during my field campaigns.

All Indonesian friends who have studied at ITC and UT, all members of PPIE and IMEA, thank you for your friendship. For Dr. Wiwin Ambarwulan, Syarif Budhiman, Anas Fauzi, Mumun Munawaroh, Dewi Anggraini, Nugroho Christanto, Hunggul Yudono, Winardi, Nasrullah, Rahayu Prihati, Dr. Trias Aditya, Zuhdan Arif, and Prabowo thank you very much for your friendship, for sharing the happy and the difficult times during our stay in Enschede.

It would have been almost impossible to conduct this PhD without the understanding, praying, and encouragement of my husband and my entirely family. To my beloved husband, Irfan B. Pramono, my sincerest thanks. To my son, Pradipta, and my daughters Candrika and Intan, my deepest apologies for being away from all of you. My thoughts were with you as you were growing from kids into teenagers. My deepest respect and thanks to my mother and my mother-in-law, your continuing praying and support were invaluable. To my sisters and brothers, thank you very much for your support.

Dedicated to :
my husband, parents, son, and daughters

List of Acronyms

AIC	:	Akaike Information Criterion
AGB	:	Above-ground Biomass
ASF	:	Alaska Satellite Facility
ASTER	:	Advanced Spaceborne Thermal Emission and Reflection Radiometer
BFMP	:	Berau Forest Management Project
CBH	:	Commercial Bole Height
CF	:	Correction Factor
CI	:	Confidence Interval
CO_2	:	Carbon Dioxide
COP	:	Conference of the Parties
DBH		Diameter at Breast Height
DEM	:	Digital Elevation Model
DM	:	Dry Matter
DN	:	Digital Number
DWT	:	Discrete Wavelet Transform
ENVI	:	Environment for Visualizing Images
ETM	:	Enhanced Thematic Mapper
EVI	:	Enhanced Vegetation Index
FAO	:	Food and Agriculture Organization
GCP	:	Ground Control Point
GEMI	:	Global Environmental Monitoring Index
GHG	:	Greenhouse Gas
GOFC-GOLD	:	Global Observation of Forest and Land Cover Dynamics
GPG-LULUCF	:	Good Practice Guidance for Land Use and Land Use Change and Forestry
GPS	:	Global Positioning System
HH	:	Horizontal – Horizontal
HV	:	Horizontal - Vertical
IDL	:	Interactive Data Language
InSAR	:	Interferometric Synthetic Aperture Radar
IPCC	:	Intergovernmental Panel on Climate Change
MIR	:	Middle Infrared
MSAVI	:	Modified Soil Adjusted Vegetation Index
MVI	:	Moisture Vegetation Index
NASA	:	National Aeronautics and Space Administration

NDFI	:	Normalized Difference Fraction Index
NDVI	:	Normalized Difference Vegetation Index
NFP	:	Netherlands Fellowship Programme
NIR	:	Near Infrared
NUFFIC	:	Netherlands Organization for International Cooperation in Higher Education
PALSAR	:	Phase Arrayed L-band Synthetic Aperture Radar
PROSEA	:	Plant Resources of South East Asia
REDD	:	Reducing Emissions from Deforestation in Developing Countries
RKL	:	*Rencana Karya Lima Tahun* (Five-years Working Plan)
RKT	:	*Rencana Karya Tahunan* (Annual Working Plan)
RMSE	:	Root Mean Squared Error
SAR	:	Synthetic Aperture Radar
POT	:	Satellite Probatoire d'Observation de la Terre
UNFCCC	:	United Nations Framework Convention on Climate Change
TM	:	Thematic Mapper
TPTI	:	*Tebang Pilih Tanam Indonesia* (Selective Cutting and Replanting System)
UTM	:	Universal Transverse Mercator
WD	:	Wood Density
WGS	:	World Geodetic System

Table of Contents

List of Figures

List of Tables

List of Appendices

CHAPTER 1

GENERAL INTRODUCTION

1.1 Background

The increase in greenhouse gas (GHG) emissions has been a major environmental issue for recent decades. Concerned about the potency of global climate change through GHG emission, especially carbon dioxide (CO_2), decision makers have explored the potential of using forests for mitigation (Ptaff *et al*., 2000). The Kyoto Protocol of the United Nations Framework Convention on Climate Change (UNFCCC) has included forestry aspects in its articles. In accordance with the Kyoto Protocol, the signatory countries under the UNFCCC committed themselves to periodically update their reports on national inventories of anthropogenic emissions or reductions in greenhouse gases to the Conference of the Parties (UNFCCC, 1998). In the forestry sectors, the inventory must include the emission of or reduction in GHG resulting from carbon stock changes (Brown, 2002).

In the Kyoto Protocol, the reduction of GHG emissions is emphasized for industrialised countries. Meanwhile, deforestation of tropical forests in developing countries is considered one of the major contributors to GHG emissions (Santilli *et al*., 2005), Therefore, avoiding deforestation has been proposed as a method of mitigation. This concept, Reducing Emissions from Deforestation in Developing Countries (REDD), was launched during the 11th Conference of the Parties (COP-11) of the UNFCCC in 2005, in Montreal (Boyd, 2010; De Jong *et al*., 2007). According to this concept, countries reducing their national deforestation should be compensated. In the Copenhagen Accord, a more comprehensive mechanism was adopted, namely REDD-plus. In the REDD-plus concept reducing emissions from deforestation and forest degradation, promoting sustainable forest management as well as enhancing carbon sinks are all integrated and regarded as mitigating GHG emissions (Ezzine-de-Blas *et al*., 2011; Sasaki and Yoshimoto, 2010; Thompson *et al*., 2011).

Forest management might be adapted with the aim to reduce CO_2 emissions by maintaining the existence of C pools (Dixon *et al*., 1994), establishing plantations and increasing forest lands (Binkley *et al*., 2002; Dixon *et al*., 1994), lengthening logging cycles (Backéus *et al*., 2005; Kapainen *et al*., 2004; Liski *et al*. 2001; Markewitz, 2006), and substituting fossil fuels by forest bio-fuels (Backéus *et al*., 2005; Baral and Guha, 2004; Dixon *et al*., 1994; Korhonen *et al*., 2002). Understanding and quantifying tropical forest biomass is therefore essential, as these forests play a major role in the global carbon cycle, wood

supply, and have been used to sequester CO_2 from the atmosphere. Measuring carbon in selectively logged forests is very relevant as it supports the implementation of REDD, as well as because selective logging is one of the degrading activities in tropical forests stated in the Global Observation of Forest and Land Cover Dynamics (GOFC-GOLD, 2009). Mapping and monitoring carbon changes is considered more difficult in degraded forests such as those subject to selective logging, than in deforestation areas (UNFCCC, 2009). Therefore, methods to improve the estimation accuracy of carbon in forests, especially selectively logged forests, are required in order to understand the global carbon cycle, predict the response of ecosystems to climate change, and support the implementation of REDD-plus. Quantifying carbon in the forest biomass may be accomplished by estimating tree biomass and assuming that 50% of the dry weight of the tree biomass consists of carbon (Intergovernmental Panel on Climate Change/IPCC, 2003).

1.2 Quantifying carbon in tropical forest biomass

Quantifying carbon in a forest biomass, especially in a tropical forest, is not a straightforward task because of the complex structure of the forest stand and the interaction between vegetation, soil, and atmosphere (De Jong, 2001). The carbon in a forest biomass can either be quantified directly or by means of remote sensing models. Direct measurement of a carbon stock by cutting and weighing tree samples is considered to be the most accurate method for calculating carbon in a forest biomass (Ketterings *et al*., 2001). This "destructive" sampling can be correlated with forest stand parameters to develop allometric equations. A forest stand parameter, such as diameter at breast height (DBH) is easily measured in the field and readily available from forest inventories. Once an allometric equation has been established, this equation can be used to estimate tree biomass. A critical question is: do we need local allometric equations to improve the accuracy of above-ground biomass estimation? Some researchers (Ketterings *et al*., 2001; Nelson *et al*., 1999) suggested that local allometric equations were essential. Others believed that generic or general equations were accurate enough to estimate above-ground biomass (Chave *et al*., 2005; Gibbs *et al*., 2007). Brown (2002) underlined that the advantage of applying generic equations was that the equations were derived from a large number of trees with a wider range of DBH. This could improve the accuracy of the biomass estimation. However, she also mentioned that these equations might not accurately reflect the true biomass of the trees in an area.

Therefore, conducting "destructive" sampling is still required to validate the selected generic equation (Brown, 2002).

To obtain accurate biomass estimation, the DBH of the inventory data must be within the DBH range of the trees used to construct the allometric equation. The characteristics of the predicted trees should also be similar to those of the trees used to develop the allometric equation. In fact, the literature reviewed lacked allometric equations constructed from trees with large diameters, while big trees with large DBH (e.g. protected species and non-commercial timber) do still exist in mature tropical forests. The contribution of these large trees (DBH > 70 cm) to the above-ground biomass ranged from 30 to 40% in mature forests (Brown 2002). In addition, the Good Practice Guidance for Land Use and Land Use Change and Forestry/GPG-LULUCF (IPCC, 2003) only presents two allometric equations for tropical forests, though there are many differences in the characteristics of tropical forests. In this thesis, new equations have been developed to achieve a better estimation of above-ground biomass for tropical lowland *Dipterocarp* forests.

Although direct measurement of forest biomass provides higher estimation accuracy than other methods, it is impractical for large areas, as well as time consuming and costly, especially for heterogeneous landscapes (Chen *et al*., 2004; Clarck *et al*., 2001; Wang *et al*., 2003). For these reasons, remote sensing is used to provide opportunities to assess carbon from local to global scales. The ultimate benefit of using remote sensing data to estimate carbon stock in forest biomass is that it can lead to a systematic observation system and together with historical archives can be used for monitoring past, present and future land cover changes over large areas (Rosenqvist *et al*., 2003). Remote sensing images provide spatial, temporal, and spectral information as well as quantitative data (Bijker, 1997; Brown, 2002; Fernández, 2002; Foody, *et al*., 2003; Rosenqvist, *et al*., 2003). With regards to the Kyoto Protocol, remote sensing can meet the requirements of articles 3, 5, 10, and 12 (Nabuurs, *et al*., 2000; Patenaude, *et al*., 2005; Rosenqvist, *et al*., 2003). The importance of remote sensing for the quantifying, monitoring, and mapping of carbon stock for the implementation of REDD is emphasized in the sourcebook of GOFC-GOLD (2009) and the UNFCCC (2010).

Remote sensing as a tool provides several advantages for quantifying, mapping, and monitoring above-ground biomass. For tropical forests, however, there are

still some problems with the application of remote sensing for estimating above-ground biomass. Quantification of above-ground biomass in tropical forests is inconsistent when generated using vegetation indices. The accuracy of the estimations depends on the biophysical parameters of the forest (Lu *et al*., 2004). A problem is also encountered when medium or coarse spatial resolution is used, as the recorded data covering a pixel in an image are a mixture of reflectance components from the earth's surface. This mixed spectral signal may reduce the estimation accuracy. Such a mixture of reflectance components within a pixel may be decomposed into fraction images of the components using spectral mixture analysis. Spectral mixture analysis has been applied widely in the mapping of vegetation abundance (Pu *et al*., 2008; Small and Lu, 2006; Tooke *et al*., 2009) and of canopy damage (Souza *et al*., 2003; Souza *et al*., 2005). However, it has rarely been applied for quantitative analysis such as biomass estimation. In this thesis the potential utility of this method for quantifying tree biomass is explored in selective logging of *Dipterocarp* forest.

An image derived from a sensor has advantages and disadvantages. Integrating multi sensor data may be a challenge when exploring major benefits from different data sources. Fusion by integrating spatial and spectral information is intended to obtain complementary information from the earth's surface from different images (Chibani, 2006). Standard methods of fusion, such as Intensity Hue Saturation, Principle Component Analysis, and Brovey Transform tend to distort the colour information (Amolins *et al*., 2007) and the spectral characteristics of the original multispectral data (Kumar *et al*., 2000). The relatively new method of Discrete Wavelet Transform to fuse images from different data sources is drawing increasing interest. Recently, the Discrete Wavelet Transform has been applied to fuse data from optical sensors and SAR (Chibani, 2006). To our knowledge, there is hardly any study that has applied fusion for quantitative purposes. In this thesis, an innovative method is introduced to fuse fraction images resulting from spectral mixture analysis and Phase Arrayed L-band Synthetic Aperture Radar (PALSAR) data.

1.3 The current and future carbon stock

Knowledge of the existing and future forest growth in conjunction with carbon stock in forest biomass is essential for implementing sustainable forest management (Boisvenue *et al*., 2004). A simulation model may provide a long term prediction of timber production in response to human intervention (Alder and Silva, 2000), or in response to a given set of climatic and soil conditions

(Kichbaum *et al*., 2001). It describes forest dynamics including growth, mortality, and associated changes in a stand (Peng, 2000). A simulation model can also be very useful since the Intergovernmental Panel on Climate Change (IPCC) increasingly focuses on accounting for carbon stock in forest biomass, and on changes occurring as a result of management activities (Markewitz, 2006). In a production forest, the length of the logging cycle and the volume of the harvested timber are the important factors affecting carbon stock in the forest ecosystem. Changing a logging cycle to possibly increase carbon stock may be considered to be a mitigation measure under article 3.4 of the Kyoto Protocol to UNFCCC (Liski *et al*., 2001). The effects on carbon stock of changing the logging cycle and the volume of harvested timber can be predicted by a simulation model.

Timber harvesting removes logwood biomass from the forest ecosystem, but at the same time harvest residues left on the forest floor form input in the soil carbon stock (Jandl *et al*., 2007). On the other hand, logging activities also disturb the soil structure and lead to soil carbon emission as soil respiration is stimulated (Kowalski *et al*., 2004). Changing the length of the logging cycle may affect the carbon stock in trees and soil in different ways. Liski *et al*. (2001) examined that decreasing the rotation length to closer to the culmination age of the mean annual increment of Scots pine and Norway spruce reduced the carbon stock in these trees, but increased the soil carbon stock. Kaipainen *et al*. (2004) observed that elongation of the logging cycle increased the carbon stock in the tree biomass, but slightly decreased the soil carbon stock in German and Finnish Scots pine forests.

The effects of the length of the logging cycle and the volume of the harvested timber on carbon stock in tropical forests have not been explored in sufficient detail. In this thesis, the effects of different logging cycles and harvested timber volumes on carbon stock in trees and soil in lowland forests with mixed *Dipterocarp* is simulated using CO2FIX V 3.1 (Schelhaas *et al*., 2004). These forests are managed according to the Indonesian selective cutting and replanting system (TPTI) with a logging cycle of 35 years and a net volume of harvested timber of around 30 m^3/ha on average, with a maximum of 55 m^3/ha.

1.4 Research objectives

The general objectives of the research are to improve the accuracy of above-ground biomass (AGB) estimation and to study current and future carbon stock in conjunction with the management of the logging cycle and the amount of harvested timber in tropical lowland mixed *Dipterocarp* forests.

The specific objectives of this research are:

- Developing local allometric equations to improve the accuracy of the AGB estimation.
- Testing the potential of spectral mixture analysis to improve the estimation accuracy of AGB in *Dipterocarp* forests.
- Estimating AGB more accurately by integrating PALSAR and Landsat-7 ETM+ (Enhanced Thematic Mapper plus) data.
- Examining and understanding the impact of the length of the logging cycle and of the volume of harvested timber on future carbon stock.

1.5 Outline of the thesis

This thesis consists of six chapters, linked together in trying to improve the accuracy of AGB estimation.

Chapter 1 illustrates the general idea of comprehensive research into biomass estimation: the background, the problems in quantifying tropical forest biomass, the weaknesses of the existing methods, and challenges to improving on previous methods. Predictions on future carbon in tree biomass and soil are presented in this chapter. In addition, chapter 1 also describes the objectives of the research.

Chapter 2 presents the development of local allometric equations for improving the accuracy of the AGB estimation. Direct measurements obtained by cutting and weighing trees are described. Statistical analyses are presented to show that compared to general equations, the local allometric equations improve the accuracy of the AGB estimation.

Chapter 3 discusses the applicability of spectral mixture analysis for improving the accuracy of AGB estimation based on remotely sensed data. The weaknesses of existing methods and the need to improve them are discussed.

The uses of spectral mixture analysis for qualitative and quantitative analysis are also discussed.

Chapter 4 introduces an innovative method using multi-sensor data to achieve a higher accuracy of the AGB estimation. The results from spectral mixture analysis described in Chapter 3 are integrated with PALSAR data using Discrete Wavelet Transform. Several equations are generated from these integrations to achieve a higher accuracy of the AGB estimation than using the method of Chapter 3.

Chapter 5 provides the resulting simulation of the current and the projection of the future carbon stock in tree biomass and soil. Managing carbon stocks in tropical forests is conducted by changing the length of the logging cycle and the volume of harvested timber. The impact of the length of the logging cycle and of the harvested timber volume on carbon stocks in trees biomass and soil are discussed.

Chapter 6 brings together all the research findings from the previous chapters. The contribution of the research findings to society and for forest management is explained. General conclusions are provided and future works are recommended.

References

Alder, D., Silva, J.N.M., 2000. An empirical cohort model for management of Terra Firme forests in the Brazilian Amazon. Forest Ecology and Management 130: 141–157.

Amolins, K., Zhang, Y., Dare, P., 2007. Wavelet based image fusion techniques - an introduction, review and comparison. ISPRS Journal of Photogrammetric & Remote Sensing 62: 249–263.

Backe´us, S., Wikstro¨m, P., La¨mås, T., 2004. A model for regional analysis of carbon sequestration and timber production. Forest Ecology and Management 216: 28–40.

Baral, A., Guha, G.S., 2005. Trees for carbon sequestration or fossil fuel substitution: The issue of cost vs. carbon benefit. Biomass and Bioenergy 27: 41–55.

Bijker, W. 1997. Radar for rain forest. A Monitoring system for land cover change in the Colombian Amazon. ITC Publication no.53. Enschede, the Netherlands.

Binkley, C. S., Brand, D., Harkin, Z., Bull, G., Ravindranath, N. H., Obersteiner, M., Nilsson, S., Yamagata, Y., Krott, M., 2002. Carbon sink by the forest sector – options and needs for implementation. Forest Policy & Economics 4: 65–77.

Boisvenue, C., Temesgen, H., Marshall, P., 2004. Selecting a small tree height growth model for mixed species stands in the southern interior of British Columbia, Canada. Forest Ecology and Management 202: 301– 312.

Boyd, W. 2010. Deforestation and emerging greenhouse gas compliance regimes: toward a global environmental law of forests, carbon and climate governance. *In*: Bosetti, V., Lubowski, R. (*eds.*), Deforestation and climate change. Reducing carbon emissions from deforestation and forest degradation, p. 1–25. Edward Elgar, Pub., Cheltenham, UK.

Brown, S. 2002. Measuring carbon in forests: Current status and future challenges. Environmental Pollution 116: 363–372.

Chave, J., Andalo, A., Brown, S., Cairns, M.A., Chambers, J.Q., Eamus, D., Fölster, H., Fromard, F., Higuchi, N., Kira, T., Lescure, J.-P., Nelson, B.W., Ogawa, H., Puig, H., Riéra, B., Yamakura, T., 2005. Tree allometry and improved estimation of carbon stocks and balance in tropical forests. Oceologia 145: 87–99.

Chen, X., Vierling, L., Rowell, E., and De Felice, T. 2004. Using lidar and effective LAI data to evaluate IKONOS and Landsat 7ETM+ vegetation cover estimates in a Ponderosa pine forest. Remote Sensing of Environment 91: 14–26.

Chibani, Y., 2006., Additive integration of SAR features into multispectral SPOT images by means of the à trous wavelet decomposition. ISPRS Journal of Photogrammetric & Remote Sensing 60: 306–314.

Clark, D.A., Brown, S., Kicklighter, D.W., Chambers, J.Q., Thomlinson, J.R., Ni, J., Holland, E.A., 2001. Net primary production in tropical forests: An evaluation and synthesis of existing field data. Ecological Application 11(2): 371–384.

De Jong, B.H.J., 2001. Uncertainties in estimating the potential for carbon mitigation of forest management. Forest Ecology and Management 154: 85–104.

De Jong, B.H., Masera, O., Olguín, M., Martínez, R., 2007. Greenhouse gas mitigation potential of combining forest management and bioenergy substitution: A case study from Central Highlands of Michoacan, Mexico. Forest Ecology and Management 242: 398–411.

Dixon, R.K., Brown, S., Houghton, R.A., Solomon, A.M., Trexler, M.C., Wisniewski, J., 1994. Carbon pools and flux of global forest ecosystems. Science 263: 185–190.

Ezzine-de-Blas, D., Börner, J., Violato-Espada, A., Nascimento, N., Piketty, M., 2011. Forest loss and management in land reform settlements: Implications for REDD governance in the Brazilian Amazon. Environmental Science & Policy 14: 188–200.

Fernández, M.Q., 2002. Polarimetric data for tropical forest monitoring. Studies at the Colombian Amazon. Doctoral Thesis, Wageningen University. The Netherlands.

Foody, G.M., Boyd, D.S., Cutler, M.E.J., 2003. Predictive relations of tropical forest biomass from Landsat TM data and their transferability between regions. Remote Sensing of Environment 85: 463–474

Gibbs, H.K., Brown, S., Niles, J.O., Foley, J.A., 2007. Monitoring and estimating tropical forest carbon stocks: making REDD a reality. Environ.Res.Lett.2. doi:10.1088/1748-9326/4/045023.

Global Observation of Forest and Land Cover Dynamics (GOFC-GOLD), 2009. A sourcebook of methods and procedures for monitoring and reporting anthropogenic greenhouse gas emissions and removals caused by deforestation, gains and losses of carbon stocks in forests remaining forests, and reforestation.

Intergovernmental Panel on Climate Change (IPCC). 2003. Good practice guidance for land use, land-use change and forestry (GPG-LULUCF). Edited by Penman, J., Gystarsky, M., Hiraishi, T., Krug, T., Kruger, D., Pipatti, R., Buendia, L., Miwa, K., Ngara, T., Tanabe, K., Wagner, F. IPCC National Greenhouse Gas Inventories Program.

Jandl, R., Lindner, M., Vesterdal, L., Bauwens, B., Baritz, R., Hagedorn, F., Johnson, D. W., Minkkinen, K.,Byrne, K.A., 2007. How strongly can forest management influence soil carbon sequestration? Review. Geoderma 137: 253–268.

Kaipainen, T., Liski, J., Pussinen, A., Karjalainen, T., 2004. Managing carbon sinks by changing rotation length in European forests. Environmental Science & Policy 7: 205–219.

Ketterings, Q.M., Coe, R., van Noordwijk, M., Ambagau, Y., Palm, C.A., 2001. Reducing uncertainty in the use of allometric biomass equations for predicting above-ground tree biomass in mixed secondary forests. Forest Ecology and Management 146: 199–209.

Kirschbaum, M.U.F., Schlamadinger, B., Cannel, M.G.R.,l., Hamburg, S.P., Karjalainen, T., Kurz, W.A., Prisley , S., Schulze, E.D., Singh, T.P., 2001. A generalized approach of accounting for biospheric carbon stock changes under the Kyoto Protocol. Environmental Science & Policy 4: 73–85.

Korhonan, R., Pingoud, K., Savolainen, I., Matthews, R., 2002. The role of carbon sequestration and the tonne-year approach in fulfilling the objective of climate convention. Environmental Science & Policy 5: 429–441.

Kowalski, A.S., Loustau, D., Berbigier, P., Manca, G., Tedeschi, V., Borghetti, M., Valitini, R., Kolari, P., Berninger, F., Rannik, U., Hari, P., Rayment, M., Mencuccini, M., Moncrieff, J., Grace, J., 2004. Paired comparisons of carbon exchange between undisturbed and regeneration stands in four managed forests in Europe. Global Change Biology 10, 1–17. doi: J. 1365 - 2486.2004.00846.x.

Kumar, A. S., Kartikeyan, B., Majumdar, K. L.., 2000. Band sharpening of IRS-multispectral imagery by cubic spline wavelets. International Journal of Remote Sensing 21: 581–594.

Liski, J., Pussinen, A., Pingoud, K., Mäkipää., Karjalainen, T., 2001. Which rotation length is favourable to carbon sequestration?. Can. J. For.Res. 31: 2004–2013.

Lu, D., Mausel, P., Brondízio, E., Moran, E., 2004. Relationship between forest stand parameters and Landsat TM spectral responses in the Brazilian Amazon Basin. Forest Ecology and Management 198: 149–167.

Markewitz, D., 2006. Fossil fuel carbon emissions from silviculture: Impacts on net carbon sequestration in forests. Forest Ecology and Management 236: 153–161.

Nabuurs, G.J., Dolman, A.J., Verkaik, E., Kuikman, P.J., Van Diepen, C.A., Whitmore, A.P., Daamen, W.P., Oenema, O., Kabat,P., Mohren, G.M.J., 2000. Article 3.3 and 3.4 of The Kyoto Protocol: consequences for industrialised countries' commitment, the monitoring needs, and possible side effects. Environmental Science & Policy 3: 123-134.

Nelson, B.W., Mesquita, R., Pereira, J.L.G., De Souza, S.G.A., Batista, G.T., Couto, L.B, 1999. Allometric regressions for improved estimate of secondary forest biomass in the central Amazon. Forest Ecology and Management 117: 149–167.

Patenaude, G., Milne, R., Dawson, T.P., 2005. Synthesis of remote sensing approaches for forest carbon estimation: Reporting to the Kyoto Protocol. Environmental Science & Policy 8: 161–178.

Peng, C., 2000. Growth and yield models for uneven-aged stands: past, present and future. Forest Ecology and Management 132: 259–279.

Ptaff, A.S.P., Kerr, S., Hughes, R.F., Liu, S., Azofeifa, G.A.S., Schimel, D., Tosi, J., Watson, V. 2000. The Kyoto Protocol and payments for tropical forest: An interdisciplinary method for estimating carbon-offset supply and increasing the feasibility of a carbon market under the CDM. Ecological Economics 35: 203–221.

Pu, R., Gong, P., Michishita, R., Sasagawa, T., 2008. Spectral mixture analysis for mapping abundance of urban surface components from the Terra/ASTER data. Remote Sensing of Environment 112: 939–954.

Rosenqvist, Å., Milne, A., Lucas, R., Imhoff, M., Dobson, C., 2003. A review
of remote sensing technology in support of the Kyoto Protocol. Environmental Science & Policy 6: 441–455.

Santilli, M., P. Mountiho, S. Schwartzman, D. Nepstad, L. Curran, and C. Nobre. 2005. Tropical deforestation and the Kyoto Protocol. Climatic Change 71: 267-276. DOI: 10.1007/s 10584- 005-8074-6.

Sasaki, N., Yoshimoto, A. 2010. Benefits of tropical forest management under the new climate change agreement - a case study in Cambodia. Environmental Science & Policy 13: 384–392.

Schelhaas, M.J., P.W. van Esch, T.A. Groen, B.H.J. de Jong, M. Kanninen, J. Liski, O. Masera, G.M.J. Mohren, G.J. Nabuurs, T. Palosuo, L. Pedroni, A. Vallejo, T. Vilén, 2004. CO2FIX V 3.1 - description of a model for quantifying carbon sequestration in forest ecosystems and wood products. ALTERRA Report 1068. Wageningen, The Netherlands.

Small, C., Lu, J. W.T., 2006. Estimation and vicarious validation of urban vegetation abundance by spectral mixture analysis. Remote Sensing of Environment 100: 441–456.

Souza, Jr. C., Firestone, L., Silva, L.M., Roberts, D., 2003. Mapping forest degradation in the Eastern Amazon from SPOT 4 through spectral mixture models. Remote Sensing of Environment 87: 494–506.

Souza, Jr., C.M., Roberts, D. A., Cocrane, M.A., 2005. Combining spectral and spatial information to map canopy damage from selective logging and forest fires. Remote Sensing of Environment 98: 329–343.

Thompson, M.C., Baruah, M., Carr, E. R., 2011. Seeing REDD+ as a project of environmental governance. Environmental Science & Policy 14: 100–110.

Tooke, T.R., Coops, N.C., Goodwin, N.R., Voogt, J.A., 2009. Extracting urban vegetation characteristics using spectral mixture analysis and decision tree classifications. Remote Sensing of Environment 113: 398–407.

UNFCCC., 1998. Kyoto Protocol to The United Nations Framework Convention on Climate Change. http://unfccc.int/resource/docs/convkp/kpeng. pdf.

UNFCCC., 2009. Cost of implementing methodologies and monitoring systems relating to estimates of emissions from deforestation and forest degradation, the assessment of carbon stocks and greenhouse gas emissions from changes in forest cover, and the enhancement of forest carbon stocks. Technical report.

UNFCCC., 2010. http://unfccc.int/methods_science/redd/methodologies/items/4538. php.

Wang, H., Hall, C.A.S., Scatena, F.N., Fetcher, N., Wu, W., 2003. Modelling the spatial and temporal variability in climate and primary productivity across the Luquillo Mountains, Puerto Rico. Forest Ecology and Management 179: 69–94.

CHAPTER 2

ALLOMETRIC EQUATIONS FOR ESTIMATING THE ABOVE-GROUND BIOMASS IN TROPICAL LOWLAND *DIPTEROCARP* FORESTS*

* This chapter is based on:

Basuki, T.M., van Laake, P.E., Skidmore, A.K., Hussin, Y.A., 2009. Allometric equations for estimating the above-ground biomass in tropical lowland *Dipterocarp* forests. Forest Ecology and Management 257: 1684 – 1694.

Abstract

Allometric equations can be used to estimate the biomass and carbon stock of forests. However, so far the equations for *Dipterocarp* forests have not been developed in sufficient detail. In this research, allometric equations are presented based on the genera of commercial species and mixed species. Separate equations are developed for the *Dipterocarpus*, *Hopea*, *Palaquium* and *Shorea* genera, and an equation of a mix of these genera represents commercial species. The mixed species is constructed from commercial and non-commercial species. The data were collected in lowland mixed *Dipterocarp* forests in East Kalimantan, Indonesia. The number of trees sampled in this research was 122, with diameters (1.30 m or above buttresses) ranging from 6 to 200 cm. Destructive sampling was used to collect the samples where diameter at breast height (DBH), commercial bole height (CBH), and wood density were used as predictors for dry weight of above-ground biomass (AGB). Model comparison and selection were based on Akaike Information Criterion (AIC), slope coefficient of the regression, average deviation, confidence interval (CI) of the mean, paired t-test. Based on these statistical indicators, the most suitable model is $\ln(AGB) = c + \alpha \ln(DBH)$. This model uses only a single predictor of DBH and produces a range of prediction values closer to the upper and lower limits of the observed mean. Model 1 is reliable for forest managers to estimate AGB, so the research findings can be extrapolated for managing forests related to carbon balance. Additional explanatory variables such as CBH do not really increase the indicators' goodness of fit for the equation. An alternative model to incorporate wood density must be considered for estimating the AGB for mixed species. Comparing the presented equations to previously published data shows that these local species-specific and generic equations differ substantially from previously published equations and that site specific equations must be considered to get a better estimation of biomass. Based on the average deviation and the range of CI, the generalized equations are not sufficient to estimate the biomass for a certain type of forests, such as lowland *Dipterocarp* forests. The research findings are new for *Dipterocarp* forests, so they complement the previous research as well as the methodology of the Good Practice Guidance for Land Use and Land Use Change and Forestry (GPG-LULUCF).

2.1 Introduction

The accurate estimation of biomass in tropical forests is crucial for many applications, from the commercial exploitation of timber to the global carbon cycle. Particularly in the latter context the estimation of the above-ground biomass (AGB) with an accuracy sufficient to establish the increments or decrements in carbon stored in the forest over relatively short periods of time (2 ~ 10 years) is increasingly important. Under the United Nations Framework Convention on Climate Change (UNFCCC), countries have to report regularly the state of their forest resources and emerging mechanisms, such as Reducing Emissions from Deforestation in Developing Countries (REDD), and they are likely to require temporally and spatially fine-gained assessments of carbon stock (UNFCCC, 2008).

Carbon stock is typically derived from biomass by assuming that 50% of the biomass is made up by carbon. The most accurate method for the estimation of biomass is through cutting of trees and weighing of their parts. This "destructive" method is often used to validate others, less invasive and costly methods, such as the estimation of carbon stock using non-destructive in-situ measurements and remote sensing (Clark *et al*., 2001; Wang *et al*., 2003). Allometric equations developed on the basis of sparse measurements from destructive sampling are related to more easily collected biophysical properties of trees, such as diameter at breast height (DBH) and commercial bole height (CBH). The estimation of carbon over large areas using remote sensing is supported by correlating the reflection of the canopy recorded at the sensor to the carbon measured directly or estimated indirectly on the ground (Chiesi *et al*.,2005; Gibb *et al*., 2007; Myeong *et al*., 2006; Tan *et al*., 2007).

In this research, tree allometric equations are developed by establishing the relationship between tree parameters such as DBH, CBH, and wood density with AGB. Various allometric equations have been developed for tropical rain forests (Araújo *et al*., 1999; Brown, 1997; Chambers *et al*., 2001; Chave *et al*., 2005, 2001; Keller *et al*., 2001; Nelson *et al*., 1999). However, there are few allometric equations developed specifically for lowland *Dipterocarp* forests, despite the fact that this type of forest covers extensive areas in tropical South-East Asia: around 59% of forests in Kalimantan and 53% of forests in Sumatra, Indonesia (Tyrie, 1999), and that they are among the most commercialized hard wood species from South-East Asia. So far, allometric equations for multi-species tropical forests of Indonesia have been published in Brown (1997),

Hashimotio *et al*. (2000), Ketterings *et al*. (2001) and Yamakura *et al*. (1986). The applicability of the equations needs to be affirmed before they can be applied to mono-typic *Dipterocarp* forests.

Brown (1997) developed allometric equations for tropical forests using data collected from Kalimantan and other tropical regions. A logistic curve based on tree age was constructed by Hashimotio *et al*. (2000) in fallow forests of East Kalimantan. The equation of Hashimotio *et al*. (2000) cannot be applied to *Dipterocarp* forests as it requires stand age as explanatory variable which is not available, and due to the differences in ecological environments between fallow and natural forests. Ketterings *et al*. (2001) established an allometric equation in mixed secondary forest in Sumatra, but this forest was not classified as *Dipterocarp* forest. Yamakura *et al*. (1986) constructed allometric equations using data collected from *Dipterocarp* forests from Sebulu, East Kalimantan. They used DBH and tree height to predict stem dry weight. The stem dry weight was used to predict branch dry weight, and stem and branch dry weight was then used to model leaf dry weight. The equations developed by Yamakura *et al*. (1986) are not practical for most uses since the equation does not directly predict the AGB.

The lack of allometric equations for *Dipterocarp* forests is also evident in the Good Practice Guidance for Land Use and Land Use Change and Forestry (IPCC, 2003; further abbreviated as GPG-LULUCF). In this document, there are only two allometric equations for tropical forests, while in fact there are many differences in the characteristics of tropical forests. The accuracy or uncertainty of models is an important aspect that is mentioned in the GPG and the different instruments of the Kyoto Protocol. To reduce uncertainty, accurate carbon accounting methods are required. The development of new, species-specific allometric equations are necessary to achieve higher levels of accuracy, and we present some new equations here to achieve a better estimation of carbon stock for tropical lowland *Dipterocarp* forests.

2.2 Methods

2.2.1 Study area

The study was executed at two sites in Berau Regency, East Kalimantan, Indonesia. The first site is located in Labanan ($1^0$45' to $2^0$10' North latitude and from $116^0$55' to $117^0$20' East longitude), Teluk Bayur District. In this location,

trees with the diameters (DBH or above buttresses) mostly ranging from 5 to 70 cm were felled. The second site is in the Puji Sempurna Raharja forest concession area, Merancang, around 60 km north-east of Labanan ($2^0$11' to $2^0$20' North latitude and $117^0$38' to $118^0$11' East longitude), where trees with diameters of 70 up to 200 cm were felled. These study areas are located within the same forest type, namely lowland mixed *Dipterocarp*. The dominant family in these forests is *Dipterocarpaceae*. These forests consist of commercial, non-commercial and protected species. The map of the study area is presented in Figure 2.1.

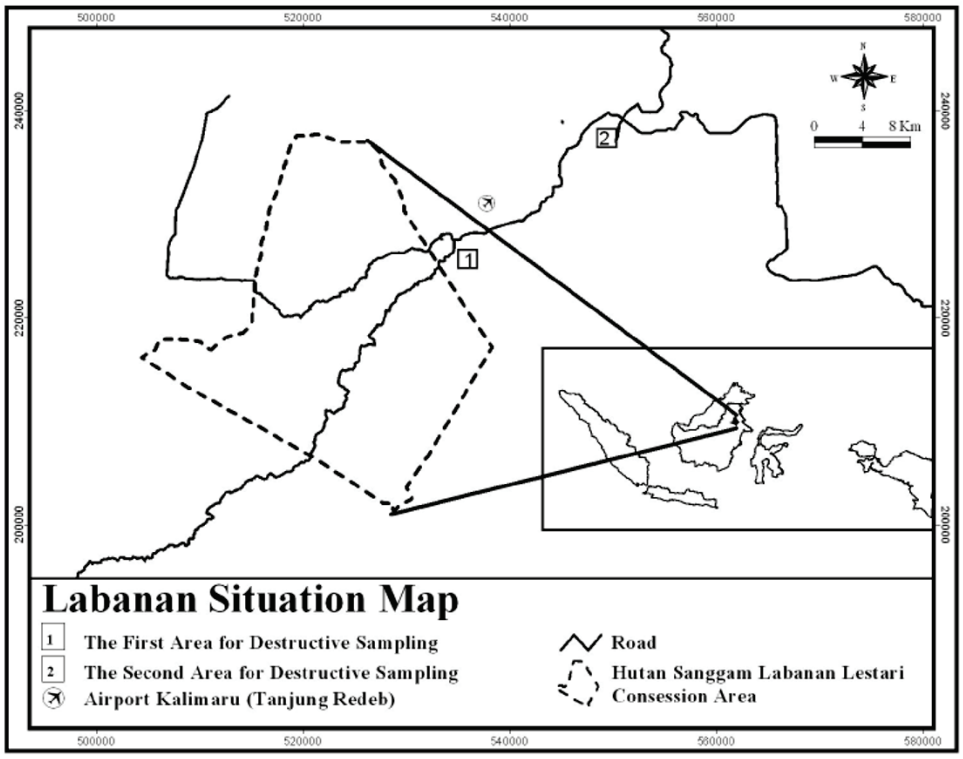

Figure 2.1: Location of the sampling sites in Labanan (the first site) and Merancang (the second site).

Based on the data (1995 – 2005) collected by the Meteorological and Geophysical Agency, the mean annual rainfall in the study area is 2300 mm. The months from June to October are dry, while the wet months are from November to May. The temperature ranges from 21 to 34 ºC and the mean is 26ºC (Berau Forest Management Project/BFMP, 1999).

At the Labanan study area, the dominant soil types are Red Yellow Podzolic or Ultisols. However, the soil properties within a soil type vary according to the terrain conditions. Minor soil types include Oxisols, Vertisols and Inceptisols (Mantel, 1999). As in Labanan, the dominant soil of the Merancang study area is Red Yellow Podzolic (66%), and the remainder is Alluvial.

2.2.2 Data collection

Trees selection was based on species grouping according to Gunawan and Rathert (1999), the inventory data of the concessioners, and a ground check. Forest inventories were conducted within 83,240 ha of the areas managed by PT Hutan Sanggam Labanan Lestari and 51,000 ha of the areas managed by PT Puji Sempurna Raharja. To obtain the representative tree samples, diameter distributions and the species grouping were taken into account during tree selection. The data were collected twice: the first data set was collected in March to April 2006, and the second data set was collected in September to October 2006. The first data set consisted of four commercial genera including *Dipterocarpus* (20 trees, 5 species), *Hopea* (20 trees, 3 species), *Palaquium* (19 trees, 3 species) and *Shorea* (24 trees, 9 species). The first data set was collected in Labanan and Puji Sempurna Raharja concession areas, Merancang. The second data set was collected in Labanan, covering commercial (excluding the four mentioned genera) and non-commercial species that consisted of 39 trees from 27 species (Samalca, 2007). These two data sets were used for destructive sampling. The diameters were 6.5 to 135 cm, 6.5 to 87 cm, 6.3 to 74 cm, 6.5 to 200 cm, and 6 to 68.9 cm for *Dipterocarpus*, *Hopea*, *Palaquium*, *Shorea* and the second data set, respectively. The overall DBH distributions were: >6 to 20 cm, 29 trees, >20 to 40 cm, 36 trees, >40 to 60 cm, 28 trees, >60 to 80 cm, 12 trees, >80 to 100, 9 trees, >100 to 120 cm, 5 trees and >120 to 200 cm, 3 trees.

Before conducting the destructive sampling, the DBH was measured. Generally the DBH was measured at 1.30 m above ground, but for trees with enlargement or buttresses, the diameter was measured at 30 cm above the main enlargement (Food and Agriculture Organization/FAO, 2004). After felling, the tree height was measured. Diameter was measured at 2 m intervals for the stems and big branches with the diameters of more than 15 cm. These measurements were used to estimate the volume and dry weight. The volume of each section was calculated using Smalian's formula as cited by De Gier (2003). The total volume was obtained by summing the volume of each section. Due to the difference in moisture content, the tree material was partitioned into leaves,

twigs (diameter <3.2 cm), small branches (diameter 3.2-6.4 cm), large branches (diameter >6.4 cm) and stem (Ketterings et al., 2001). The fresh weight of the leaves, twigs, branches and stems with diameters equal or less than 15 cm was weighed in the field using spring weighing scales of 50 kg and 25 kg capacity with accuracy $\pm 1\%$. A table scale was used to weigh smaller specimens. The latter balance had a capacity of 2000 g with accuracy ± 0.5 %.

The samples from the partitioned trees were taken in three replications and stored in sealed plastic bags, and then sent to the laboratory to determine their moisture content. In the laboratory, an analytical balance with capacity of 420 g and accuracy of 0.001 g was used to weigh the samples. Dry weights were obtained by drying the samples at a temperature of 105 ºC until a constant weight was achieved (Stewart *et al*., 1992; Ketterings *et al*., 2001).

To determine the wood density, samples were taken from the lower, middle and upper parts of the stems. The samples were taken as a pie shape or cylinder, so the inner and outer parts of the trunks with their barks were included (Nelson *et al*., 1999). Wood density was measured by the water replacement method. To avoid shrinkage during volume measurement, the samples were first saturated. In so doing, rehydration was conducted for 48 hours. The volume of each sample was determined from the volume of the water displaced when submerged. The wood density was calculated as dry oven weight divided by saturated volume. The results for the individual specimens are presented in Appendix 2.1.

The dry weight of the stems and branches with the diameter of > 15 cm was calculated by multiplying the fresh volume of each section by wood density. For the other partitioned trees, the dry weight was calculated through fresh weight multiplied by dry weight/fresh weight ratio of the corresponding samples. The dry weight of a tree was obtained by summing the dry weight of the stem, branches, twigs, and leaves.

2.2.3 Data analysis

Based on the data collected, several equations were developed. Firstly, the equations were developed for four individual genera *Dipterocarpus*, *Hopea*, *Palaquium* and *Shorea*. Secondly, these four genera were mixed to develop an equation for commercial species. Finally, the four genera together with the

second data set (Samalca, 2007) were used to develop an allometric equation for mixed species.

Before establishing the allometric equation, scatter plots were used to see whether the relationship between independent and dependent variables was linear. Furthermore, several allometric relationships between independent and dependent variables were tested. The independent variables included DBH, CBH, and wood density, whereas the dependent variable was the dry weight of the AGB. Because the data exhibited heteroscedasticity, a power function was an inappropriate model in this study, so we transformed the data for linear regression using a natural logarithm. The transformation equalized the variance over the entire range of biomass values which satisfies the prerequisite of linear regression (Sokal and Rohlf, 1995 and Sprugel, 1983). However, this transformation introduced a systematic bias in the calculation which was corrected using a correction factor (CF) when back-transforming the calculation into biomass (Chave *et al*., 2005; Sah *et al*., 2004; Son *et al*, 2001; and Sprugel, 1983).

Model comparison and selection were based on average deviation (Brand *et al*., 1985; Cairns *et al*., 2003; Chave *et al*., 2005; and Nelson *et al*., 1999), slope coefficient of the regression (Nelson *et al*., 1999), Akaike Information Criterion (AIC) (Burnham and Anderson, 2002 and Chave *et al*., 2005), confidence interval (CI) of the predictions, and paired t-test. Coefficients of determination (R^2) more than 90% are reported in this paper.

The average deviation was computed from the absolute difference between predicted and observed dry weight and expressed as the percentage of observed dry weight, then all deviations were averaged (Brand *et al*., 1985; Cairns *et al*., 2003; Chave *et al*., 2005; and Nelson, 1999). The equation to calculate average deviation is shown in equation 2.1. The deviation was calculated after the prediction was back-transformed to the unit values and corrected using a CF. The average deviation has been calculated as follows:

$$\bar{S}(\%) = \frac{100}{n} \sum_{i=1}^{n} |\hat{Y}i - Yi| / Yi \qquad (2.1)$$

where $\bar{S}$ is the average deviation, Y_i = the observed dry weight, $\hat{Y}_i$ = the predicted dry weight, n = number of observations.

The formula of AIC used as the criterion for model selection (Chave *et al*., 2005) is:

$$AIC = -2\ln(L) + 2p \quad (2.2)$$

where L is the likelihood of the fitted model and p is the total number of parameters in the model. The optimal model will minimize the AIC value (Chave et al., 2005). AIC is used to compare non-nested models.

2.2.4 Comparing the equations to previously published equations

The proposed mixed species model was applied to the data of Ketteings *et al*. (2001). Besides that, we also employed the models of Brown (1997), one of the pan-tropic equations of Chave *et al*. (2005), and Ketterings *et al*. (2001) to the current data.

The allometric equation developed by Brown (1997) for tropical moist forest is:

$$AGB = \exp(-2.134 + 2.53 \ln(DBH)) \quad (2.3)$$

where AGB is above-ground biomass in kg/tree and DBH is in cm. The equation of Brown (1997) was constructed from the data collected by several authors from different tropical countries and at different times. The diameters used to establish this equation ranged from 5 to 148 cm, and the number of sample trees was 170. Besides the model of Brown (1997), one of the pan-tropic models of Chave *et al*. (2005) was chosen as a comparison of the proposed models. Pan-tropic models were developed from various tropical forests based on the compilation of data since 1950s from 27 study sites in America, Asia and Oceania (Chave *et al*. 2005). The samples were collected from 2410 trees with DBH that ranged from 5 to 156 cm. The best pan-tropics model for moist tropical forest based on DBH measurements and wood density was applied to the current data. The equation is:

$$AGB = \rho \exp(-1.499 + 2.148 \ln(DBH) + 0.207 (\ln(DBH))^{\wedge 2} - 0.0281(\ln(DBH))^{\wedge 3}) \quad (2.4)$$

where AGB is in kg/tree, ρ = species specific wood density (g/cm^3). In addition to the models mentioned above, the model of Ketterings *et al*. (2001) was chosen. Ketterings' data consisted of 29 trees from 14 genera with the diameters

ranging from 7.6 cm to 48.1 cm. The allometric equation developed by Ketterings *et al*. (2001) is:

$$AGB = r\,\rho_{avg}\,(DBH)^{\wedge 2+c} \quad (2.5)$$

where AGB is in kg/tree, r is a parameter that is constant over wide range of geographical areas, ρ_{avg} is the average wood density for the study areas, and c is a parameter estimated from relationship between tree height and DBH. For the study areas, c is 0.397, ρ is 0.604 g/cm^3, and r is 0.11.

2.3 Results

2.3.1 Developing allometric equations

The model initially developed is presented in equation 2.6:

$$\ln(AGB) = c + \alpha \ln(DBH) \quad (2.6)$$

where AGB is dry weight in kg/tree, DBH is in cm, c is the intercept, and α is the slope coefficient of the regression. The values of the coefficients are presented in Table 2.1 and the regression lines are presented in Figure 2.2.

For this model, the adjusted R^2 ranged from 0.963 to 0.989 and the lowest was found for mixed species. The average deviation was therefore the highest for the mixed species. Among the genera, *Shorea* had the highest average deviation (19.6%). The allometric equation for every genus, commercial species, and mixed species had a significant slope coefficient at $p<0.001$ (Table 2.1).

Model 1 uses only DBH as a predictor. In fact, tree biomass is affected by its height and wood density as well. Therefore, CBH and wood density were incorporated as additional independent variables. Even though measuring the total tree height was easy for felled trees, CBH was used instead of total height due to practical difficulty of measuring standing trees in the field and the properties of the tree architecture in the study areas. Regarding tree architecture, the bulk of tree biomass measured in the field was in the form of main stems and not in branches and leaves. It accounted of 45% to 90% with the average of 67% of the AGB. By incorporating CBH (in meters) as the second predictor in model 2, the model becomes a multiple linear regression as follows:

$$\ln(AGB) = c + \alpha \ln(DBH) + \beta \ln(CBH) \quad (2.7)$$

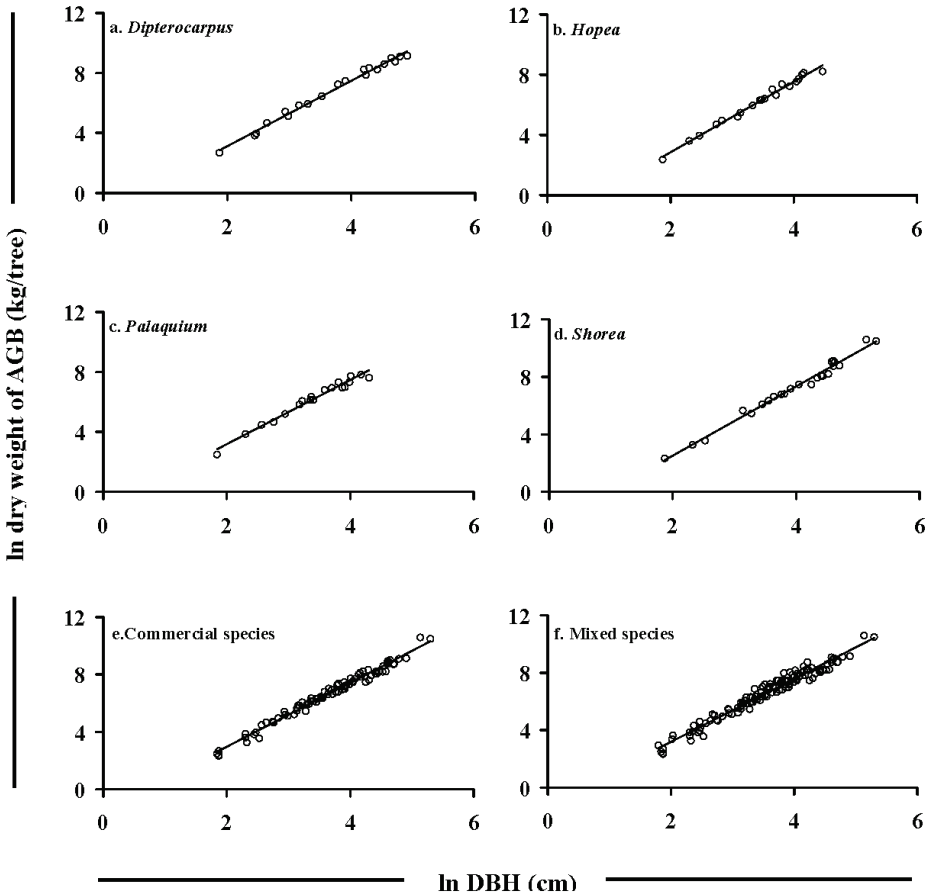

Figure 2.2: Linear regression of natural log transformation of DBH (cm) and above-ground biomass (AGB) (kg/tree) of *Dipterocarpus* (a), *Hopea* (b), *Palaquium* (c), *Shorea* (d), commercial species (e) and mixed species (f). The number of trees for every regression is 20, 20, 19, 24, 83 and 122, respectively.

Since correlation between DBH and AGB has been high, the addition of CBH in model 2 only increased slightly R^2 and also reduced slightly the average deviation. Table 2.1 shows that at the genus level, the β coefficients from the inclusion of CBH are significant at $p<0.05$ for *Dipterocarpus* and *Hopea*, and not statistically significant for *Shorea* (Table 2.1).

As mentioned above, wood density is an important factor when calculating biomass (Baker *et al*., 2004, Chave *et al*., 2005, Nogueira *et al*., 2007), so it was added as a predictor variable. Adding wood density in the model is important in order to estimate the biomass for mixed species and big trees, since biomass

estimates for larger DBH trees are more variable and have a disproportionately large contribution to forest biomass.

By incorporating wood density in the third model, the equation becomes:

$$\ln(AGB) = c + \alpha \ln(DBH) + \beta \ln(WD) \quad (2.8)$$

where WD is wood density for every measured tree. The β coefficient in model 3 was not statistically significant for *Dipterocarpus*, *Hopea* and *Shorea*, whereas for the commercial and mixed species equations, it was highly significant at $p<0.001$ (Table 2.1).

Table 2.1: Model parameter used to estimate the above-ground biomass of *Dipterocarp* forests.

Species grouping	N	Allometric Equation	Coefficient		Standard error of the coefficient	Adjusted R^2	Standard error of residual	Average Deviation (%)	CF
			symbol	Value					
Diptero carpus	20	ln (AGB) = c	c	-1.232***	0.200	0.989***	0.210	18.65	1.022
		+ α ln (DBH)	α	2.178***	0.053				
		ln (AGB) = c	c	-2.187***	0.428	0.992***	0.183	14.15	1.017
		+ α ln (DBH)	α	2.007***	0.084				
		+ β ln (CBH)	β	0.575*	0.236				
		ln (AGB) = c	c	-1.190**	0.336	0.989***	0.213	18.84	1.023
		+ α ln (DBH)	α	2.175***	0.057				
		+ β ln (WD)	β	0.082^{ns}	0.488				
Hopea	20	ln (AGB) = c	c	-1.813***	0.213	0.987***	0.184	14.08	1.017
		+ α ln (DBH)	α	2.339***	0.061				
		ln (AGB) = c	c	-2.856***	0.480	0.990***	0.165	12.76	1.014
		+ α ln (DBH)	α	2.116***	0.109				
		+ β ln (CBH	β	0.656*	0.277				
		ln (AGB) = c	c	-1.708***	0.301	0.987***	0.188	13.87	1.018
		+ α ln DBH)	α	2.335***	0.063				
		+ β ln (WD)	β	0.174^{ns}	0.344				
Palaqui Um	19	ln (AGB) = c	c	-1.098***	0.281	0.975***	0.230	18.78	1.027
		+ α ln DBH)	α	2.142***	0.082				
		ln (AGB) = c	c	-1.663***	0.275	0..984***	0.181	13.72	1.017
		+ α ln DBH)	α	1.817***	0.114				
		+ β ln (CBH)	β	0.612**	0.177				
		ln (AGB) = c +	c	-0.723*	0.286	0.980***	0.201	16.86	1.020
		α ln (DBH)	α	2.145***	0.071				
		+ β ln (WD)	β	0.704*	0.273				
Shorea	24	ln (AGB) = c	c	-2.193***	0.253	0.984***	0.2601	20.49	1.034
		+ α ln (DBH)	α	2.371***	0.063				
		ln (AGB) = c	c	-2.758***	0.417	0.985***	0.250	18.60	1.032
		+ α ln DBH)	α	2.178***	0.131				
		+ β ln (CBH)	β	0.463^{ns}	0.277				
		ln (AGB) = c	c	-1.533***	0.405	0.986***	0.244	19.14	1.030
		+ α ln (DBH)	α	2.294***	0.070				
		+ β ln (WD)	β	0.560^{ns}	0.278				

Table 2.1: (*Continued*)

Species grouping	N	Allometric Equation	Coefficient symbol	Coefficient Value	Standard error of the coefficient	Adjusted R^2	Standard error of residual	Average Deviation (%)	CF
Commercial species	83	ln (AGB) = c + α ln (DBH)	c	-1.498***	0.127	0.981***	0.252	21.61	1.032
			α	2.234***	0.034				
		ln (AGB) = c + α ln (DBH) + β ln (CBH)	c	-2.266***	0.213	0.985***	0.227	18.63	1.026
			α	2.030***	0.056				
			β	0.542***	0.125				
		ln (AGB) = c + α ln (DBH) + β ln (WD)	c	-1.045***	0.150	0.985***	0.225	18.77	1.057
			α	2.203***	0.031				
			β	0.639***	0.138				
Mixed *species*	122	ln (AGB) = c + α ln (DBH)	c	-1.201***	0.141	0.963***	0.335	30.32	1.058
			α	2.196***	0.039				
		ln (AGB) = c + α ln (DBH) +β ln (CBH)	c	-1.935***	0.234	0.967***	0.318	27.49	1.052
			α	1.981***	0.067				
			β	0.541***	0.141				
		ln (AGB) = c + α ln (DBH) + β ln (WD)	c	-0.744***	0.154	0.970***	0.303	26.51	1.047
			α	2.188***	0.035				
			β	0.832***	0.157				

Note: The statistical analyses are significant at 95 % confidence interval. ***p<0.001; **p<0.01; *p<0.05; and non-significant, ^{ns}p>0.05. N= the number of tree samples, AGB = above-ground biomass based on dry weight (kg/tree), DBH = diameter at breast height (cm), CBH = commercial bole height (m), WD = wood density (g/cm^3), and CF = correction factor

To compare model 2 and 3, AIC was calculated and the results are presented in Table 2.2. The AIC values for model 3 were lower than that for model 2, except for *Dipterocarpus* and *Hopea*. Based on the species grouping, the highest AIC values were found for the mixed species followed by the commercial species and the lowest were in the genera.

Table 2.2: Akaike Information Criterion (AIC) for model 2 and 3

Species grouping	Model	AIC
Dipterocarpus	2	321
	3	326
Hopea	2	282
	3	303
Palaquium	2	271
	3	264
Shorea	2	458
	3	437
Commercial species	2	1490
	3	1464
Mixed species	2	2176

Our estimates of wood densities were compared with the data from GPG and from Plant Resources of South East Asia (PROSEA) (Soerianegara and Lemmens, 1993). The results show that increasing DBH is not followed by an increase in wood density. This finding is in agreement with the previous research by Baker *et al*. (2004), Nogueira *et al*. (2005, 2007). The comparison of the wood density values based on the current study and those from the published data of GPG and PROSEA (Soerianegara and Lemmens, 1993) is presented in Appendix 2.1. In the GPG, for *Shorea* only *Shorea spp. balau* group, *Shorea spp.* (dark red meranti), *Shorea spp.* (light red meranti), etc. are mentioned but their species are not presented. In fact, the commercial timber red meranti consists of many species, such as *S. parvifolia*, *S. smithiana*, *S. macroptera*. The wood density for the dominant species from every genus is superimposed with the wood density from the corresponding species of the published data (PROSEA) and presented in Figure 2.3.

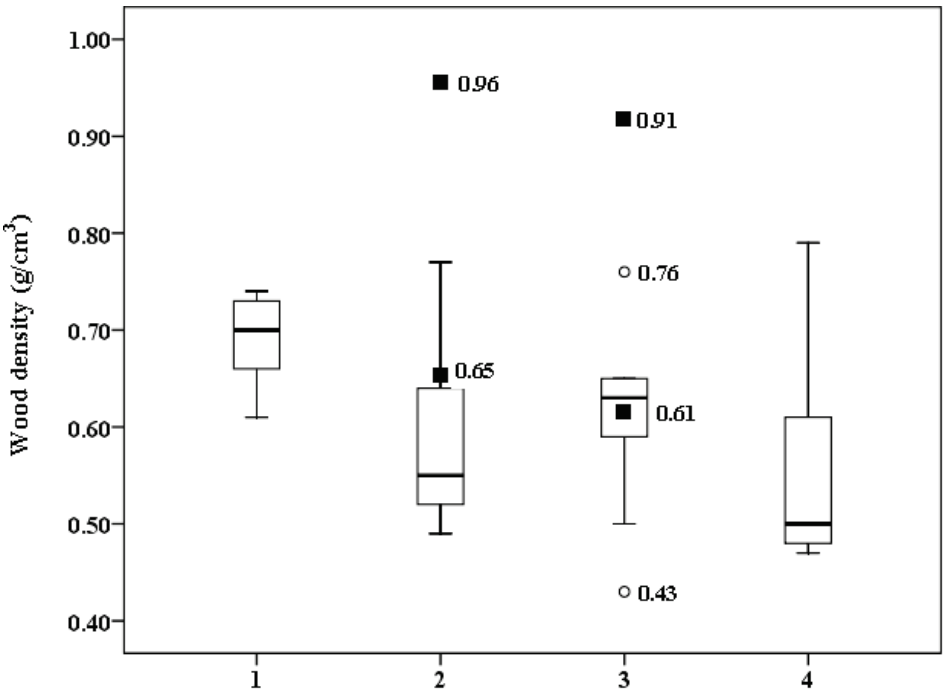

Figure 2.3: Wood density of 1: *D. pacyphyllus* (n=8), 2: *H. cernua* (n=18), 3: *P. gutta* (n=13) and 4: *S. retusa* (n=6), the dominant species of *Dipterocarpaceae*, *Hopea*, *Palaqium* and *Shorea*, respectively. The cycle shapes with values of 0.76 and 0.43 are the outlier of *H. cernua* from the current data. The rectangle shapes indicate the highest and the lowest wood density of *P gutta* and *H cernua* from the data of PROSEA.

Two outliers of wood density, indicated by the circles, are found from *Palaquium gutta* of the current data. The first is at a DBH of 50 cm with a wood density of 0.43 g/cm^3, and the second is at a DBH of 28.6 cm with a wood density of 0.76 g/cm^3. The data from the PROSEA are indicated by the rectangular shapes which show the highest and the lowest values of wood densities of *H. cernua* and *P. gutta*.

2.3.2 Comparing the equations to previously published equations

Model 1 of the mixed species regression was applied to the data of Ketterings *et al*. (2001). The predicted AGB using the first model to the Ketterings' data produced the same trend as the observed data (Figure 2.4).

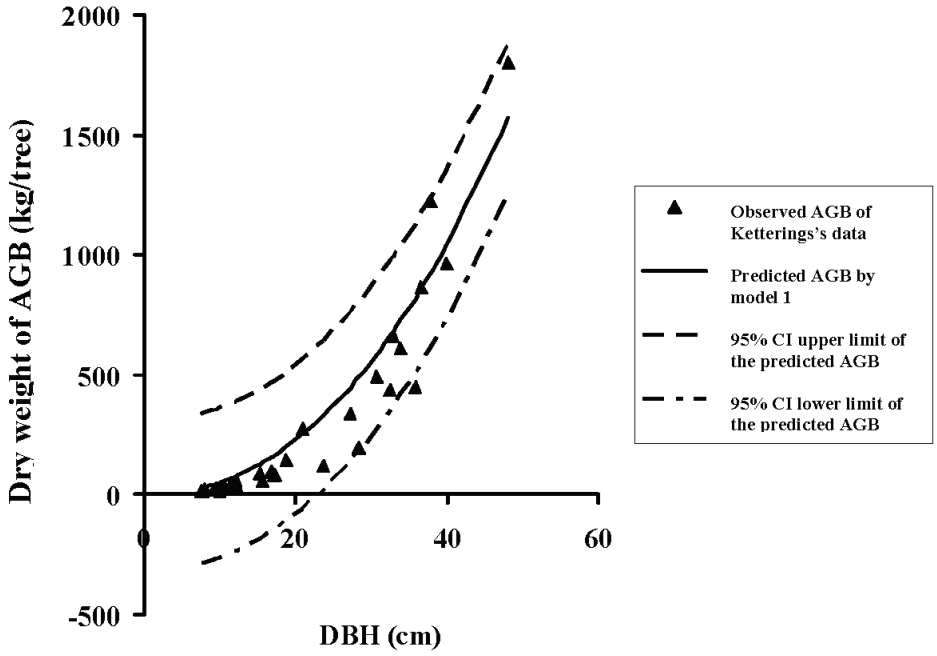

Figure 2.4: Regression line for model 1 of the mixed species (122 sample trees) as applied to the data published by Ketterings *et al*. (2001).

The average deviation for individual trees of the previously published models is always higher than that of models 1, 2, and 3 of the mixed species, and has higher deviation at the genus level (Table 2.3). At the genus level, prediction of AGB using the equation of Brown (1997) resulted average deviation ranging from 43 to 107 % and from 52 to 94% for the equation of Chave *et al*. (2005).

Table 2.3: Average deviation of the model to estimate the above-ground biomass

Species grouping	The employed equation	Average deviation ($\overline{S}$)*) (%)
Dipterocarpus	Model 1	18,65
	Model 2	14.15
	Model 3	18.84
	Brown (1997)	62.78
	Chave *et al*. (2005)	89.67
	Ketterings *et al*. (2001)	46.81
Hopea	Model 1	14.08
	Model 2	12.76
	Model 3	13.87
	Brown (1997)	42.94
	Chave *et al*. (2005)	52.08
	Ketterings *et al*. (2001)	49.46
Palaquium	Model 1	18.78
	Model 2	13.72
	Model 3	16.86
	Brown (1997)	43.94
	Chave *et al*. (2005)	54.13
	Ketterings *et al*. (2001)	50.71
Shorea	Model 1	20.49
	Model 2	18.60
	Model 3	19.14
	Brown (1997)	107.16
	Chave et al. (2005)	94.44
	Ketterings *et al*. (2001)	32.15
Commercial species	Model 1	21.61
	Model 2	18.63
	Model 3	18.77
	Brown (1997)	66.77
	Chave *et al*. (2005)	73.85
	Ketterings *et al*. (2001)	44.02
Mixed species	Model 1	30.32
	Model 2	27.49
	Model 3	26.51
	Brown (1997)	51.95
	Chave *et al*. (2005)	55.09
	Ketterings *et al*. (2001)	51.89

Note: *) $\overline{S}(\%) = \frac{100}{n} \sum_{i=1}^{n} | \hat{Y}i - Yi | / Y_i$, $\overline{S}$ = average deviation,

Y_i = observed values, = $\hat{Y}_i$ predicted values

When the equations of Chave *et al*. (2005) and Brown (1997) were applied to our data, the predicted values were over estimated. By contrast, the model of Ketterings *et al*. (2001) underestimated the AGB. This evident can be seen from the CI values presented in Table 2.4. At 95 % CI, upper and lower limit of the mean AGB from the model of Brown (1997) and Chave *et al*. (2005) were higher than the observed values. In addition, paired t-test presented in Table 2.5 shows that for one tailed at α=0.05, the mean of the observed data and the proposed models is significantly different from the predicted mean using the previously published models. Figure 2.5 shows the observed values and the prediction line using model 1, model of Brown (1997) and Ketterings *et al*. (2001).

Table 2.4: Confidence interval (CI) of the mean from various models for mixed species (122 trees)

Parameters	Observed	Model 1	Model 2	Model 3	Brown	Chave	Ketterings
Mean AGB (kg)	2284.21	2416.69	2280.74	2458.60	3832.45	4180.43	1239.39
95% CI Lower limit of mean AGB (kg)	1376.51	1456.35	1526.76	1570.11	2297.53	2581.58	759.25
95% CI Upper limit of mean AGB (kg)	3191.90	3377.35	3034.73	3347.09	5367.38	5779.27	1719.25
The number of trees	122	122	122	122	122	122	122

Table 2.5: Paired t-test at 95 % confidence interval of the mean of the above-ground biomass (kg) for mixed species (122 trees).

Pair	t-statistic	Sig. (one tailed)
Observed-model of Brown (1997)	-4.184	0.000
Observed-model of Chave *et al.*.(2005)	-4.849	0.000
Observed-model of Ketterings *et al*. (2001)	4.330	0.000
Model 1-model 2	2.575	0.006
Model 1-model 3	-0.921	0.179
Model 1-model of Brown (1997)	-3.978	0.000
Model 1-model of Chave et al. (2005)	-4.346	0.000
Model 1-model of Ketterings et al. (2001)	6.669	0.000

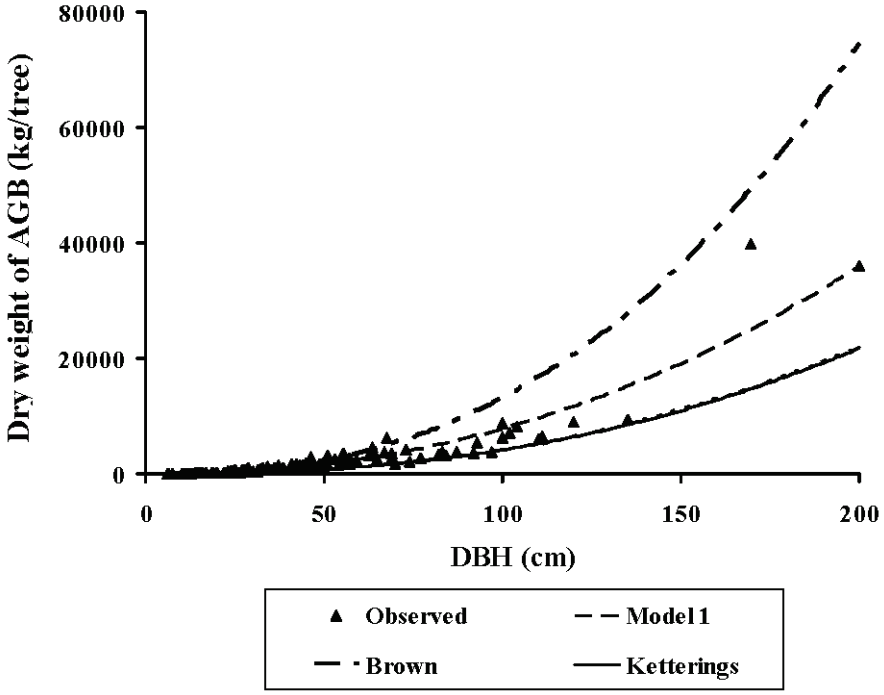

Figure 2.5: Diameter at breast height (DBH) versus dry weight of the above-ground biomass (AGB) for the mixed species (122 sample trees) from the observed data and the prediction lines using model 1, model of Brown (1997) and Ketterings *et al*. (2001).

2.4 Discussion

2.4.1 Allometric equations

When the first and the second data sets were used to generate the equations for mixed species, the deviations of the predicted biomass was higher than the observed one. This is due to the higher variation in tree characteristics among those species and genera between the first and the second data set. Based on the raw data, it can be observed that the second data set for the DBH of 6, 36, and 68 cm has dry weights of 19, 1100, and 6300 kg biomass, respectively, whereas for the first data set at those diameters the biomass is 10 to 14, 900, and 3800 kg, respectively. These results are in agreement with the research of Nelson *et al*. (1999) who found that by using the same allometric equation with DBH as the independent variable, the deviation in species-specific regressions varies from 10.9 to 14.7% for trees with the diameters from 5.1 to 38.2 cm, but if these species were mixed, the average deviation was 19.8%.

In the equation based on the individual genus, *Hopea* has the lowest average deviation, because the sample of this genus only consists of 3 species. On the other hand, within the *Shorea* group, the average deviation is the highest because it consists of 10 species and the diameter range is wider (6.5 to 200 cm).

At the genus level for model 2, the lower significance level of β when compared to the α coefficient may be caused by the effect of multicollinearity. In a multiple linear regression, multicollinearity causes partial regression coefficients for one or both independent variables to be less precise, and t-values to become less significant (Nelson et al, 1999). In the current data, the tolerance values for every genus and mixed species do not indicate multicollinearity. However, based on Pearson correlations between DBH and CBH, it shows a fair correlation for every genus, except *Palaquium*. So, this correlation induces multicollinearity in model 2, but the multicollinearity is weak because the β coefficient is still significant at $p<0.05$, except for *Shorea*. Multicollinearity disappears for the allometric equations of commercial and mixed species, because these equations were constructed from a larger number of samples where some of them have weak multicollinearity and the others do not indicate multicollinearity at all.

The role of wood density in the allometric equation is more prominent for the mixed species than in the genera. As presented in Table 2.1, the β coefficients of commercial and mixed species equations are significant at the 95 % CI. The evidence that the variation of wood density among the genera is higher than within a single genus is also supported by Baker *et al*. (2004) and Chave *et al*. (2006).

The importance of including wood density in biomass estimation can be examined for big trees, such as *Shorea superba* and *Shorea sp*. The *S. superba* with a diameter of 170 cm has a AGB dry weight of 39.7 tons, whereas the other (*Shorea sp*) with a diameter of 200 cm has a lower dry weight of AGB, that is 36 tons. It is likely that the differences in wood density and tree architecture explain the differences in the dry weight of these two species. Although *S. superba* has smaller DBH and shorter CBH, it has higher wood density compared to that of *Shorea sp*, resulting in the same dry weight of commercial bole (27.8 ton). The characteristics of these species show that their wood density, DBH and CBH are 0.86 g/cm^3, 170 cm and 26 m for *S. superba*,

and for *Shorea sp*., they are 0.57 g/cm^3, 200 cm, and 28 m, respectively. In this research, the genus of *Shorea* consists of several big trees, however, adding wood density to the model does not significantly influence β coefficient (Table 2.1).

The measurements of wood density of different species from the lowland *Dipterocarp* forests can be useful to complement the proposed methodology for estimating carbon stock change. In addition, for several of the species reported here no wood density values have previously been published. In the GPG, only a single value for wood density is given for certain species (see Appendix 3A.1. of GPG). With respect to the GPG methodology for estimating carbon stock change, the major source of uncertainty for estimating carbon stock using the default method is related to the applicability of these parameters for the diverse age and composition structure of specific stands (IPCC, 2003). Thus, the various values of wood density from different characteristics of forests must be considered. As an example, in this study the wood density of *Dipterocarpus grandiflorus* is 0.56 g/cm^3 for a DBH of 18.8 cm and 0.75 g/cm^3 for a DBH of 44 cm (Appendix 2.1), while in the GPG the wood density of this species is 0.62 g/cm^3, without any indication of the diameter.

2.4.2 Fitting and applicability of the models

Even though most AIC values of model 3 are lower than model 2 (Table 2.2), the values are relatively the same. Therefore for fitting the models, the emphasis will be given more on the coefficient of the regression, average deviation, the range of CI, and paired t-test. Of the proposed models, model 1 gives a better prediction than model 2. This can be observed from the inclusion of CBH into the model. It increases R^2 slightly and the average deviation decreases slightly, but the slope less significant and the standard error of α coefficient also increases. Based on the lower and upper limit CI of the mixed species, model 1 is closer to the range of the mean of the observed values (Table 2.4). In contrast, the upper and lower limit of CI of model 2 does not reach the range of CI of the observed values. For the mixed species, model 1 is significantly different from model 2 (Table 2.5). Model 1 is therefore the preferred model for estimating the AGB of *Dipterocarp* forests.

Within the genus, model 3 does not give effect over model 1 since β coefficient does not significantly influence the model (Table 2.1). However, adding wood density as a predictor is an alternative to estimate the biomass of big trees and

mixed species. The β coefficient is significant when wood density is incorporated into mixed species and the average deviation decreases. The effect of wood density to the dry weight is evident for big trees from the current data set as explained previously and from the different data set of Brown as explained in the next paragraph.

A possible explanation for high deviation for the model of Brown and Chave *et al*. (2005) is the difference in wood density and tree architecture. Although, some of Brown's and Chave's data were collected in Kalimantan, it does not imply that the characteristics of the trees from Kalimantan, as used by Brown (1997) and Chave *et al* (2005), are the same as the trees used in this study. As can be seen from Brown's data, one of the trees from Kalimantan with the diameter of 130 cm had dry weight of 42.8 ton (Brown, 1997), whereas from the current research, *Shorea* sp with a diameter of 200 cm has dry weight of 36 ton. However, the prediction line of Ketterings' equation lies below the observed values and the prediction line of model 1 (Figure 2.5). This may be caused by the marked difference between the sampled trees in this study and Ketterings' data. The only species which are found both in Ketterings' data and this study are *Shorea* and *Alseodaphne,* sp. The lower prediction of Ketterings' equation is because the trees used to construct Ketterings' equation were much smaller than those from the current study, as elaborated in the previous section. In addition to the explanations above, the inclusion of wood density in assessing biomass carbon will reduce uncertainty due to the variation among differences of sites (Chave, *et al*. 2006 and Baker *et al*., 2004).

Based on the application of the proposed model and the previously published data, for accurate biomass estimation, one must consider site specific equations. This finding is supported by Cairns *et al*. (2003) and Nelson *et al*. (1999) when they apply a previously published equation to their data. Nelson *et al*. (1999) overestimated biomass prediction by 10 to 60% for trees with a DBH from 5 to 25 cm, and showed an even greater over estimation for trees with larger DBH. In contrast with these results, Chave *et al*. (2005) and Gibbs *et al*. (2007) stated that for tropical forests, local species-specific allometric equations are not needed; instead, generalized allometric relationships must be employed. Moreover, grouping species by broad forests types or ecological zones is highly more effective than generating allometric equations for local conditions or species-specific allometric equations, because the local equations will not improve accuracy significantly. However, based on the analysis of the 95 % CI

of the mean, the prediction using the pan-tropic allometric equation by Chave *et al*. (2005) showed that the lower limit of the prediction is much higher than the observed values (Table 2.4). The lower boundaries of the observed data, the prediction using model 1, and the prediction using pan-tropic model are 1376.5, 1456.3, and 2581.6, respectively. The average deviations of the lower limit CI of these two predictions from the observed data are 6 % and 87 %.

Paired t-test presented in Table 2.5 supports the CI discussed above. At 95 % CI, the mean of the observed and the proposed models are significantly lower than the mean of the models of Brown (1997) and Chave *et al*. (2005), but higher compared to that of Ketterings *et al*. (2001).

With regards to GPG (Appendix 4A.2), the developed model can be used to complement the existing equations by Brown which are used in GPG.

2.4.3 Sources of error

In developing the equations in this study several potential sources of errors could be identified:

- Wood density differs among the tree sections: it is higher at breast height than at the top of bole (Nogueira *et al*., 2005) and also higher at the base of the tree stem than that at the base of the living crown (Cordero and Kanninen, 2002). In the current study, the samples for wood density analysis were taken from the upper, middle and lower of the main trunk. However, these data were also used to estimate the weight of the big branches that were impossible to be weighed. This might cause over-estimation of the weight for individual trees.
- The number of species for developing the allometric equations may not be enough to represent the gamut of species present at the study areas. Based on the data collected by Bertault and Kadir (1998) in the undisturbed forest, the average of tree species was 182 per hectare.
- The majority of samples had a diameter of less than 120 cm; there were only 3 trees with a diameter of more than 120 cm, which were 135, 170 and 200 cm. Ideally, there should be several trees which have diameters between 135 cm and 200 cm for developing mixed species equation.

2.5 Conclusions

Model 1, $\ln(AGB) = c + \alpha \ln(DBH)$, is the most suitable allometric equation for *Dipterocarp* forests. The range of 95% CI of model 1 is closer to the observed

values, so it can be applied to studies of the carbon balance. This allometric equation can be used to improve and complement the GPG, especially for tropical forests that are dominated by *Dipterocarp* species. In addition, model 3 is an alternative model since wood density is an important factor for estimating the biomass for mixed species.

Diameter is the only explanatory variable in model 1, it is easy to measure and generally available in standard forest inventory. The inclusion of CBH into DBH as predictor variable does not improve the performance of model 1.

Based on the application of the proposed model to the previously published data and the application of the published equation to the current data, it can be concluded that the application of site specific equation must be considered.

Acknowledgements

We would like to express our appreciation to the anonymous reviewers for their constructive comments on the manuscript. This work is supported by a grant from the Netherlands Fellowship Programme (NFP) which is administered by the Netherlands Organization for International Cooperation in Higher Education (NUFFIC).

References

Araújo, T.M., Higuchi, N., de Carvalho Júnior, J.A., 1999. Comparison of formulae for biomass determination in a tropical rain forest site the state of Pará, Brazil. Forest Ecology and Management 177: 43-52.

Baker, T.R., Phillips, O.L., Malhi, Y., Almeida, S., Arroyo, L., Di Fiore, A., Killeen, T.J., Laurance, S.G., Laurance, W.F., Lewis, S.L., Lloyd, J., Monteagudo, A., Neill, D.A., Patiño, S., Pitman, N.C.A., Silva, N., Martínez, R.V., 2004. Variation in wood density determines spatial patterns in Amazonian forest biomass. Global Change Biology 10: 545-562.

Berau Forest Management Project (BFMP), 1999. The climatic and hydrology of Labanan concession. Ministry of Forestry, Jakarta.

Brand, G.J., Smith, W.B., 1985. Evaluating allometric shrub biomass equations fit to generated data. Can. Journal of Botany 63: 64-67.

Brown, S., 1997. Estimating biomass and biomass change of tropical forests: a primer. FAO. Forestry Paper 134. Rome, 87 pp.

Burnham, K.P., Anderson, D.R. 2002. Model selection and multimodel inference. A practical information-theoretic approach. 2nd ed. Springer Science+Business Media, Inc., New York.

Cairns, M.A., Olmsted, I., Granados, J., Argaez, J., 2003. Composition and aboveground tree biomass of a dry semi-evergreen forest on Mexico's Yucatan Peninsula. Forest Ecology and Management 186: 125-132.

Chambers, J.Q., dos Santos, J., Ribeiro, R.J., Higuchi, N., 2001. Tree damage, allometric relationship, and above-ground net primary production in central Amazon forest. Forest Ecology and Management 152: 73-84.

Chave, J., Andalo, A., Brown, S., Cairns, M.A., Chambers, J.Q., Eamus, D., Fölster, H., Fromard, F., Higuchi, N., Kira, T., Lescure, J.-P., Nelson, B.W., Ogawa, H., Puig, H., Riéra, B., Yamakura, T., 2005. Tree allometry and improved estimation of carbon stocks and balance in tropical forests. Oceologia 145: 87-99.

Chave, J., Muller-Landau, H.C., Baker, T.R., Easdale, T.A., Steege, H.T., Webb, C.O., 2006. Regional and phylogenetic variation of wood density across 2,456 Neotropical tree species. Ecological Applications 16, 56-2367.

Chave, J., Riéra, B., Dubois, M., 2001. Estimation of biomass in a Neotropical Forest of French Guiana: spatial and temporal variability. Journal of Tropical Ecology 17: 79-96.

Chiesi, M., Maselli, F., Bindi, M., Fibbi, L., Cherubini, P., Arlotta, E., Tirone, G., Matteucci, G., Seufert, G., 2005. Modelling carbon budget of Mediterranean forests using ground and remote sensing measurements. Agricultural and Forest Meteorology 136: 22-34.

Clark, D.A., Brown, S., Kicklighter, D.W., Chambers, J.Q., Thomlinson, J.R., Ni, J., Holland, E.A., 2001. Net primary production in tropical forests: An evaluation and synthesis of existing field data. Ecological Application 11(2): 371-384.

Cordero, L.D., Kanninen, M., 2002. Wood specific gravity and above ground biomass of *Bombacopsis quinata* plantation in Costa Rica. Forest Ecology and Management 165: 1-9.

De Gier, A., 2003. A new approach to woody biomass assessment in woodlands and shrublands. In: P. Roy (*Ed*), Geoinformatics for Tropical Ecosystems, India, p. 161-198.

FAO, 2004. National forest inventory: Field manual template, Rome. http://www.fao.org /docrep/008/ae578e/ae578e00.htm (accessed on January 2, 2007).

Gibbs, H.K., Brown, S., Niles, J.O., Foley, J.A., 2007. Monitoring and estimating tropical forest carbon stocks: making REDD a reality. Environ.Res.Lett.2. doi:10.1088/1748-9326/4/045023.

Gunawan, A., Rathert, G., 1999. Monitoring, data management and analysis of the BFMP permanent sample plots (STREK plots) at Berau. Berau Forest Management Project. European Union- Ministry of Forestry and Estate Crops, Jakarta.

Hashimotio T., Kojima K., Tange T., Sasaki S., 2000. Changes in carbon storage in fallow forests in the tropical lowlands of Borneo. Forest Ecology and Management 126: 331-337.

Intergovernmental Panel on Climate Change (IPCC). 2003. Good practice guidance for land use, land-use change and forestry (GPG-LULUCF). Edited by Penman, J., Gystarsky, M., Hiraishi, T., Krug, T., Kruger, D., Pipatti, R., Buendia, L., Miwa, K., Ngara, T., Tanabe, K., Wagner, F. IPCC National Greenhouse Gas Inventories Programme.

Keeler, M., Palace, M., Hurtt, G., 2001. Biomass estimation in the Tapajos National Forest, Brazil examination of sampling and allometric uncertainties. Forest Ecology and Management 154: 371-382.

Ketterings, Q.M., Coe, R., van Noordwijk, M., Ambagau, Y., Palm, C.A., 2001. Reducing uncertainty in the use of allometric biomass equations for predicting above-ground tree biomass in mixed secondary forests. Forest Ecology and Management 146: 199-209.

Mantel, S., 1999. Development of environmental framework: Soils and terrain conditions of Labanan. Summary Report. Berau Forest Management Project. European Union- Ministry of Forestry and Estate Crops, Jakarta.

Myeong, S., Nowak, D.J., Duggin, M.J., 2006. A temporal analysis of urban forest carbon storage using remote sensing. Remote sensing of Environment 101: 277-282.

Nelson, B.W., Mesquita, R., Pereira, J.L.G., de Souza, S.G.A., Batista, G.T., Couta, L.B., 1999. Allometric regressions for improved estimate of secondary forest biomass in the Central Amazon. Forest Ecology and Management 117: 149-167.

Nogueira, E.M., Fearnside, P.M., Nelson, B.W., França, M.B., 2007. Wood density in forests of Brazil's 'arc of deforestation': Implications for biomass and flux of carbon from land-use change in Amazonia. Forest Ecology and Management 248: 119-135.

Nogueira, E.M., Nelson, B.W., Fearnside, P.M., 2005. Wood density in dense forest in central Amazonia, Brazil. Forest Ecology and Management 208: 261-286.

Sah, J.P., Ross, M.S., Kaptur, S., Snyder, J.R., 2004. Estimating aboveground biomass of broadleaved woody plants in the understory of Florida Keys Pine forests. Forest Ecology and Management 203: 319-329.

Samalca, I., 2007. Estimation of forest biomass and its error: A case in Kalimantan, Indonesia. MSc thesis: ITC, Enschede, 74 p.

Sist, P., Saridan, A., 1998. Description of the primary lowland forest of Berau. *In*: Bertault, J-G., Kadir, K. (*eds.*), Silvicultural research in a lowland mixed Dipterocarp forest of East Kalimantan, 51 - 73. CIRAD-forêt, FORDA, PT Inhutani I, Jakarta.

Soerianegara, I., Lemmens, R.H.M.J., (Eds.), 1993. Plant Resources of South-East Asia (PROSEA). Timber trees: Major commercial timbers, 5 (1). Pudoc Scientific Pub. Wageningen.

Sokal, R.R., Rohlf, F.J., 1995. Biometry. The principles and practice of statistic in biological research. 3rd ed. W.H. Freeman and Co, New York.

Son, Y., Hwang, J.W., Kim, Z.S., Lee, W.K., J.S. Kim, J.S., 2001. Allometry and biomass of Korean pine (*Pinus koraiensis*) in Central Korea. Bioresource Technology 78: 251-255.

Sprugel, D.G., 1983. Correcting for bias in log-transformed allometric equations. Ecology 64 (1): 209-210.

Stewart, J.L., Dunsdon, A.J., Hellin, J.J., Hughes, C.E., 1992. Wood biomass estimation of Central American dry zone species. Tropical Forestry Papers 26. Oxford Forestry Institute, Department of Plant Sciences, Univ. of Oxford.

Tan, K., Piao, S., Peng, C., Fang, J., 2007. Satellite-based estimation of biomass carbon stocks for northeast China's forests between 1982 and 1999. Forest Ecology and Management 240: 114-121.

Tyrie, G., 1999. Ten years of tropical lowland rainforest research in Labanan, East Kalimantan the STREK plots. Berau Forest Management Project. European Union- Ministry of Forestry and Estate Crops, Jakarta.

UNFCCC (United Nations Framework Convention on Climate Change), 2008. Report of the Conference of the Parties on its thirteenth session, held in Bali from 3 to 15 December 2007. Addendum, Part 2. Document FCCC/CP/2007/6/Add.1. UNFCCC, Bonn, Germany.

Wang, H., Hall, C.A.S., Scatena, F.N., Fetcher, N., Wu, W., 2003. Modeling the Spatial and temporal variability in climate and primary productivity across

the Luquillo mountains, Puerto Rico. Forest Ecology and Management 179: 69-94.

Yamakura, T., Hagihara, A., Sukardjo, S., Ogawa, H., 1986. Above-ground biomass of tropical rainforest stands in Indonesian Borneo. Plant Ecology 68 (2): 71-82.

Appendix 2.1. The wood density of the current study and the published data

N.	Species	This research		GPG-LULUCF**)		PROSEA**)	
		Diameter (cm)	WD*) (g/cm^3)	Diameter (cm)	WD*) (g/cm^3)	Diameter (cm)	WD*) (g/cm^3)
1	*Dipterocarpus convertus*	11.5	0.52				
2	*D. crinitus*	83.0	0.65				0.740 - 1.070
3	*D. crinitus*	104.0	0.77				
4	*D. grandiflorus*	18.8	0.64		0.62		0.650 - 0.945
5	*D. grandiflorus*	44.0	0.75				
6	*D. grandiflorus*	49.5	0.62				
7	*D. humeratus*	14.0	0.54				0.730 - 0.800
8	*D. humeratus*	27.0	0.69				
9	*D. pacyphyllus*	34.0	0.70				
10	*D. pacyphyllus*	67.0	0.73				
11	*D. pacyphyllus*	69.0	0.70				
12	*D. pacyphyllus*	73.0	0.61				
13	*D. pacyphyllus*	93.0	0.74				
14	*D. pacyphyllus*	111.0	0.66				
15	*D. pacyphyllus*	120.0	0.66				
16	*D. pacyphyllus*	135.0	0.73				
17	*D. palmbanicus*	6.5	0.67				0.595 - 0.785
18	*D. palmbanicus*	11.8	0.78				
19	*D. palmbanicus*	19.8	0.65				
20	*D. palmbanicus*	23.5	0.70				
21	*Hopea cernua*	6.5	0.65				0.650 - 0.960
22	*H. cernua*	10.0	0.57				
23	*H. cernua*	11.8	0.49				
24	*H. cernua*	15.5	0.51				
25	*H. cernua*	17.0	0.67				
26	*H. cernua*	22.0	0.52				
27	*H. cernua*	23.0	0.64				
28	*H. cernua*	28.0	0.55				
29	*H. cernua*	31.5	0.55				
30	*H. cernua*	32.5	0.66				
31	*H. cernua*	34.0	0.54				
32	*H. cernua*	38.5	0.54				

Appendix 2.1 (*Continued*)

No	Species	This research		GPG-LULUCF**)		PROSEA**)	
		Diameter (cm)	WD*) (g/cm^3)	Diameter (cm)	WD*) (g/cm^3)	Diameter (cm)	WD*) (g/cm^3)
33	*H. cernua*	41.0	0.51				
34	*H. cernua*	45.0	0.77				
35	*H. cernua*	51.0	0.56				
36	*H. cernua*	57.0	0.53				
37	*H. cernua*	59.0	0.58				
38	*H. cernua*	64.0	0.51				
39	*H. dryobalanoides*	62.4	0.69				0.480-0.980
40	*H. mengrawan*	87.0	0.66				0.510 - 0.980
41	*Palaquium gutta*	10.0	0.50				0.610 - 0.910
42	*P. gutta*	19.0	0.65				
43	*P. gutta*	24.0	0.65				
44	*P. gutta*	28.6	0.76				
45	*P. gutta*	29.0	0.65				
46	*P. gutta*	30.0	0.61				
47	*P. gutta*	36.0	0.61				
48	*P. gutta*	40.5	0.65				
49	*P. gutta*	48.0	0.59				
50	*P. gutta*	50.0	0.43				
51	*P. gutta*	54.0	0.63				
52	*P. gutta*	55.0	0.53				
53	*P. gutta*	65.0	0.63				
54	*P. rostratum*	6.3	0.56				0.480-0.760
55	*P. rostratum*	15.8	0.58				
56	*P. rostratum*	25.0	0.62				
57	*P. rostratum*	45.0	0.67				
58	*Palaquium sp*	13.0	0.44				
59	*Palaquium sp*	74.0	0.38				
60	*Shorea agamii*	100.0	0.50				0.665
61	*S. atrinervosa*	50.0	0.60				0.770 - 1.110
62	*S. atrinervosa*	100.0	0.71				
63	*S. macroptera*	23.0.0	0.54				0.370 - 0.770
64	*S. macroptera*	45.0	0.48				
65	*S. parvifolia*	31.5	0.51				0.290 - 0.835
66	*S. parvifolia*	57.0	0.52				

Appendix 2.1. (*Continued*)

No.	Species	This research		GPG-LULUCF**)		PROSEA**)	
		Diameter (cm)	WD*) (g/cm^3)	Diameter (cm)	WD*) (g/cm^3)	Diameter (cm)	WD*) (g/cm^3)
67	*S. parvifolia*	102.0	0.61				
68	*S. parvifolia*	110.0	0.60				
69	*S. parvistipulata*	35.0	0.45				
70	*S. retusa*	26.5	0.50				
71	*S. retusa*	70.0	0.48				
72	*S. retusa*	77.0	0.61				
73	*S. retusa*	84.0	0.47				
74	*S. retusa*	92.0	0.50				
75	*S. retusa*	97.0	0.79				
76	*S. smithiana*	10.2	0.32				0.300 - 0.720
77	*Shorea sp.*	6.5	0.55				
78	*Shorea sp.*	12.5	0.39				
79	*Shorea sp.*	38.1	0.50				
80	*Shorea sp.*	43.0	0.54				
81	*Shorea sp.*	82.0	0.38				
82	*Shorea sp.*	200.0	0.57				
83	*S. superba*	170.0	0.86				0.695 - 1.095
	Shorea spp., balau group				0.70		
	Shorea spp., dark red meranti				0.55		
	Shorea spp., light red meranti				0.40		
	Shorea spp., white meranti				0.48		
	Shorea spp., yellow meranti				0.46		

Note: *) Wood density expressed as oven dry weight (g) per saturated volume (cm^3)
**) Published data

CHAPTER 3

THE POTENTIAL OF SPECTRAL MIXTURE ANALYSIS TO IMPROVE THE ESTIMATION ACCURACY OF TROPICAL FOREST BIOMASS*

* This chapter is based on:
Basuki, T.M., Skidmore, A.K., van Laake, P.E., van Duren, I., Hussin, Y.A., 2011. The potential of spectral mixture analysis to improve the estimation accuracy of tropical forest biomass. Geocarto International (online and in press). http://dx.doi.org/10.1080/10106049.211-634928.

Abstract

A main limitation of pixel-based vegetation indices or reflectance values for estimating above-ground biomass (AGB) is that they do not consider the mixed spectral components on the earth's surface covered by a pixel. In this research, we decomposed mixed reflectance in each pixel before developing models to achieve higher accuracy in estimation of AGB. Spectral mixture analysis was applied to decompose the mixed spectral components of Landsat-7 Enhance Thematic Mapper (ETM)+ imagery into fractional images. Afterwards, regression models were developed by integrating training data and fraction images. The results showed that the spectral mixture analysis improved the accuracy of biomass estimation of *Dipterocarp* forests. When applied to the independent validation data set, the model based on the vegetation fraction reduced 5 – 16 % the root mean square error compared to the models using a single band 4 or 5, multiple bands 4, 5, 7 and all non-thermal bands of Landsat ETM+.

3.1 Introduction

Accurate estimation of above-ground forest biomass, carbon stocks, and change in biomass is essential to monitor impacts of forest management and policies. These require good quality spatial baseline information. Remote sensing has proven to be an important tool in the assessment of above-ground biomass (AGB) at regional, national and global level (Brown, 2002; Patenaude *et al*., 2005; Rosenqvist *et al*., 2003, UNFCCC, 2009). The use of products from optical sensors, in combination with empirical models, is a commonly applied method to assess AGB. Using regression, a link may be made between spectral reflectance or vegetation indices and biomass (Foody *et al*., 2003; Lu *et al*., 2004; Okuda *et al*., 2004). The normalized difference vegetation index (NDVI) is the most frequently used compared to other vegetation indices (Lu *et al*., 2004). However, the results using this index for biophysical assessments in tropical forests are inconsistent. Accuracy depends on which specific biophysical parameters need to be quantified and the characteristics of the study areas (Lu *et al*., 2004). Some of previous researchers found that NDVI is significantly correlated with AGB (Gonzalez-Alonso *et al*., 2006; Zheng *et al*., 2007) while others found that it could not be applied to assess this parameter (Lu *et al*., 2004; Sader *et al*. 1989). These contradictory results can be attributed to saturation of the NDVI value at high biomass levels (Mutanga and Skidmore 2004; Okuda *et al*., 2004) as well as atmospheric contamination (Huete *et al*., 1994 and Xiao *et al*., 2003).

To improve assessments, several models based on spectral reflectance or vegetation indices have been developed and tested. Lu *et al*. (2004) integrated forest inventory data, six reflective TM bands, and several vegetation indices to estimate AGB. They concluded that for forest with a complex stand structure, band TM5 and linear transformed indices were strongly correlated with the AGB. Steininger (2000) studied relationships between spectral reflectance generated from Landsat Thematic Mapper data in tropical forests of Brazil and Bolivia. It was observed that spectral band 5 was the best estimator for AGB in these Brazilian forests. However, it was restricted to dry weight biomasses estimates less than 150 ton/ha only.

The Enhanced Vegetation Index (EVI) was developed to reduce atmospheric influences and improve signal sensitivity in high biomass regions (Huete *et al*., 1997) while the Global Environmental Monitoring Index (GEMI) was designed to minimize atmospheric and soil effects (McDonald *et al*., 1998; Pinty and

Verstraete, 1992). The latter index partially reduced background reflectance under sparse vegetation cover (McDonald *et al*., 1998). Modified Soil Adjusted Vegetation Index (MSAVI) and near infrared reflectance were also useful to retrieve biophysical parameters. Zheng *et al*. (2004) examined that MSAVI and infrared reflectance strongly correlated with AGB for pine forest. For lowland mixed *Dipterocarp* forests, however, the use of remote sensing based methods to estimate AGB or forest stand parameters highly varied in their results. Nssoko, (2007) and Okuda *et al*. (2004) found very low correlation between AGB and Landsat reflectance values, NDVI; and EVI. In contrast to Nssoko (2007) and Okuda *et al*. (2004), Foody *et al*. (2003) obtained a relatively good coefficient of determination (R^2 = 0.69) when neural network was applied to predict AGB. In addition, Tangki and Chappell (2008) reported that average radiance in band 4 of Landsat-5 TM highly correlated (R^2 = 0.76) with AGB in the Ulu Segama Forest Reserve in Sabah, Malaysia, part of Borneo Island. But, the model used by Tangki and Chappell (2008) was not validated, which means that the applicability of the model for other areas is uncertain. Consequently, we have to look for a method to fill in this knowledge gap.

One of the limitations in estimating AGB using vegetation indices is that a signal recorded by a sensor in one pixel is in fact a spectral mixture of radiance or reflectance of all components on the earth's surface covered by that pixel. In spectral mixture analysis, each pixel is considered as a combination of multiple components weighted by relative surface abundance (Tompskins, *et al*., 1997). This enables us to model an image as a linear mixture of a few basic pure spectral components known as endmembers (Adams and Gillespie 2006; Small, 2004; Tompskins *et al*., 1997). Spectral mixture analysis has been used to determine and map urban vegetation abundances (Powell *et al*., 2007; Pu *et al*., 2008; Small, 2001; 2003; 2005; Small and Lu, 2006; Tooke *et al*., 2009). It was also applied for long term monitoring of cover types over large areas using medium resolution imagery (Hostert, *et al*., 2003 and Rogan *et al*, 2002), coarse resolution imagery (DeFries *et al*., 2000) as well as combining medium and coarse resolution images (Uenishi *et al*., 2005).

Related to vegetation analysis, spectral mixture analysis is commonly applied to study vegetation abundance outside tropical forests. In tropical forests, this method is mostly used to assess canopy damage in Amazon forests (Souza and Barreto, 2000; Souza *et al*. 2003; Souza *et al*., 2005). Souza *et al*. (2005) developed a normalized difference fraction index (NDFI). They combined it

with a contextual classification algorithm to map canopy damage derived from logging, fires and other disturbances. This integrated method was successfully applied with an overall accuracy of 90.4 %. In addition, Lu *et al*. (2003) used spectral mixture analysis in tropical forests for classifying successional and mature forests. It was observed that the spectral mixture analysis approach produced an overall classification accuracy of 78.2 % and resulted in a 7.4 % increase in accuracy, when compared to a maximum likelihood classification (Lu *et al*., 2003). Spectral mixture analysis is rarely applied for quantitative analysis in tropical forest. Lu *et al*. (2005) applied this method to estimate AGB in tropical forests. They found that spectral mixture analysis provided high relationship between the AGB and vegetation fraction in successional forest, but in the primary forest the correlation was very low.

Mixture of spectral components may be happen in a selectively logged forest. The gaps in the forest canopy resulting from selective logging are smaller than the pixel size of optical sensors such as Landsat or ASTER. This means that pixels represent a mix of forest canopy cover, bare soil, and other components that are found on the earth surface. Sist *et al*., (2003) studied the effect of conventional selective logging and reduced impact logging on canopy openness in *Dipterocarp* forests in East Kalimantan, Indonesia. Before logging, the mean canopy openness in conventional selective logging and reduced impact logging were 3.6 % and 3.1 %, respectively. After logging, it ranged from 17.5 to 20.7 % in conventional selective logging and 4 to 18 % in reduced impact logging. In the same areas, Vega (2005) found that felling a single tree in such forests created a gap fraction ranging from 30 to 100 % for pixels with a resolution of 15 m.

Having identified the lack of accurate AGB assessments and the potential of applying spectral mixture analysis for quantitative analysis in selectively logged tropical forests, this study aims to test the potential of spectral mixture analysis to improve the estimation accuracy of AGB in *Dipterocarp* forests. These forests cover extensive areas in tropical South-East Asia, so it is necessary to obtain a suitable method for estimating its biomass. The improvement of the accuracy of AGB estimation can be expected because spectral mixture analysis has potential to obtain the proportion of vegetation from mixture spectral components in the study area, and thus the main component for AGB estimation.

In developing the models based on spectral mixture analysis, all of non-thermal bands of Landsat-7 ETM+ were used. Therefore, as the comparison to the proposed models, we generated a multiple regression based on the spectral band 1, 2, 3, 4, 5, and 7 of the Landsat-7 ETM+. In addition, moisture vegetation indices, a single band and multiple bands 4, 5, and 7 of Landsat-7 ETM+ were used as the estimators for the AGB.

3.2 Materials and methods

3.2.1 Study area

The research was conducted in a forest concession managed by PT Hutan Sanggam Labanan Lestari in Berau Regency, East Kalimantan, Indonesia. The concession lies between 1°45' to 2°10' north latitude and between 116°55' to 117°20' east longitude, the situation map is illustrated in Figure 3.1.

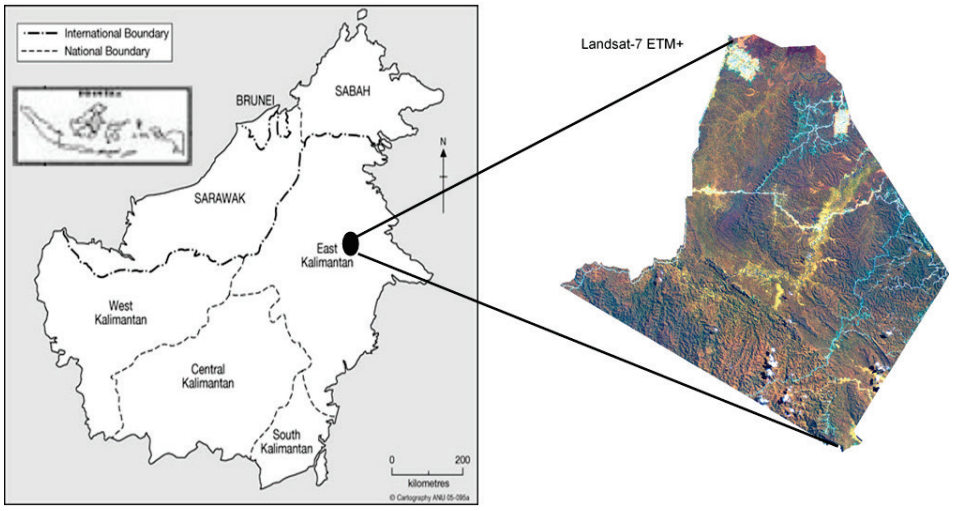

Figure 3.1: Location of the study area

The concession area is 83,240 ha. The forest type in the study area is called lowland mixed *Dipterocarp* forest. It is dominated by the family of *Dipterocarpaceae*. According to Sist and Saridan (1998), this family contributes about 25% of the total tree density, 50% of the total tree basal area and 60.2% of the stand volume. The second most abundant family is *Euphorbiaceae* comprising 13.5% of the total tree density and 9.1% of the basal area. Selective logging was applied for commercial timber harvesting from 1976 to 2003.

3.2.2 Image pre-processing

A Landsat-7 ETM+ image (path 117 and row 59) acquired in May 31, 2003 was used to generate spectral reflectance and moisture vegetation indices. Image pre-processing was conducted to minimize atmospheric, geometric and radiometric errors. Haze removal was applied to reduce atmospheric effects. Geometric correction of the image using a first order polynomial was carried out using 15 ground control points (GCPs) collected from the study area (Wijaya, 2005), resulting in a total root mean squared error (RMSE) less than a 0.5 pixel. The image was geo-rectified to the Universal Transverse Mercator (UTM) coordinate system with datum World Geodetic System (WGS) 1984 and zone 50 North and resampled to 32 m spatial resolution. Prior to derivation of the spectral indices and spectral mixture analysis, the digital numbers (DNs) of the image were converted to radiance and then to reflectance using an exoatmospheric model described by National Aeronautics and Space Administration (NASA) (2005).

3.2.3 Spectral mixture analysis

The formula for spectral mixture analysis used in this study (Tompkins *et al*., 1997) is:

$$R_b = \sum_{i=1}^{m} f_i r_{ib} + E_b \qquad (3.1)$$

where R_b is the reflectance of a pixel at band b, f_i is the fractional abundance of endmember i (from a total of m endmembers), r_{ib} is the reflectance at band b of endmember i, and E_b is the error in band b of the model fit.

The spectral mixture analysis was run using Environment for Visualizing Images (ENVI) 4.7 and Interactive Data Language (IDL) 7.1 software. To reduce noise, reflectance bands 1, 2, 3, 4, 5, and 7 of Landsat 7 ETM+ were transformed using minimum noise fraction. Afterwards, the minimum noise fraction image was analyzed to obtain the spectrally most pure pixel, using the pixel purity index (Boardman *et al*., 1995). The highest pixel purity index values were used to identify the location of sample endmembers on the original image (Souza *et. al*., 2005). The sample endmembers were also evaluated by their location on the extremes of the image feature space by assuming that these represent the purest pixels in the images (Lu *et al*., 2003; Lu *et al*., 2005). Endmember selection is a crucial step, since this determines the success of the spectral unmixing. Improper choice of endmembers will cause negative and

super positive (>1) fraction images. By prior knowledge of the study area and trial and error of endmember selection, it was found that for the study area the most suitable endmembers consisted of vegetation, soil and shade. Using the selected endmembers, spectral mixture analysis was applied resulting in the fraction images for vegetation, soil, shade, and error fractions. The fraction images were investigated to identify fraction overflow or fractions that had values less than 0 or more than 1. The spectral mixture analysis was run iteratively until a minimum fraction overflow was obtained. The number of pixel having fraction overflow was quantify using a developed script and run by ENVI-IDL software. The most suitable model with an average fraction overflow of 3% was used for further analysis. Water bodies, settlements, shrubs, and roads were masked because these features were not of interest in the study.

3.2.4 Spectral indices

Spectral indices including NDVI, Simple Ratio, Enhanced Vegetation Index, Advanced Vegetation Index, Soil Adjusted Vegetation Index, Modified Soil Adjusted Vegetation Index, Global Environmental Monitoring Index, and Atmospherically Resistant Vegetation Index have been applied for AGB assessment in the study area previously (Nssoko, 2007; Wijaya *et al*., 2009). In the current research, two single bands (band 4, 5) and the moisture vegetation indices based on the combination of reflectance band 4 and 5 (MVI5) and the combination of reflectance band 4 and 7 (MVI7) were applied. The single bands and indices were chosen because these had a better performance for biophysical estimations in other tropical forests (Freitas *et al*., 2005; Lu *et al*., 2004; Steininger, 2000; Tangki and Chappell, 2008). The formulas for moisture vegetation indices of MVI5 and MVI7 as follows:

$$MVI5 = (NIR - MIR5)/(NIR + MIR5) \quad (3.2)$$

$$MV17 = (NIR - MIR7)/(NIR + MIR7) \quad (3.3)$$

where MVI5= Moisture Vegetation Index band 4 and 5
MVI7=Moisture Vegetation Index band 4 and 7
NIR =Near Infrared Reflectance (band 4) of Lansat-7 ETM+,
MIR5 =Middle Infrared of band 5 Landsat-7 ETM+,
MIR7 =Middle Infrared of band 7 Landsat-7 ETM+

In addition, multiple linear regression models were developed using all bands of Landsat-7 ETM+ (band 1 to 5, and 7) and also from the first three bands which have the highest correlation with the AGB. These multiple bands have not been applied for the current study area.

3.2.5 Estimation of reference above-ground biomass

The fieldwork was conducted from May to June 2006. Seventy seven (77) random sampling plots were identified based on a Landsat-7 ETM+ (May 31, 2003). The plots were divided randomly into two groups, 50 plots were used for developing models and 27 plots for validations. The location of the plots distributed from flat on swampy areas and near rivers to undulating and hilly regions. The terrain had flat to steep slopes. The protected forests were located on hilly areas with steep slopes. The coordinates of the plots were recorded using Global Positioning System (GPS).

A circular plot with the size of 500 m^2 was used. A slope correction was applied in case the plot was located on a slope. The radius of the circle ranged from 12.62 m to 15.78 m. Within each of 77 plots, tree diameters equal or greater than 10 cm were measured using a meter tape at breast height (DBH). In this study, woody plants which have DBH equal to or greater than 10 cm are defined as trees (Lu *et al*., 2005). The AGB in this paper is restricted to the above-ground of the trees which have DBH ≥ 10 cm.

The AGB was estimated using a local allometric equation developed by Basuki *et al*. (2009). This equation was developed using a regression analysis of 122 trees with diameters ranging from 5 to 200 cm and consisting of 48 species. The equation to estimate AGB was:

$$\ln(AGB) = 2.196*\ln(DBH) - 1.201 \quad (3.4)$$

where: AGB is above-ground biomass in dry weight (kg/tree) and DBH is in cm. The adjusted R^2 of the model is 0.963. The AGB was obtained by de-transforming ln(AGB) values. The descriptive statistics of the AGB of the sampling plots for the training and validation data are presented in Table 3.1.

Table 3.1: Descriptive statistics of the above-ground biomass (ton/ha) for the training (50 plots) and the validation (27 plots) data.

Above-ground biomass (ton/ha)	Training samples (50 plots)	Validation samples (27 plots)
Minimum	102.62	102.26
Mean	343.79	329.20
Maximum	839.32	812.15
Standard deviation	156.61	191.98

3.2.6 Statistical analysis

Prior to development models, Pearson correlation coefficient was used to evaluate the strength of linear correlation between two variables. Multiple and simple linear regressions were employed to establish relationships between AGB and the independents variables. The independent variables consisted of spectral band 4; band 5; band 4, 5, 7; band 1, 2, 3, 4, 5, 7; MVI5, MVI7 and the vegetation, soil, and shade values generated from the fraction images. The values of the independent variables were calculated as the average of a 3 by 3 pixel window (Lu *et al*., 2004). Multicollinearity was inspected for multiple linear regressions models. Variance inflation factor (Brauner and Shacham, 1998) was used to determine whether a model has multicollinearity between the independent variables. The most suitable model for estimating the AGB was selected based on the value of coefficient determination (R^2) of the regression (Lu *et al*., 2005) and for the model which minimized the root mean square error (RMSE) of the validation data.

3.3 Results

3.3.1 Fraction images

The fraction images produced from the spectral mixture analysis highlight the heterogeneity of the forest cover in the study area (Figure 3.2). In the soil fraction image (Figure 3.2b), light grey areas where represent pixels with a high fraction of bare soil. On the fraction shade image (Figure 3.2c), unlogged forests have a darker colour indicating a lower fraction of shade compared to logged over forests.

3.3.2 Remote sensing based estimation of above-ground biomass

Table 3.2 shows the Pearson correlation between fraction images, spectral reflectance of Landsat-7 ETM+ and the AGB. It can be seen that vegetation and

shade fraction have strong Pearson correlation with the AGB. For the Landsat-7 ETM+, band 4 has the highest correlation with the AGB followed by band 5 and 7. Therefore, these three bands together were also used to generate multiple linear regressions to predict the AGB.

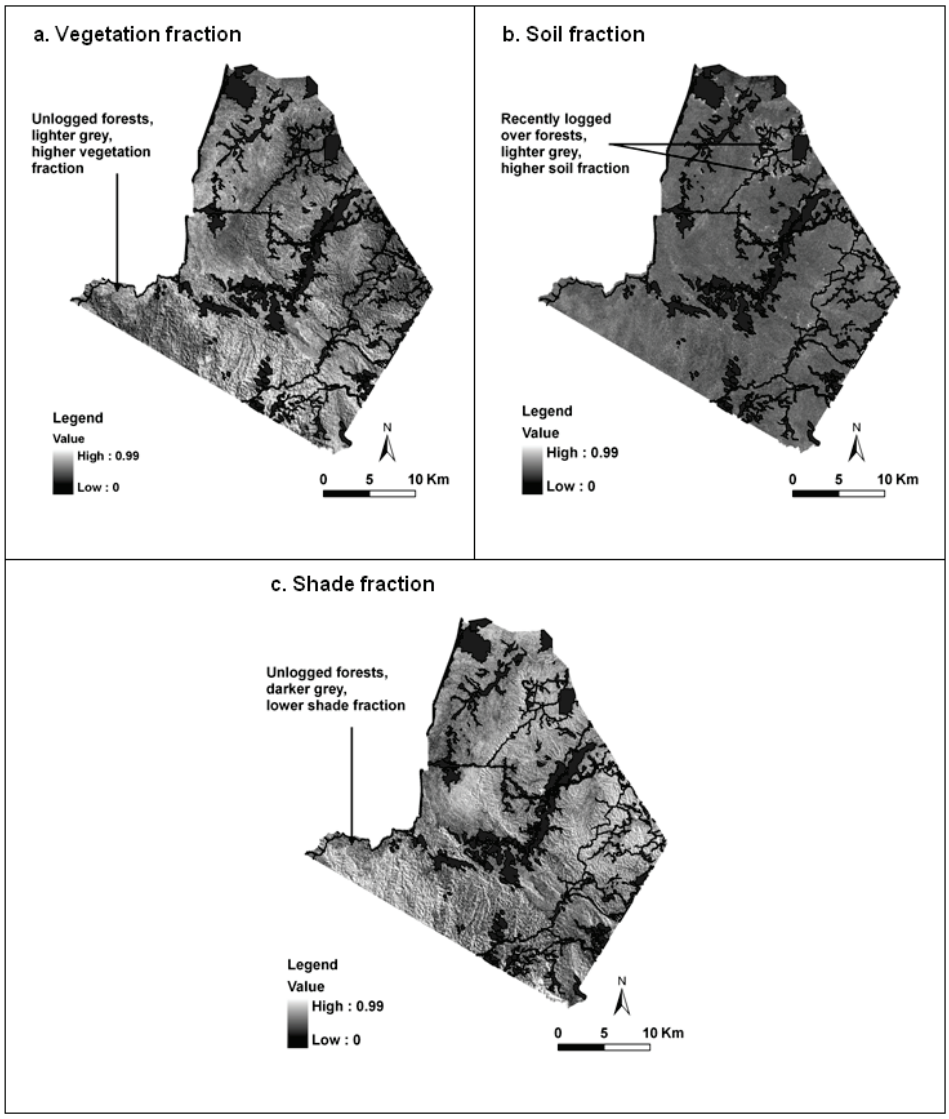

Figure 3.2: Fraction endmembers of Landsat-7 ETM+ produced by spectral mixture analysis, vegetation (a), soil (b), and shade (c).

Table 3.2: Pearson correlation at 95 % confidence interval between the above-ground biomass (ton/ha) and the fraction endmembers or spectral reflectance of Landsat-7 ETM+ for 50 sample plots.

Fraction endmembers			Landsat-7 ETM+		
Fraction	Pearson correlation	p-value	Band	Pearson correlation	p-value
Vegetation	0.800	0.000	1	0.205	0.076^{ns}
Soil	-0.312	0.014	2	0.231	0.053 ^{ns}
Shade	-0.756	0.000	3	-0.097	0.252 ^{ns}
			4	0.757	0.000
			5	0.564	0.000
			7	0.369	0.040

The statistical analysis of the regression models and the independent validation are provided in Table 3.3. The model estimators based on the vegetation indices and a single band or band combination of the Landsat-7 ETM+ provides coefficient determination less than 0.6 (Table 3.3). Among these estimators, the use all non-thermal bands (band 1 – 5, and 7) produces the highest R^2, and the lowest are found for moisture vegetation indices.

Compared to the estimators of band 4, band 5, and non-thermal band of Landsat-7 ETM+ as well as moisture vegetation indices, the models based on the fraction images improve the R^2 of the regression models and reduced the RMSE of the validation data as presented in Table 3.3. In this case, the multiple linear regressions based on the vegetation and soil fractions and the simple linear regression of the vegetation fraction have a similar coefficient of determination. When all the fraction images were employed to predict AGB, multicollinearity occurred between the vegetation and the shade fraction, therefore the shade fraction was not applied to develop the models.

To test the applicability of the proposed regression models, validation was conducted using independent data from 27 plots and the results are also provided in Table 3.3. The validation was conducted for each regression model, except for MVI5 and MVI7 because these vegetation indices have low correlation with the AGB. Among the regression models, the proposed model developed from the vegetation fraction has the lowest RMSE value of the validation data. The scatter plots of the measured and the predicted AGB using independent data are illustrated in Figure 3.3.

Table 3.3: Linear regression between remote sensing based vegetation and soil fractions or the spectral reflectance of Landsat-7 ETM+ and the above-ground biomass (ton/ha) using the training data (50 plots) and the RMSE value of the independent validation data (27 plots).

Independent variable	Regression model			Validation
	Equation	Adjusted R^2	Significance level of p-value	RMSE (ton/ha)
Vegetation fraction	AGB = -258.055 + 1350.342*veg	0.632	0.000	130.4
Vegetation and soil fractions	AGB = -200.793 +1303.543*veg – 723.260*soil	0.635	0.000	133.4
Reflectance band 4	AGB = -1663.499 + 8461.377*ref4	0.565	0.000	137.8
Reflectance band 5	AGB = -1075.753 + 14811.499*ref5	0.304	0..000	155.5
Reflectance band 4, 5, 7	AGB = -1658.158 + 8058.407*ref4 + 2778.176*ref5 – 5691.019*ref7	0.548	0.000	137.5
Reflectance band 1, 2, 3, 4, 5, 7	AGB = -1272.352 + 3766.575*ref1 + 8502.767*ref2 – 33838.339*ref3 + 7325.874*ref4 + 5086.444*ref5 – 4270.166*ref7	0.582	0.000	144.0
MVI5	AGB = - 390.551 + 1729.827*MVI5	0.021	0.160^{ns}	-
MVI7	AGB = -1779.172 + 2759.609*MVI7	0.041	0.085^{ns}	-

Note: AGB = above-ground biomass, RMSE = root mean square error, veg = vegetation, ref = reflectance, MVI5 = moisture vegetation index derived from reflectance of band 4 and 5, MVI7= moisture vegetation index derived from reflectance of band 4 and 7

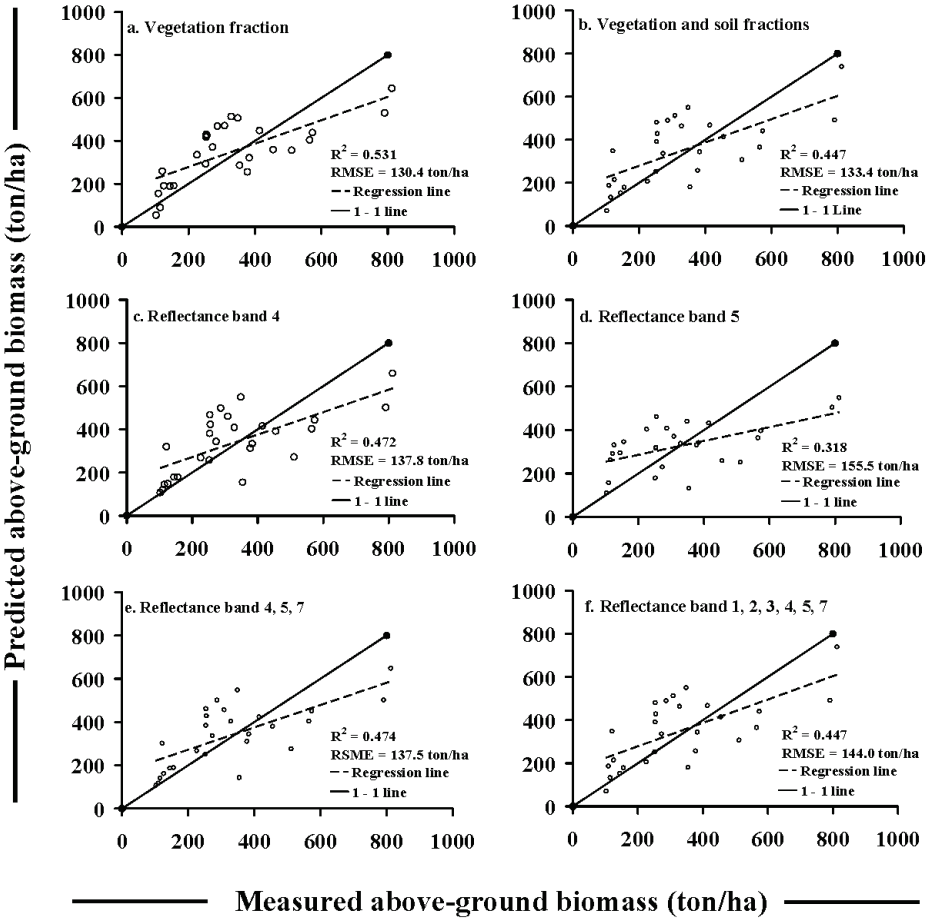

Figure 3.3: Scatter plots of the measured and the predicted values of above-ground biomass (ton/ha) using different independent variables applied to the validation data set. The measured above-ground biomass was the result of applying an allometric equation. The predicted values were calculated using regression models including vegetation fraction (a), vegetation and soil fractions (b), reflectance of Landsat-7 ETM+ band 4 (c), band 5 (d), band 4, 5, 7 (e), and band 1, 2, 3, 4, 5, and 7 (f).

3.4 Discussion

The proposed models based on the fraction images have a higher adjusted R^2 compared to the moisture vegetation indices and the simple and multiple regression models of the Landsat-7 ETM+ bands. This indicates the importance of decomposing spectral reflectance of pixels in medium resolution images such as Landsat-7 ETM+ into fractions of vegetation, soil and shade. The decomposition is essential to obtain the proportion of the vegetation within the mixed components since this is the variable ultimately needed to estimate the

AGB. Besides this, separation of shade from the vegetation is needed because in a complex forest structure, canopy shading is an important aspect influencing vegetation reflectance captured by a sensor, and consequently it could affect biomass estimation (Asner and Warner, 2003; Steininger, 2000).

The decomposition of mixed endmembers is useful for qualitative as well as quantitative analysis. Visual interpretation of fraction images helps to differentiate newly harvested areas from primary or mature forests. This phenomenon supports previous research undertaken by Lu *et al*. (2003) in Amazonian tropical forests. They applied spectral mixture analysis and concluded that secondary succession forests could be discriminated from mature forests due to different proportion of vegetation, shade, and soil covered by a pixel. Besides that, Souza *et al*. (2005) found that intact forests had significantly higher green vegetation fractions than that of conventionally logged forests, as well as logged and burned forests.

The models explain 63 % of the variation of the AGB. This coefficient of determination is lower than that obtained by Lu *et al*. (2005) in the successional forests in Brazil. In the successional forests, Lu *et al.* (2005) found that their regression model derived from a vegetation fraction image produced a coefficient of determination of around 0.80. In the primary forest the shade fraction image only explained less than 20 % of the variation of AGB. Possible reasons for the different results in the current study and the research conducted by Lu *et al*. (2005) are the differences in the forest stand structures and thus the determination of the endmembers which is site specific. The training data to develop our models consist of sample plots from the successional and primary forests, whereas Lu *et al* (2005) developed the regression model separately from the successional and primary forest.

The proposed models are a major improvement compared to the conventional models. They have a higher coefficient of determination compared to the previous study conducted by Wijaya *et al*. (2010) at the same study area. In the current study, the fraction images explained 63 % of the variation in the AGB. By contrast, Wijaya *et al*. (2010) found that the coefficient of determination between AGB with the common spectral indices e.g. SR, NDVI, EVI, ARVI, SAVI, GEMI, Tasseled caps and Grey Level Co-occurrence Matrix mean (GLCM_mean) was less than 0.296. The improved accuracy of AGB estimation using the fraction images is because in the spectral mixture analysis the

proportion of the vegetation, soil and shade has been determined before developing the regression models. Further analysis of the data revealed that the models based on fraction images reduced the RMSE compared to a single or multiple bands spectral reflectance of Landsat-7 ETM+ when applied to the independent validation data set (Table 3.3). Based on this solid analysis we can conclude that breaking down images into vegetation fraction images provides the best predictor for biomass and therefore this methodology should be used in similar studies.

The use of all bands (1 to 5, and 7) of the Landsat-7 ETM+ produces a higher R^2 value of the regression model compared to band 4 and combination of band 4, 5, and 7. However, the improvement is not significant because the Pearson correlation between the visible bands and the AGB is low (Table 3.2).

The results of using single bands (e.g. band 4 or 5) for the current forest area are different from the research undertaken by Steininger (2000) and Tangki and Chappell (2008). These could be caused by differences in forest stand structure and the amount of biomass. The regression model of Steininger (2000) was based on secondary forest with a maximum dry weight of AGB of 150 ton/ha. Steininger found a strong coefficient of determination (R^2 = 0.722) between AGB and TM band 5. In our study the maximum dry weight of the AGB was 839 ton/ha and originated from logged over and primary forests. Tangki and Chappell (2008) conducted their research in *Dipterocar*p forest, similar to our study area, but the maximum of AGB in their forest was only 500 ton/ha.

The results of using moisture vegetation indices as biomass estimators vary from one forest to another. In our forest area, these indices were not suitable to predict AGB. However, Boyd *et al*. (1999) and Lu *et al*. (2004) found a better correlation between moisture vegetation indices and biomass. Boyd *et al*. (1999) obtained R^2 of 0.22 when moisture vegetation index from near infra red and middle infra red of NOAA Advanced Very High Resolution Radiometer (AVHRR) was applied to estimate AGB in tropical forest in southern Cameroon. Lu *et al*. (2004) observed that moisture vegetation indices produced different correlation with AGB in Altamira, Bragantina and Penta de Pedras which are located in Brazilian Amazon. The moisture vegetation index of Landsat TM band 4 and 5 was used to estimate AGB with R^2 of 0.40, 0.18, and 0.19, respectively for Altamira, Bragantina and Penta de Pedras. The reason for these different results is because of variations in forests structure including tree

height, species composition, and the amount of biomass and vegetation vigour. These phenomena imply that application of vegetation indices or spectral signature of Landsat TM or ETM+ depends on the biophysical characteristics of the forests and is site specific.

Looking at the validation, the scatter plots of the models derived from fraction images produce similar patterns (Figure 3.3a and 3.3b). The model derived from reflectance of band 4 yields over estimation for the AGB less than 354 ton/ha (Figure 3.3c). The regression model of band 4, 5, 7 and the non-thermal band of Landsat-7 ETM+ show a similar pattern (Figure 3.3e and 3.3f). However, all the graphs show the increases of the measured AGB are followed by the increase of predicted ones until an AGB reaches around 400 ton/ha. After that point, the predicted values are lower than the measured ones. These phenomena are probably saturation effects, where the increase biomasses are not followed by the increase of predictor variables.

The spectral mixture analysis has potential to improve the accuracy of the AGB estimation compared to the common vegetation indices or spectral reflectance. However, this methodology needs expertise and careful selection of endmembers as this is the crucial step in the analysis. In determining endmembers, especially using pixel purity index, the process is interactive in comparison to spectral reflectance or vegetation indices that directly derived from the image. The proposed models can be applied to estimate AGB estimation up to 400 ton/ha, above this value the saturation problem may be presence.

In this research, only three endmembers are applied. Including non-photosynthetic vegetation such as branches and stems may be more appropriate for these forests. Additional non-photosynthetic vegetation endmembers have been successfully applied to map forest degradation (Souza *et al*., 2003) and to map canopy damage from selective logging and forest fires (Souza *et al*., 2005). For the forest in this study, however, determining such endmembers is difficult because the resulting fraction images were overflow having negative and super positive (>1) values.

3.5 Conclusions

Our findings demonstrate that spectral mixture analysis can increase the accuracy of AGB assessment for mixed *Dipterocarps* forests. The proposed

models based on the spectral mixture analysis explain 63 % of the variability the AGB. The proposed models improve the estimation accuracy of the AGB compared to more conventional models, such as spectral reflectance of band 4; band 5; band 4, 5, 7; non thermal band and moisture vegetation indices. Decomposing mixed spectral components into fractions of individual components is essential before developing the regression models in selective logging forests. Endmembers selection is a critical step in the methodology. The problem in dense forest with complex stand structure and very high biomass is that saturation in light absorption occurs, which cannot be solved by applying this technique.

Acknowledgements

We would like to thank the staffs of Labanan concession area, Bp. Ir. Dody Herika and his staffs for their assistance during field campaign; Willem Nieuwenhuis, ITC, for helping some scripts, Dr. Nichola M. Knox, ITC, for her assistance in proof reading. This research is supported by a grant from the Netherlands Organization for International Cooperation in Higher Education (NUFFIC).

References

Adams, J.B., Gillespie, A.R., 2006. Remote Sensing of Landscapes with Spectral Images. A Physical Modeling Approach. Cambridge Univ. Press, UK.

Asner, G.P., Warner, A.S., 2003. Canopy shadow in IKONOS satellite observations of tropical forests and savannas. Remote Sensing of Environment 87: 521-533.

Basuki, T.M., van Laake, P.E., Skidmore, A.K., Hussin, Y.A., 2009. Allometric equations for estimating the above-ground biomass in tropical lowland Dipterocarp forests. Forest Ecology and Management 257: 1684-1694.

Boardman, J. M., Kruse, F. A., Green, R. O., 1995. Mapping target signature via partial unmixing of AVIRIS data. Summaries of the Fifth JPL Airborne Earth Science Workshop. JPL Publication 95(1): 23–26.

Boyd, D. S., Foody, G.M., Curran, P.J., 1999. The relationship between the biomass of Cameroonian tropical forests and radiation reflected in middle infrared wavelengths (3.0 – 5.0 μm). Int. Journal of Remote Sensing 20: 1017 – 1023.

Brauner, N., Shacham, M., 1998. Identifying and removing sources of imprecision in polynomial regression. Mathematics and Computers Simulation 48: 75-91.

Brown, S., 2002, Measuring Carbon in Forests: Current Status and Future Challenges. Environmental Pollution 116: 363-372.

DeFries, R. S., Hansen, M. C., Townshend, J. R. G., 2000, Global continuous fields of vegetation characteristics: A linear mixture model applied to multi-year 8 km AVHRR data. Int. Journal of Remote Sensing 21: 1389 – 1414.

Foody, G.M., Boyd, D.S., Cutler, M.E.J., 2003, Predictive relations of tropical forest biomass from Landsat TM data and their transferability between region. Remote Sensing of Environment 85: 463-474.

Freitas, S.R., Mello, M.C.S., Cruz, C.B.M., 2005, Relationships between forest structure and vegetation indices in Atlantic rainforest. Forest Ecology and Management 218: 353-362.

González-Alonso, F., Merino-de-Miguel, S., Roldán-Zamarrón, A., Garcí-Gigorro, S., Cuevas, J.M., 2006. Forest biomass estimation through NDVI-composites. The role of remotely sensed data to assess Spanish forests as carbon sinks. Int. Journal of Remote Sensing 27 (24): 5409-5415.

Hoster, P., Röder, A., Hill, J., 2003. Coupling spectral unmixing and trend analysis for monitoring long-term vegetation dynamics in Mediterranean rangelands. Remote sensing of environment 87: 183-197.

Huete, A., Justice, C., Liu, H., 1994. Development of vegetation and soil indices for MODIS-EOS. Remote Sensing of Environment 49: 224-234.

Huete, A.R., Liu, H.Q., Batchily, K., van Leeuwen, W., 1997. A comparison of vegetation indices over a global set of TM images for EOS-MODIS. Remote Sensing of Environment 59: 440-451.

Lu, D., Moran, E., Batistella, M., 2003. Linear mixture model applied to Amazonian vegetation classification. Remote Sensing of Environment 87: 456-469.

Lu, D., Batistella, M., Moran, E., 2005. Satellite estimation of aboveground biomass and impacts of forest stand structure. Photogrammetric Engineering & Remote Sensing 71(8): 967-974.

Lu, D., Mausel, P., Brondízio, E., Moran, E., 2004. Relationship between forest stand parameters and Landsat TM spectral responses in the Brazilian Amazon Basin. Forest Ecology and Management 198: 149-167.

McDonald, A.J., Gemmell, F.M., Lewis, P.E., 1998. Investigation of the utility of spectral vegetation indices for determining information on coniferous forests. Remote Sensing of Environment 66: 250–272.

Mutanga, O., Skidmore, A.K., 2004. Hyperspectral band depth analysis for a better estimation of grass biomass (*Cenchrus ciliaris*) measured under controlled laboratory conditions. International Journal of Applied Earth Observation and Geoinformation 5: 87-96.

NASA., 2005. Landsat 7 science data users handbook (Online). Available at http://ltpwww.gsfc.nasa.gov/IAS/handbook/handbook_toc.html.

Nssoko, G.E., 2007. Sensitivity of spectral vegetation indices to trees biomass in tropical rainforests: a case of Labanan concession area, East Kalimantan, Indonesia. Unpublished MSc thesis: ITC, Enschede, 48pp.

Okuda, T., Suzukia, M., Numataa, S., Yoshidaa, K., Nishimuraa, S., Adachib, N., Niiyamac, K., Manokarand, N., Hashim, M., 2004. Estimation of aboveground biomass in logged and primary lowland rainforests using 3-D photogrammetric analysis. Forest Ecology and Management 203: 63-75.

Powell, R.B., Roberts, D.A., Dennison, P.E., Hess, L.L., 2007. Remote Sensing of Environment 106: 253-267.

Patenaude, G., Milne, R., Dawson, T.P., 2005. Synthesis of remote sensing approaches for forest carbon estimation: Reporting to the Kyoto Protocol. Environmental Science and Policy 8: 161-178.

Pinty, B., Verstraete, M. M., 1992. GEMI: a non-linear index to monitor global vegetation from satellites. Vegetatio 101: 15–20.

Pu, R., Gong, P., Michishita, R., Sasagawa, T., 2008. Spectral mixture analysis for mapping abundance of urban surface components from the Terra/ASTER data. Remote Sensing of Environment 112: 939-954.

Rogan, J., Franklin, J., Roberts, D. A., 2002. A comparison of methods for monitoring multi temporal vegetation change using Thematic Mapper imagery. Remote Sensing of Environment 80: 143-156.

Rosenqvist, Å., Milne, A., Lucas, R., Imhoff, M., Dobson, C., 2003. A review of remote sensing technology in support of the Kyoto Protocol. Environmental Science and Policy 6: 441-455.

Sader, S.A., Waide, R.B., Lawrence, W., Joyce, A.T., 1989. Tropical forest biomass and successional age class relationship to vegetation index derived from LANDSAT TM data. Remote Sensing Environment 28: 143–156.

Sist, P., Saridan, A., 1998. Description of the primary lowland forest of Berau. *In*: Bertault, J-G., Kadir, K. (*eds.*), Silvicultural research in a lowland

mixed Dipterocarp forest of East Kalimantan, 51 - 73. CIRAD-forêt, FORDA, PT Inhutani I, Jakarta.

Sist, P., Sheil, D., Kartawinata, K., Priyadi, H., 2003. Reduced-impact logging in Indonesian Borneo: some results confirming the need for new silvicultural prescriptions. Forest Ecology and Management 179: 415-427.Small, C., 2001. Estimation of urban vegetation abundance by spectral mixture analysis. Int.Journal of Remote Sensing 22(7): 1305-1334.

Small, C., 2003. High spatial resolution spectral mixture analysis of urban reflectance. Remote Sensing of Environment 88: 170-186.

Small, C., 2004. The Landsat ETM+ spectral mixing space. Remote Sensing of Environment 93: 1-17.

Small, C., 2005. A global analysis of urban reflectance. Int. Journal of Remote Sensing 26(4): 661-681.

Small, C., Lu, J. W.T., 2006. Estimation and vicarious validation of urban vegetation abundance by spectral mixture analysis. Remote Sensing of Environment 100: 441-456.

Souza Jr., C., Barreto, P., 2000. An alternative approach for detecting and monitoring selectively logged forests in the Amazon. Int. Journal of Remote Sensing 21(1): 173-179.

Souza Jr. C., Firestone, L., Silva, L.M., Roberts, D., 2003. Mapping forest degradation in the Eastern Amazon from SPOT 4 through spectral mixture models. Remote Sensing of Environment 87: 494-506.

Souza Jr., C.M., Roberts, D. A., Cocrane, M.A., 2005. Combining spectral and spatial information to map canopy damage from selective logging and forest fires. Remote Sensing of Environment 98: 329-343.

Steininger, M.K., 2000. Satellite estimation of tropical secondary forest above-ground biomass data from Brazil and Bolivia. Int. Journal of Remote Sensing 21(6&7): 1139-1157.

Tangki, H., Chappell, N.A., 2008. Biomass variation across selectively logged forest within a 225-km^2 region of Borneo and its prediction by Landsat TM. Forest Ecology and Management 256: 1960-1970.

Tompkins, S., Mustard, J.F., Pieters, C. M., Forsyth, D.W., 1997. Optimization of endmembers for spectral mixture analysis. Remote sensing of environment 59: 472-489.

Tooke, T.R., Coops, N.C., Goodwin, N.R., Voogt, J.A., 2009. Extracting urban vegetation characteristics using spectral mixture analysis and decision tree classifications. Remote Sensing of Environment 113: 398-407.

Uenishi, T.M., Oki, K., Omasa, K., Tamura, M., 2005. A land cover distribution composite image from coarse spatial images using an unmixing method. Int. Journal of Remote Sensing 26(5): 871-886.

UNFCCC., 2009. Cost of implementing methodologies and monitoring systems relating to estimates of emissions from deforestation and forest degradation, the assessment of carbon stocks and greenhouse gas emissions from changes in forest cover, and the enhancement of forest carbon stocks. Technical report.

Vega, B., 2005. Image fusion of optical and microwave data to assess criteria and indicator (C&I) related to forest encroachment, for certification process of Sustainable Forest Management (SFM). Unpublished MSc thesis: ITC, Enschede, 79 p.

Wijaya, A., 2005. Application of multi-stage classification to detect illegal logging with the use multi-source data: a case study in Labanan forest management unit, East Kalimantan, Indonesia. Unpublished MSc. thesis, ITC, Enschede, 64 p.

Wijaya, A., Kusnadi, S, Gloaguen, R., Heilmeir, H., 2010. Improved strategy for estimating stem volume and forest biomass using moderate resolution remote sensing data and GIS. Journal of Forestry Research 21(1): 1-12. DOI 10.1007/s11676-010-0001-7.

Xiao, X., Braswell, B., Zhang, Q., Boles, S., Frolking, S., and Moore III, B., 2003. Sensitivity of vegetation indices to atmospheric aerosols: continental-scale observations in Northern Asia. Remote Sensing of Environment 84: 385-392.

Zheng, D., Rademacher, J., Chen, J., Crow, T., Bresee, M., Le Moine, J., Ryu, S-R., 2004, Estimating aboveground biomass using Landsat 7 ETM^+ data across a managed landscape in northern Wisconsin, USA. Remote Sensing of Environment 93: 402-411.

Zheng, G., Chen, J.M., Tian, Q.J., Ju, W.M., Xia, X.Q., 2007, Combining remote sensing imagery and forest age inventory for biomass mapping. Journal of Environmental Management 85: 616-623.

CHAPTER 4

ESTIMATING TROPICAL FOREST BIOMASS MORE ACCURATELY BY INTEGRATING ALOS PALSAR AND LANDSAT-7 ETM+ DATA*

* This chapter is based on:

Basuki, T.M., Skidmore, A.K., Hussin, Y.A., van Duren, I., 2011. Estimating tropical forest biomass more accurately by integrating ALOS PALSAR and Landsat-7 ETM+ data. International Journal of Remote Sensing (resubmitted after revision).

Abstract

Integration of multisensor data provides the opportunity to explore benefits emanating from different data sources. A fusion between fraction images derived from spectral mixture analysis of Landsat-7 Enhance Thematic Mapper (ETM)+ and Phase Arrayed L-band Synthetic Aperture Radar (PALSAR) is introduced. The aim of this fusion is to improve the estimation accuracy of the above-ground biomass (AGB) in lowland mixed *Dipterocarp* forest. Spectral mixture analysis was applied to decompose mixture spectral components of Landsat-7 ETM+ into vegetation, soil, and shade fractions. These fraction images were integrated with PALSAR data using the Discrete Wavelet Transform (DWT) and the Brovey transform. As a comparison, the spectral reflectance of the Landsat-7 ETM+ was fused directly with PALSAR data. Backscatter of horizontal-horizontal (HH) and horizontal-vertical (HV) polarizations was used as well to estimate the AGB. Forest inventory was carried out in 77 randomly distributed plots, the data being used for either model development or for validation. A local allometric equation was applied to calculate the AGB per plot. Regression models were developed by integrating field measurements of 50 sample plots with remotely sensed data, e.g. fraction images, reflectance of Landsat-7 ETM+, and PALSAR data. The developed models were validated using 27 independent sample plots. The results showed that not all the fused images significantly improved the accuracy of the estimation of the AGB. The model based on the Brovey transform using the reflectance of Landsat-7ETM+ and PALSAR only produced a R^2 of 0.03 to 0.10. By contrast, fusion between the PALSAR data and fraction images using the Brovey transform improved the accuracy to a R^2 of 0.33 to 0.46. Further improvement in the accuracy of estimating AGB was observed when the DWT was applied to integrate PALSAR with the reflectance of Landsat-7ETM+ (R^2 = 0.69 to 0.72) and PALSAR with fraction images (R^2 = 0.70 to 0.74).

4.1 Introduction

Above-ground biomass (AGB) estimation in tropical forests has become a topic of high interest because its carbon stock forms part of the global carbon cycle. Forests can exchange carbon with the atmosphere through forest degradation and deforestation (Luckman *et al*., 1998; Phat *et al*., 2004) and forest regrowth (Luckman *et al*., 1998; Schimel *et al*., 2001). The use of optical and microwave remote sensing in combination with field measurements may provide a method to improve estimation of forest biomass over large areas (Rauste, 2005). However, in AGB assessment data derived from these sensors have both advantages and disadvantages.

Optical sensors with medium spatial resolution, such as Landsat-7 Enhance Thematic Mapper (ETM)+, have multispectral bands in the visible, near infrared, middle infrared and thermal infrared. Synthetic Aperture Radar (SAR) penetrates through surficial materials and vegetation canopies and can provide information on surface roughness, volume and mass of objects, as well as moisture content**.** Optical sensors collect reflected solar energy, which cannot penetrate into vegetation canopies, cloud, haze and fog. Another disadvantage of optical medium spatial resolution imagery is that reflectance recorded by a sensor within a single pixel may be a combination of the reflectance by pure components on the ground's surface in that pixel. Decomposition of pixels into their separate components and followed by quantifying the vegetation fraction are crucial steps before employing these data for AGB estimation (Lu *et al*., 2005). In tropical forests the complex forest structure causes canopy shading, influencing vegetation reflectance captured by a sensor. This could have an affect on AGB estimation (Gemmell, 1995; Steininger, 2000).

The application of SAR to assess biomass is offering opportunities for AGB estimation in tropical regions where high cloud cover often occurs. Radar is an active microwave system, which can work day and night, independent of solar energy. It can penetrate clouds and record energy returned from surface features. Besides these advantages, SAR also has limitations, such as in hilly regions, where no information is recorded at all in radar shadow areas (Trevett, 1986).

SAR has been employed to assess AGB in different regions. For instance, it has been applied in Australia to estimate AGB of Eucalyptus forests (Austin *et al*., 2003) and woody vegetation in the Southern Brigalow Belt, Central Queensland

(Liang *et al*, 2005; Lucas *et al*., 2006); in Canada's western sub-arctic and low arctic (Chen *et al*., 2009); in pine forests in the USA (Hyde *et al*., 2007); and in the Huvsgul Lake Basin, Mongolia, on Taiga species (Tsolmon *et al*., 2002). In tropical Amazon forests in Brazil, Kuplich *et al*. (2005) and Santos *et al*. (2003) have employed SAR for estimating AGB. Regarding the application in these tropical forests, the AGB can be estimated with reasonable accuracy using cross-polarized L and P band SAR imagery. However, saturation in AGB estimation is an important issue when computation is directly derived from simple regression between AGB and coefficient backscatter. The shorter the wavelength, the faster the point of saturation is reached (Kellndorfer *et al*., 2003; Lu, 2006; Lucas *et al*., 2006). Luckman *et al*. (1998) observed that backscatter of JERS-1 SAR through HH (horizontal-horizontal) polarization saturated at an AGB of around 60 ton/ha in tropical forest. The point of saturation in AGB estimation is affected by wavelength, e.g. C, L, and P bands; polarization, e.g. HH, HV (horizontal-vertical) and VV (vertical-vertical); incidence angles; and the characteristics of vegetation structure and ground conditions (Lu, 2006; Lucas *et al*., 2004; Rosenqvist *et al*., 2003, Saatchi *et al*., 2011). Fusion between remotely sensed data derived from optical and radar sensors may reduce the problems mentioned above and improve the accuracy of AGB estimation in tropical forests (Lu *et al*., 2005; Rauste, 2005).

Fusion uses an algorithm to integrate two or more different images to form a new image (Pohl and Genderen, 1998). The aim of fusion is to integrate spatial and spectral information (Acerbi *et al*., 2006) and to provide complementary information about a surface (Chibani, 2006; Pajares and de la Cruz, 2004). Fusion is also used to obtain a better visual analysis and more accurate classification of land cover (Pradhan, *et al*., 2006). Chaved *et al*. (1991) highlighted some points to consider when integrating information from different sensors: digital images from both sensors should be geometrically corrected to match one another, the method applied to fuse the images should not distort the spectral characteristics of the multispectral image, and the resulting image should have a high spatial resolution and similar spectral properties as the original image.

Various methods have been employed to fuse images. Standard methods include Intensity Hue Saturation, Principle Component Analysis, and Brovey transforms (Hussin and Shaker, 1996; Li *et al*., 2002; Musa *et al*., 2004; Wang *et al*., 2005). The standard fusion methods mentioned above tend to distort

colour information (Amolins *et al*., 2007) and sometimes the resulting image cannot preserve spectral characteristics of the original multispectral data (Kumar *et al*., 2000). A relatively new approach to fusing images is applying wavelet transform (Alparone *et al*., 2004; Amolins *et al*., 2007; Li *et al*., 2002; Pradhan *et al*., 2006; Yunhao *et al*., 2006). Ranchin and Wald (2000) demonstrated that fusion based on wavelet transform could improve spatial resolution with minimum distortion of spectral characteristics of the original image. The basic concept of wavelet decomposition is to analyze the signal according to different scales or resolutions (Martínez and Gilabert, 2009). Wavelet fusion decomposes a high spatial resolution and a multispectral resolution into the same spatial resolution by means of wavelet transform. Detailed information on the high spatial resolution data is injected into a multi spectral image (Amolins *et al*., 2007). To integrate the data, corresponding wavelet coefficients are combined, and the fused image is obtained by performing an inverse wavelet transform (Canty, 2010; Li *et al*., 2002; Ranchin and Wald, 2000).

Fusion using wavelet transform has usually been applied to optical remotely sensed data (Lemeshewsky, 1999; Ranchin and Wald, 2000). It integrates panchromatic images of high spatial resolution with multispectral resolution images of low spatial resolution (Li *et al*., 2002; Núñez *et al*., 1999, Shi *et al*., 2003). Recently, synthetic aperture radar has been fused with images resulting from optical sensors using wavelet transform (Alparone *et al*., 2004; Chibani, 2005; Chibani, 2006; Simone *et al*., 2002). Fusion with this transform is commonly employed to enhance features in urban areas and for land cover classification. Chibani (2005) enhanced the detection of lines, edges and field boundaries on radar image by fusing this radar with panchromatic image of Satellite Probatoire d'Observation de la Terre (SPOT) based on wavelet transform. Classification accuracy increased when Cakir (1999) conducted wavelet transform to integrate SPOT XS with SAR imagery and Huang *et al*. (2008) fused Quick Bird with IKONOS. Based on the reviewed literature, the potential use of image fusion has not been explored sufficiently for quantitative purposes, such as quantifying of forest biomass.

Based on the weaknesses of data derived from optical and microwave sensors as mentioned above, as well as on the lack of potential use of image fusion, an innovative approach to quantify AGB is proposed. The objective of the research is to improve the accuracy in estimating AGB in *Dipterocarp* forests by

integrating PALSAR with Landsat-7 ETM+. The reason to fuse these data is that the PALSAR has longer wavelengths, can penetrate deeper into canopies and has a higher spatial resolution than Landsat-7 ETM+ data. On the other hand, the optical data have multispectral bands. Therefore combining these data types has the potential to gain higher accuracies in biomass estimation. An innovative approach in this research was that the spectral reflectance of the Landsat-7 ETM+ was not directly fused with PALSAR data. Before fusing, the mixture of spectral components present in the pixels of the Landsat-7 ETM+ image were decomposed into vegetation, soil, and shade fractions using spectral mixture analysis. Then, the fraction images resulting from the decomposition were integrated with PALSAR data using the Brovey and Discrete Wavelet Transforms (DWT). For comparison, the spectral reflectance of Landsat-7 ETM+ was directly fused with PALSAR data, and the AGB estimated using backscatter from HH and HV polarizations only.

4.2 Materials and methods

4.2.1 Study area

The study area is located in a forest concession managed by PT Hutan Sanggam Labanan Lestari in Berau Regency, East Kalimantan, Indonesia. However, the area is extended (Figure 4.1) beyond this forest concession to fulfil prerequisites for applying the DWT for the fusion.

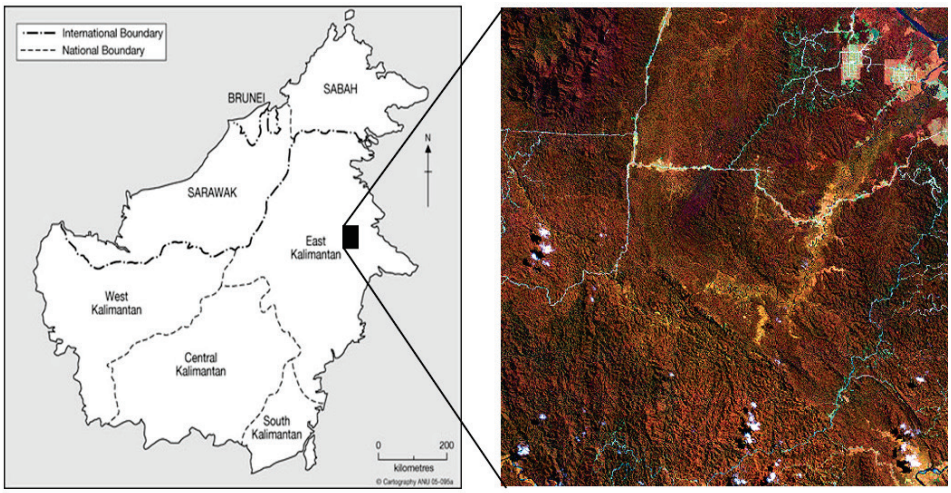

Figure 4.1: Location of the study area

The forest type of the study area is lowland mixed *Dipterocarp* forests. *Dipterocarpaceae* and *Euphorbiaceae* are the first and second most abundant families in these forests (Sist and Saridan, 1998). A selective cutting and planting system was applied for timber harvesting.

4.2.2 Image pre-processing

Landsat-7 ETM+ and PALSAR images were used in this research. A Landsat-7 ETM+ image acquired in May 31, 2003, from path 117 and row 59 was used to complement the PALSAR images. The PALSAR images were acquired in June 12, 2007. The forest was assumed to be in a stable condition, as forest harvesting had not been allowed in this concession between 2004 and the acquisition of the PALSAR data.

Image processing was conducted to minimize geometric and radiometric errors. Geometric correction of the Landsat-7 ETM+ image was conducted using 15 ground control points (GCPs) resulting in a pixel error below 0.5. The first order polynomial of a geometric model was applied and the image was geocoded to the Universal Transverse Mercator (UTM) coordinate system with datum World Geodetic System (WGS) 1984 and zone 50 North. The digital numbers (DNs) of the image were converted to radiance and then to reflectance using an exoatmospheric model as described in National Aeronautics and Space Administration/NASA (2005). DN values of bands 1, 2, 3, 4, 5, and 7 of Landsat-7 ETM+ were converted into reflectance.

The PALSAR image was received in level 1.1 which is in a slant range projection. Its spatial slant and azimuth resolutions were 9.50 m and 4.50 m, respectively. This L-band image had an incidence angle of 38.76 degrees with like (HH) and cross (HV) polarizations. Conversion from slant range into ground projection was conducted using the Alaska Satellite Facility (ASF) MapReady version 2.2.5. This free software (http://www.asf.alaska.edu/sardatacenter/softwaretools, accessed November 8, 2009) was also employed to correct terrain and radiometric distortions, as well as for geocoding. This image was radiometrically calibrated by converting amplitude values (Digital Numbers (DNs)) into a power image in units of σ_o. The σ_o is the ratio between the power that comes back from a patch of ground and the power sent to the patch of ground (Alaska Satellite Engineering Group, http://www.asf.alaska.edu/sardatacenter/softwaretools, accessed November 8, 2009). The conversion of DNs to σ_o (in power scale) is:

$$\sigma_0 = a_2 (DN_2 - a_1 N_r) \quad (4.1)$$

where DN is the original pixel value, Nr is the noise as a function of range, a_1 is the noise scale factor, and a_2 is the linear conversion determined during calibration of the processor. The σ_o amplitude values act as independent variables in the prediction of AGB (Fransson *et al*., 2000).
SAR is acquired in a side looking direction and induces distortions of rough terrain in the image such as foreshortening, shadow, and layover. In this case, terrain correction was carried out to minimize these distortions. The image was corrected using heights obtained from a Digital Elevation Model (DEM). The DEM had a 30 m spatial resolution and was derived from ASTER data downloaded from http://www.gdem.aster.ersdac.or.jp/, accessed November 10, 2009. Radiometry of the PALSAR was corrected using local incidence angles derived from the DEM. Kellndorfer *et al*. (1998) formulated this as follows:

$$\sigma_{corr} = \sigma_{orig} \sin(\alpha DEM) / \sin(\alpha ELL) \quad (4.2)$$

where σ_{corr} is the radar backscatter coefficient corrected for local incidence angle, σ_{orig} is the original backscatter coefficient, αELL is the incidence angle measured from the ellipsoid, and αDEM is the actual incidence angle calculated from the DEM.

The image was geocoded into the Universal Transverse Mercator (UTM) coordinate system with datum WGS 1984 and zone 50 North. It was resampled using the nearest neighbour method to produce an image with a spatial resolution of 16 m. This was a requirement for the wavelet analysis explained in the next section. In order to fuse the images, PALSAR was registered to the LANDSAT-7 ETM+ by a second order polynomial. The errors in the x and y direction were 4.71 and 4.60 m, respectively, with a total root mean squared error (RMSE) of 6.58 m.

4.2.3 Spectral mixture analysis

For remotely sensed data with medium resolution such as Landsat-7 ETM+, a signal from within a pixel recorded by the sensor could be a mixture of the reflectance from all component endmembers on the earth's surface covered by that pixel. An endmember is a pure spectral component (Adams and Gillespie, 2006). Spectral mixture analysis decomposes mixture endmembers. In spectral mixture analysis, it is assumed that a pixel in each spectral band is linear

combinations of multiple components weighted by relative surface abundance, and is expressed as (Tompskins *et al*., 1997):

$$R_b = \sum_{i=1}^{m} f_i r_{ib} + E_b \quad (4.3)$$

where: R_b is the reflectance of a pixel at band b, fi is the fractional abundance of endmember i (from a total of m endmembers), r_{ib} is the reflectance at band b of end member i, and E_b is the error in band b of the model fit.

Reflectance bands 1, 2, 3, 4, 5, and 7 of Landsat 7 ETM+ were transformed using minimum noise fraction. The transformed image was used to determine the most spectrally pure pixel, using the pixel purity index (Boardman *et al*., 1995). Pixels having high purity index values were used to identify the location of sample endmembers on the original image (Souza et al., 2005). In addition, sample endmembers were also identified by their location on the extremes of the image feature space (Lu *et al*., 2005). The selected sample endmembers were used to decompose the mixed spectral reflectance of the original image and produced fraction images consisting vegetation, soil, shade, and error fractions. All of the procedures for the spectral mixture analysis mentioned above were run using Environment for Visualizing Images (ENVI) 4.7 and Interactive Data Language (IDL) 7.1 software. Only forest areas were used for further analysis, whereas water bodies, settlements, shrubs, and roads were mask out.

4.2.4 The Brovey transform

The Brovey transform is intended to produce red, green and blue images, therefore only three bands at a time should be merged from the input multispectral data (Leica Geosystem, 2008). To choose three bands for the Brovey transform, a correlation analysis between each band of Landsat_7 ETM+ with the AGB was carried out. The three bands of Landsat-7 ETM+ with the highest correlation to the AGB were employed to fuse with the HH and HV polarizations of the PALSAR images. In addition, the fraction images (vegetation, soil and shade) resulting from the spectral mixture analysis were also used as input in this fusion. The formulas (modified from Leica Geosystem, 2008) are:

[B1 / B1 + B2 + B3] **x** [High resolution image] = B1_new (4.4)

[B2 / B1 + B2 + B3] **x** [High resolution image] = B2_new (4.5)

[B3 / B1 + B2 + B3] **x** [High resolution image] = B3_new (4.6)

where
B1, B2, and B3 are bands of the Landsat-7 ETM+ or fraction images,
High resolution image is a HH and HV polarization of PALSAR, and
B1_new, B2_new, and B3_new are the bands resulting from the Brovey transform.

4.2.5 The Discrete Wavelet Transform and its application for image fusion

A wavelet is a local wavelike function and its transform is a convolution of the wavelet function with a signal (Addison, 2002). During decomposition, the wavelet may be moved along the signal (translated), and be stretched or squeezed (dilated) (Addison, 2002; Mallat, 1989). Basically, wavelet transform quantifies the matching of the wavelet with the signal at different locations and scales (Addison 2002; Claudia *et al*., 2010). A high positive wavelet coefficient will be produced if the wavelet matches the shape of the signal, in contrast a large negative coefficient will be obtained when the wavelet and the signal are out of phase (Addison 2002; Claudia *et al*. 2010). In addition, the transform yields a low coefficient if the wavelet and signal do not coincide.

The DWT transforms signals over a discrete set of scales and the transforms can be realized using a variety of fast algorithms and customized hardware (Bruce *et al*., 2001; Pu and Gong, 2004). An application of DWT for image fusion can be illustrated as a bank of filters, where at every level of decomposition, the signal is split into high and low frequency components. Further decomposition can be applied to the low frequency components until the desired resolution is reached, as explained in detail by Mallat (1989), Strang and Nguyen (1997), Shensa (1999), and Amolins *et al*. (2007). The original image can be reconstructed by inverse transformation of all of the components of each deconstructed level in turn, starting from the coarsest spatial resolution (Amolins *et al*., 2007).

A prerequisite for the DWT is that the transform convolves the data by a factor of 2^n for the integer of n (Addison, 2002; Canty, 2010). Four quadrants are generated from every spatial resolution level of decomposition (Chibani and Houacine, 2003; Canty, 2010). These quadrants consist of one approximate image (low resolution and a reproduction of the original), and three detailed images (horizontal, vertical and diagonal detail) (Chibani and Houacine, 2003; Claudia *et al*., 2010).

In image fusion, detailed information from one image (with high spatial resolution) can be extracted and injected into low spatial resolution or multi spectral resolution images (Chibani, 2005; Amolins *et al*., 2007). The details of an image generally characterize different physical structures of the scene (Mallat, 1989), therefore, the resulting fused image contains complementary information to the fine and coarse resolution images. In this study, the PALSAR image is a high spatial resolution image and the Landsat-7 ETM+ image, as well as the fraction images resulting from spectral mixture analysis, is the multispectral images with low spatial resolution. The orthogonal wavelet transform was applied to the PALSAR image, the original reflectance of the Landsat-7 ETM+ data, and to the image resulting from the spectral mixture analysis. The PALSAR was down scaled twice and the data from the optical remotely sensed data were decomposed once to achieve a 64 m spatial resolution. The images from the PALSAR were fused with the optical remotely sensed imagery. Finally, an inverse transform was applied to reconstruct a fused image with high spatial resolution. A weighted model was employed in the inverse transform (Amolins *et al*., 2007; Canty, 2010) using the equation:

$$C^Z_{optical} = a^Z \mathbf{x}\ C^Z_{PALSAR} + b^Z, \text{ for } Z=D, V, \text{ and } H \qquad (4.7)$$

where $C^Z_{optical}$ is the optical remotely sensed imagery having information injected, C^Z_{PALSAR} is the detailed image of PALSAR, a^Z is the mean of the optical remotely sensed data, b^Z is the standard deviation of the PALSAR data, and D, V, and H are the diagonal, vertical and horizontal directions.

4.2.6 Forest inventory

Forest inventory was undertaken from May to June 2006. Random sample plot allocation was based on a Landsat-7 ETM+ image (May 31, 2003). The image acquired in 2003 was used because for the present study area, there was no cloud free image since May 2003 until the field campaign. Seventy seven

sample plots were divided randomly into two groups: 50 plots were used as training samples and 27 plots were used for validation. The coordinates of the plots were recorded using Global Positioning System (GPS).

The size of each plot was 500 m^2 and circular, but with corrections for slope of the terrain. The radius ranged from 12.62 m to 15.78 m. Within each of the 77 plots, tree diameters equal or greater than 10 cm were measured at breast height (DBH). Based on the inventory, the DBH of the sample plots ranged from 10 to 192 cm. The DBH data from the forest inventory were converted into AGB using a local allometric equation (Basuki *et al*., 2009). The equation to estimate AGB is:

$$\ln(AGB) = 2.196 \times \ln(DBH) - 1.201 \quad (4.8)$$

where AGB is above-ground biomass in dry weight (kg/tree) and DBH is in cm. The amount of AGB was obtained by de-transforming ln(AGB) (Basuki *et al*., 2009). The estimated AGB was used as the reference data and descriptive statistics are provided in Table 4.1. Paired t-test at 95 % confidence interval indicated that there were no differences between the training and the validation data.

Table 4.1: Descriptive statistics for the above-ground biomass (ton/ha) for the training (50 plots) and the validation (27 plots) data.

Above-ground biomass (ton/ha)	Training samples (50 plots)	Validation samples (27 plots)
Minimum	102.62	102.26
Mean	343.79	329.20
Maximum	839.32	812.15
Standard deviation	156.61	191.98

4.2.7 Analysis

Regression models were developed to examine the relationships between dependent variable (AGB) and independent variables. The independent variables were the amplitude backscatter values of HH and HV polarizations from the PALSAR data, and the single band and multiple band combinations of the fused images using the Brovey and Wavelet methods. Multiple regressions were proposed after examining free multicollinearity among the independent variables. The independent variables were the average of the extracted values

from 3 x 3 pixels around the centre points of the sampling plots (Tsolmon *et al*., 2002; Austin *et al*., 2003; Lucas *et al*., 2006). Every model was cross validated using an independent data set (n=27).

4.3 Results

4.3.1 The fused images

The highest correlation between the spectral reflectance of Landsat-7 ETM+ and AGB is observed in band 4, followed by band 5 and 7 as provided in Table 4.2. Therefore the reflectance of these bands and the PALSAR data were used as input for the Brovey transform. This transformation was also applied to integrate the fractions of vegetation, soil and shade with the HH and HV polarizations.

Table 4.2: Pearson correlation at 95% of confidence interval between the above-ground biomass (ton/ha) and the individual spectral reflectance of Landsat-7 ETM+ for 50 sample plots.

Band	Pearson correlation	p value
1	0.205	0.076
2	0.231	0.053
3	-0.097	0.252
4	0.757	0.000
5	0.564	0.000
7	0.369	0.040

In agreement with previous studies (Kumar *et al*., 2000; Ranchin and Wald, 2000; Li *et al*, 2002), fusion using the Brovey transform distorted the characteristics of radiometry of the multispectral image, as is illustrated in Figure 4.2c. However, fusion using this transform yielded a better visual performance of the resulting image when the PALSAR data were integrated with the fraction image from the Spectral Mixture Analysis (compare Figure 4.2b and 4.2d). Fusion, using the DWT, visually produced a similar result to the multispectral image. In this case, Figure 4.2a should be compared with 4.2e, and 4.2b with 4.2f.

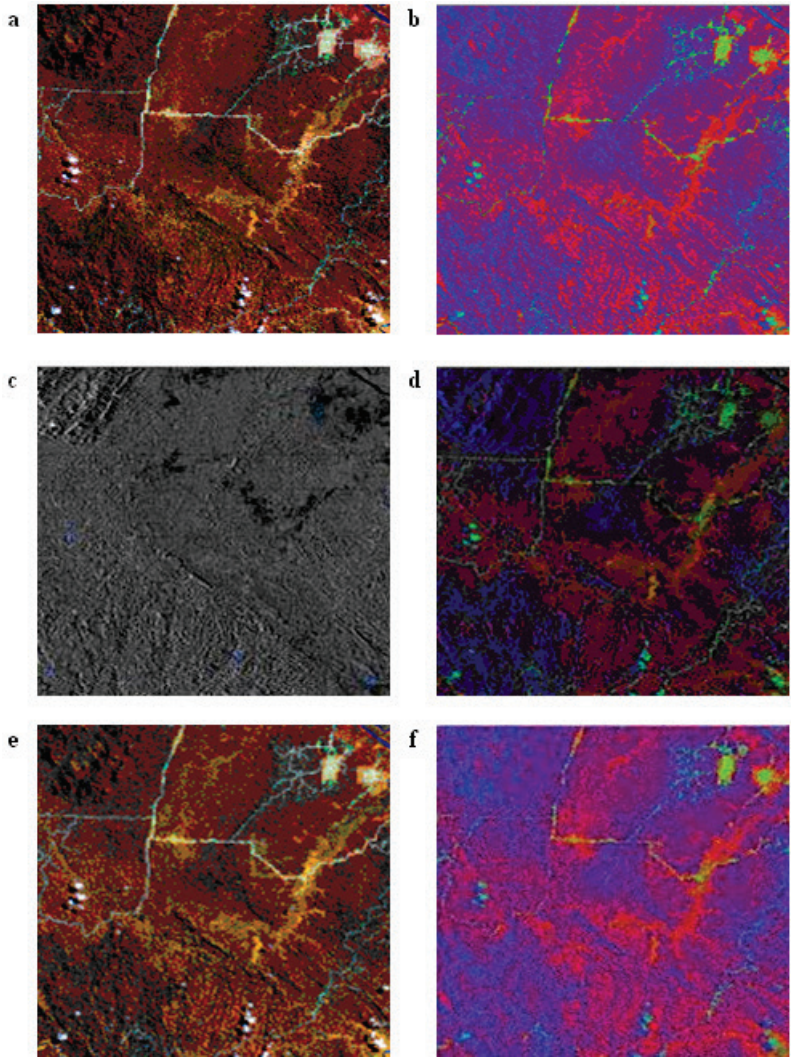

Figure 4.2: The original Landsat-7 ETM+ image (a), the fraction image resulting from Spectral Mixture Analysis (b), the fusion of HV polarization of PALSAR with reflectance of band 4, 5, and 7 of Landsat-7 ETM+ using the Brovey transform (c), with fraction image resulting from Spectral Mixture Analysis using the Brovey transform (d), with reflectance of Landsat-7 ETM+ using the Discrete Wavelet Transform (e), with the fraction image resulting from Spectral Mixture Analysis using the Discrete Wavelet Transform (f).

4.3.2 Biomass retrieval using remote sensing signal

The proposed models integrating fraction images with PALSAR data (Table 4.3) have much improved the estimation of AGB compared to the single polarization of PALSAR, both for the Brovey and the DWT. The R^2 was

increased when PALSAR data were incorporated in the fractional images, rather than using original spectral reflectance of the Landsat-7 ETM+. However, the model derived from the Brovey transform had a lower coefficient of determination than that of single and multiple band combination estimators resulting from the DWT. By contrast, only weak correlation was observed between AGB and radar backscatter of HH polarization (R = 0.268) as well as of HV polarization (R = 0.363), therefore the proposed models were only derived from the fused images as provided in Table 4.3.

Table 4.3: Regression models at 95% of confidence interval between the fused images (spectral reflectance of Landsat-7 ETM+ or fraction images and PALSAR data) and the above-ground biomass (ton/ha) using 50 sample plots.

Method	Independent variable	Equation	Adjusted R^2	p value	RMSE	
					(ton/ha)	(% of the mean)
Brovey transform	Fusion of reflectance band 4, 5, and 7 with HH polarization	-	0.031	0.220	154.2	45.2
	Fusion of reflectance band 4, 5, and 7 with HV polarization	-	0.101	0.049	148.5	43.4
	Fusion of vegetation, soil, and shade fractions with HH polarization	AGB = 167.654 + 2363.802brov_ veg_soil_shade_hh	0.332	0.000	128.0	37.8
	Fusion of vegetation, soil and shade fractions with HV polarization	AGB = 123.910 + 16014.500brov_veg _soil_shade_hv	0.461	0.000	114.9	33.9

Table 4.3: (*Continued*)

Method	Independent variable	Equation	Adjusted R^2	p value	RMSE	
					(ton/ ha)	(% of the mean)
Discrete wavelet transform	Fusion of reflectance band 4 with HH polarization	AGB = -1352.896 + 7162.091*ref4_hh	0.691	0.000	87.1	25.5
	Fusion of reflectance band 4, 5, and 7 with HH polarization	AGB = -1439.984 +7683.668*ref4hh + 1968.451*ref5_hh – 7439.332*ref7_hh	0.699	0.000	85.9	25.2
	Fusion of reflectance band 4 with HV polarization	AGB = -1353.881 + 7143.904*ref4_hv	0.720	0.000	82.8	24.3
	Fusion of reflectance band 4, 5, and 7 with HV polarization	AGB = -132.133 + 8201.965*ref4_hv – 2356.026*ref5_hv – 1816.364*ref7_hv	0.719	0.000	83.0	24.3
	Fusion of reflectance band 1, 2, 3 , 4, 5, and 7 with HV polarization	AGB = –940.170 – (6459.237*ref1_hv) +(5211.665*ref2_hv) – (5577.381*ref3_hv) + 8085.999*ref4_hv – 1687.023*ref5_hv – 881.406*ref7_hv	0.711	0.000	84.2	24.7
	Fusion of vegetation fraction with HH polarization	AGB = –191.764 + 1152.929*veg_hh	0.704	0.000	85.3	25.0
	Fusion of vegetation and soil fractions with HH polarization	AGB = –83.304 + 1073.298*veg_hh – 1436.975*soil_hh	0.746	0.000	78.9	23.1
	Fusion of vegetation, soil, and shade fractions with HH polarization	AGB = –198.478 + 1187.383*veg_hh – 1382.406*soil_hh + 125.005*shade_hh	0.742	0.000	79.6	23.3

Table 4.3: (*Continued*)

Method	Independent variable	Equation	Adjusted R^2	p value	RMSE (ton/ ha)	RMSE (% of the mean)
Discrete wavelet transform	Fusion of vegetation fraction with HV polarization	AGB = –180.053 + 1116.703*veg_hv	0.710	0.000	84.3	24.7
	Fusion of vegetation and soil fractions with HV polarization	AGB = –93.942 + 1075.756*veg_hv – 1253.127*soil_hv	0.743	0.000	79.4	23.3
	Fusion of vegetation, soil and shade fractions with HV polarization	AGB = –348.334 + 1313.120*veg_hv – 1175.127*soil_hv + 288.930*shade_hv	0.744	0.000	79.3	23.2
Spectral mixture analysis	Vegetation fraction	AGB = –258.055 +1350.342*veg	0.632	0.000	94.9	28.0
	Vegetation and soil fractions	AGB = –200.793 + 1303.543*veg – 723.260*soil	0.635	0.000	94.7	27.9

Note: AGB = above-ground biomass, brov = Brovey transform, veg = vegetation, hh = horizontal- horizontal, hv = horizontal- vertical

Fusion using wavelet transform between the original reflectance of Landsat-7 ETM+ and HV polarization produced a higher R^2 than with HH polarization (Table 4.3). However, fusion using wavelet transform between fraction images with HV polarization did not always provide a higher R^2 than those of HH polarization. For the model based on spectral mixture analysis and wavelet transform, multiple regressions of the fraction images increased the coefficient of determination. However, the highest R^2 of the proposed models was gained through multiple regression of the vegetation and soil fractions with the radar backscatter using the DWT. Multiple regressions were also conducted on the fused image of fraction images with HH and HV polarization, and this produced a R^2 of 0.752. However, due to multicollinearity between those fractions, the model was excluded. Table 4.3 also presents the models based on fraction images derived from spectral mixture analysis. This is to provide a clearer comparison between models based on fusion and those based on non fusion images.

Validation was tested using 27 sample plots of independent data for the fused images. Although the model based on the fusion of fractional images with HV polarization using the Brovey transform has a fair correlation with the AGB (R^2 = 0.461), but validation using the independent data set yielded a high RMSE as presented in Table 4.4. Compare to the models based on the Brovey transform, the models only based on the fraction images reduce the RMSE of the validation from 28 to 35 %.

Table 4.4: Validation using an independent data set from 27 plots

Method	Independent Variable	RMSE	
		(ton/ha)	% of the mean
Brovey transform	Fusion of vegetation, soil, and shade fractions with HH polarization	200.92	59.3
	Fusion of vegetation, soil and shade fractions with HV polarization	188.39	55.6
Discrete wavelet transform	Fusion of reflectance band 4 with HH polarization	123.5	36.5
	Fusion of reflectance band 4, 5, and 7 with HH polarization	118.3	34.9
	Fusion of reflectance band 1, 2, 3, 4, 5, and 7 with HH polarization	117.3	34.6
	Fusion of reflectance band 4 with HV polarization	120.0	35.4
	Fusion of reflectance band 4, 5, and 7 with HV polarization	119.0	35.1
	Fusion of reflectance band 1, 2, 3, 4, 5, and 7 with HV polarization	117.0	34.5
Discrete wavelet transform	Fusion of vegetation fraction with HH polarization	117.0	34.5
	Fusion of vegetation and soil fractions with HH polarization	122.7	36.2
	Fusion of vegetation, soil, and shade fractions with HH polarization	122.9	36.3
	Fusion of vegetation fraction with HV polarization	118.6	35.0
	Fusion of vegetation and soil fractions with HV polarization	121.2	35.8
	Fusion of vegetation, soil and shade fractions with HV polarization	127.7	37.7
Spectral mixture analysis	Vegetation fraction	130.5	38.5
	Vegetation and soil fractions	135.6	40.1

4.4 Discussion

Overall, the proposed regression models using the fused images of the fractional images did improve the estimation accuracy of the AGB than the fused image using the original spectral reflectance. This shows that the proportion of mixed spectral components (e.g. vegetation, soil, and shade) should be computed before integration with the PALSAR data in order to achieve higher accuracy of the AGB estimation. The separation of the mixed spectral component is essential because most the study areas are forests that have been logged. In selectively logged forests the ground is not totally covered by trees. Such logged forests are a mix of vegetation, soil and shade, and on medium resolution imagery these spectral components are also mixed. For example, Vega (2005) found that felling a single tree in such forests created a gap ranging from 30 to 100 % for pixels with a resolution of 15 m. Within this gap, reflectance from the soil may be mixed with the reflectance from the surrounding trees and recorded within a pixel by the sensor.

The fusion using the DWT improves the estimation accuracy of AGB. This indicates the data from these two sensors complement each other and integrating them is beneficial. Landsat-7 ETM+ with its multispectral bands provides information on different properties of the earth's surface. For instance, the near infrared band is useful to detect vegetation with its high reflectance. The information from these multispectral bands is complemented by the PALSAR data. The benefit of using the L band of the PALSAR is not only its ability to penetrate deeper into the canopy, but also the nature of the SAR data showing multiple scattering within the canopy. Penetration of microwave radiation into the canopy depends on the wavelength and the type of polarization (Balzter *et al*., 2003).

In addition to the above explanation, the wavelet method preserves high and low frequency features during the spectral decomposition, which means that variation in AGB directly causes change in the spectral characteristics, i.e. change in the peaks and valleys along the spectral curve (Pu and Gong, 2004). The weaker relationship between total AGB and extracted independent variables from the fused image using the Brovey transform is caused by the algorithm to enhance the visual interpretation of the red, green and blue combination (Wang *et al*., 2005). Colour distortion can occur if the Brovey transform is employed to fuse multi sensor data with large differences in spectral range (Alparone *et al*., 2004). With respect to the integration data, it

can be learnt that fusion does not always improve the resulting image as the AGB estimator. It depends on the applied method to integrate the data. In the present study, Brovey transform cannot integrate properly the advantages of the PALSAR and Landsat-7 ETM+ to the fused image. Therefore, model based on the fusion between PALSAR and fraction images using the Brovey transform cannot produce higher R^2 compare to the model only based on the fraction images.

Using a single polarization data, the HV produces higher correlation with the AGB than HH polarization. Most HH polarization responses consist of surface scattering, while HV reflects volumetric multiple scattering. Therefore, cross polarized data are responding to volume and biomass, especially with L-band since they penetrate the forest canopy (Lucas *et al*., 2006).

Regarding the application of a single L band of SAR data, Luckman *et al*. (1998) found that the HH-polarized L band of JERS-1 SAR saturated at a AGB of 60 ton/ha in Amazon forests in Brazil. In woodland areas in Queensland, Australia, Lucas *et al*. (2006) observed that the maximum saturation level for HH polarization of the L band was 75 to 80 ton/ha, and 98 ton/ha for HV polarization. Wang and Qi (2008) found saturation at a higher level of biomass compared to the previous researchers when applying a modified radiative transfer model using the L band of JERS-1 SAR in dense moist evergreen forests. Using this model, the increase in woody backscatter was not reduced until the biomass reached 100 ton/ha. After that point, the increase in woody backscatter was reduced, but biomass still increased to around -8dB at about 500 ton/ha of total AGB.

The RMSE of the proposed regression models based on the DWT ranges from 117 to 128 ton/ha or 35 to 38 % of the mean AGB. This can be caused by high variability of the reference AGB, it vary from 102 to 839 ton/ha. As comparison, Lefsky *et al*. (2005) also found RMSE about 118.5 ton/ha when estimating AGB using LIDAR (Light Detection and Ranging) image. Saatchi *et al*. (2011) examined that the estimation accuracy of AGB was affected by the size of sample plots, the type of wavelength and polarization and the corporation with the Interferometric SAR (InSAR) to measure tree height.

It was suggested that a minimum sample plot of 0.25 ha is needed to reduce the effect of speckle noise (Saatchi *et al*., 2011). With a small sample plot, the

occurrence of a tree with large DBH will create high heterogeneity in forest stand structure and large variation in coefficient of variation, whereas in a larger sample plot the variation is averaged (Saatchi *et al*., 2011). Based on the field observation, some big trees such as *Koompasia excelsa*, *Canarium sp*., *Shorea sp*., *Dipterocarpus sp*. existed in the sample plots. The DBH of these big trees were greater than 100 cm.

Saatchi *et al*., (2011) found that at a maximum AGB of 300 ton/ha, the RMSE of the validation using L band with full polarization (HH, HV, and VV) were 39.5 and 48.0 ton/ha for sample plots of 0.50 and 1.0 ha, respectively, and for the full polarization integrated with the InSAR at the same plots size, the RMSE were 30.8 ton/ha and 29.0 ton/ha. For P band with the same maximum AGB and 0.5 ha of sample plot, they obtained the RMSE were 26.6 and 20.2 ton/ha and for 1.0 ha of sample plot the RMSE were 18.7 and 15.1 ton/ha for full polarization and full polarization integrated with InSAR, respectively (Saatchi *et al*., 2011). For the current study area, a further study to reduce the RMSE of the AGB estimation may be conducted by increasing the size of sample plot, the use of P band, or incorporation with the InSAR.

4.5 Conclusions

The proposed model shows the potential use of PALSAR data when integrated with Landsat-7 ETM+ or fraction images. The integration of radar and optical imagery increased the estimation accuracy of AGB in mixed *Dipterocarp* forest. The proposed models fused fraction images with PALSAR data, thereby significantly increasing the coefficient of determination, compared to models based only on radar backscatter. The current regression models also reduced RMSE compared to the model derived only from spectral mixture analysis.

Acknowledgements

We appreciate to B.T. Sasongko, MSc., Bogor Agriculture University for the discussion of PALSAR. The authors are grateful to Dr. M.J. Canty for the DWT script and W. Nieuwenhuis for technical assistance. My colleagues, Claudia Pittiglio thank you for deep discussion in wavelet theory. This research is supported by a grant from the Netherlands Fellowship Programme (NFP).

References

Acerbi-Junior, F.W., Clevers, J.G.P., Schepmna, M.E., 2006. The assessment of multi-sensor image fusion using wavelet transforms for mapping the Brazilian Savanna. Int. Journal of Applied Earth Observation and Geoinformation 8: 278–288.

Adams, J.B., Gillespie, A.R., 2006. Remote sensing of landscapes with spectral images. A Physical Modeling Approach. Cambridge Univ. Press, UK.

Addison, P.S., 2002. The illustrated wavelet transform handbook. Introductory theory and applications in science, engineering, medicine and finance, Inst. of Physics Publishing, UK.

Alaska Satellite Facility Engineering Group. ASF map ready user manual. http://www.asf.alaska.edu/sardatacenter/softwaretools (accessed November 8, 2009).

Alparone, L., Baronti, S., Garzelli, A., Nencini, F., 2004. Landsat ETM+ and SAR image fusion based on Generalized Intensity Modulation. IEEE Transactions on Geoscience and Remote Sensing 42: 2832–2839.

Amolins, K., Zhang, Y., Dare, P., 2007. Wavelet based image fusion techniques — An introduction, review and comparison. ISPRS Journal of Photogrammetric & Remote Sensing 62: 249–263.

Austin, J.M., Mackey, B.G., van Nief, K.P., 2003. Estimating forest biomass using satellite radar: An exploratory study in a temperate Australia Eucalyptus forest. Forest Ecology and management 176: 575–583.

Balzter, H., Skinner, L., Luckman, A., Brooke, R., 2003. Estimation of tree growth in a conifer plantation over 19 years from multi-satellite L-band SAR. Remote Sensing of Environment 84: 184–191.

Basuki, T.M., van Laake, P.E., Skidmore, A.K., Hussin, Y.A., 2009. Allometric equations for estimating the above-ground biomass in tropical lowland *Dipterocarp* forests. Forest Ecology and Management 257: 1684–1694.

Boardman, J. M., Kruse, F. A., Green, R. O., 1995. Mapping target signature via partial unmixing of AVIRIS data. Summaries of the Fifth JPL Airborne Earth Science Workshop. JPL Publication 95: 23–26.

Bruce, L.M., Morgan, C., Larsen, S., 2001. Automated detection of subpixel hyperspectral targets with continuous and discrete wavelet transforms. IEEE Transactions on Geoscience and Remote Sensing 39: 2217–2226

Cakir, H.I., Khorram, S., Dai, X.L., de Fraipont, P. , 1999. Merging SPOT XS imagery using the wavelet transform method to improve classification accuracy. 0-7803-5207-6/99/$10.00©1999 *IEEE*, p. 71–73.

Canty, M.J., 2010. Image analysis, classification and change detection in Remote sensing. With algorithms for ENVI/IDL. Second edition. Taylor & Francis Group, New York.

Chavez, P.S., Sides, S.C., and Anderson, J.A., 1991. Comparison of three different methods to merge multiresolution and multi spectral data: Landsat TM and SPOT panchromatic. Photogrammetric Engineering & Remote Sensing 57: 295–303.

Chen, W., Blain, D., Li, J., Keohler, K., Fraser, R., Zhang, Y., Leblanc, S., Olthof, I., Wang, J., Mcgovern, M., 2009. Biomass measurements and relationships with Landsat-7/ETM+ and JERS-1/SAR data over Canada's western sub-arctic and low arctic. Int. Journal of Remote Sensing 30: 2355– 2376.

Chibani, Y., Houacine, A., 2003. Redundant versus orthogonal wavelet decomposition for multisensory image fusion. Pattern Recognition 36: 879–887.

Chibani, Y. ,2005. Selective synthetic aperture radar and panchromatic image fusion by using the `a trouswavelet decomposition. EURASIP Journal on Applied Signal Processing 14: 2207–2214.

Chibani, Y., 2006., Additive integration of SAR features into multispectral SPOT images by means of the à trous wavelet decomposition. ISPRS Journal of Photogrammetric & Remote Sensing 60: 306–314.

Fransson, J.E.S., Walter, F., and Ulander, L. M. H., 2000. Estimation of forest parameters using CARABAS-II VHF SAR data. IEEE Transaction on Geoscience and Remote Sensing 38: 720–727.

Gemmell, F.M., 1995. Effects of forest cover, terrain, and scale on timber volume estimation with Thematic Mapper data in the rocky mountain site. Remote Sensing of Environment 5: 291–305.

Huang, X., Zhang, L., Li, P., 2008. A multiscale feature fusion approach for classification of very high resolution satellite imagery based on wavelet transform. Int. Journal of Remote Sensing 29: 5923–5941.

Hussin, Y.A., Shaker, S. R., 1996. Optical and radar satellite image fusion techniques for monitoring natural resources and land use changes. The German Int. Journal of Electronic and Communications. AEU EUSAR'96 Special Issue, pp. 169–176.

Hyde, P., Nelso, R., Kimes, D., and Levine, E., 2007. Exploring LiDAR–RaDAR synergy—predicting aboveground biomass in a southwestern ponderosa pine forest using LiDAR, SAR and InSAR. Remote Sensing of Environment 106: 28–38.

Kellndorfer, J.M., Pierce, L.E., Dobson, M.C., 1998. Toward consistent regional-to-global-scale vegetation characterization using orbital SAR system. IEEE Transactions on Geoscience and Remote sensing 36: 1396–1411.

Kellndorfer, J.M., Dobson, M.C., Vona, J.D., and Clutter, M., 2003. Toward precision forestry: plot-level parameter retrieval for Slash Pine plantations with JPL IRSAR. IEEE Transactions on Geoscience and Remote Sensing 41: 1571–1582.

Kumar, A. S., Kartikeyan, B., Majumdar, K. L.., 2000. Band sharpening of IRS-multispectral imagery by cubic spline wavelets. Int. Journal of Remote Sensing 21: 581–594.

Kuplich, T.M., Curran, P.J., Atkinson, P.M., 2005. Relating SAR image texture to the biomass of regenerating tropical forests. Int. Journal of Remote Sensing 26: 4829–4854.

Lefsky, M.A., Turner, D.P., Guzy, M., Cohen, W.B. 2005., Combining lidar estimates of aboveground biomass and Landsat estimates of stand age for spatially extensive validation of modelled forest productivity. Remote Sensing of Environment 95: 549–558.

Leica geosystem, 2008. ERDAS field guide™. pp. 335.

Lemeshewsky, G. P., 1999. Multispectral multisensor image fusion using wavelet transforms. In: Proc. SPIE Int. Soc. Opt. Eng., Visual image processing VIII, Orlando, USA, 3716, pp. 214–222.

Li, S., Kwok, J.T., Wang, Y., 2002. Using the discrete wavelet frame transformation to merge Landsat TM and SPOT panchromatic images. Information Fusion 3: 17–23.

Liang, P., Moghaddam, M., Pierce, L., Lucas, R. M., 2005. Radar backscatter model for multi-layer mixed species forests. IEEE Transactions on Geoscience and Remote Sensing 43: 2612–2626.

Lu, D., Batistella, M., Moran, E., 2005. Satellite estimation of aboveground biomass and impacts of forest stand structure. Photogrammetric Engineering & Remote Sensing 71: 967–974.

Lu, D. 2006. The potential and challenge of remote sensing-based biomass estimation. Int.l Journal of Remote Sensing 27: 1297–1328.

Lucas, R.M., Moghaddam, M., Cronin, N., 2004. Microwave scattering from mixed-species forests, Queensland, Australia. IEEE Transactions on Geoscience and Remote Sensing 42: 2142–2159.

Lucas, R.M., Cronin, N., Lee, A., Moghaddam, M., Witte, C., Tickle, P., 2006. Empirical relationships between AIRSAR backscatter and LiDAR-derived

forest biomass, Queensland, Australia. Remote Sensing of Environment 100: 407–425.

Luckman, A., Baker, J., Honzák, M., Lucas, R., 1998. Tropical forest biomass density estimation using JERS-1 SAR: Seasonal variation, confidence limits, and application to image mosaic. Remote sensing of environment 63: 126–139.

Mallat, S.G., 1989, A theory for multiresolution signal decomposition: the wavelet representation. IEEE Transactions on Pattern Analysis and Machine Intelligence 11: 674–693.

Martinez, B., Gilabert, M.A., 2009. Vegetation dynamics from NDVI time series analysis using the wavelet transform. Remote Sensing of Environment 113: 1823–1842.

Musa, M. K., Hussin, Y.A. Weir, M.C., 2004. Multi-data fusion for sustainable forest management. Asian Journal on Geoinformatics 4: 57–70.

Núnêz, J., Otazu, X., Fors, O., Prades, A., Palà, V., Arbiol, R., 1999. Multiresolution-base image fusion with additive wavelet decomposition IEEE Transactions on Geoscience and Remote Sensing 37: 1204–1211.

Pajares, G., de la Cruz, J.M., 2004. A wavelet-based image fusion tutorial. Pattern Recognition 37: 1855–1872.

Phat, N.K., Knorr, W., Kim, S., 2004. Appropriate measures for conservation of terrestrial carbon stocks—Analysis of trends of forest management in Southeast Asia. Forest Ecology and Management 191: 283–299.

Pittiglio, C., Skidmore, A.K., de Bie, C.A.J.M., Murwira, A. A common dominant scale emerges from images of diverse satellite platforms using the wavelet transform. Int. Journal of Remote Sensing 32(13): 3665-3687.

Pohl, C. and van Genderen, J.L., 1998. Multisensor image fusion in remote sensing: concepts, methods, and applications. Int. Journal of Remote Sensing 19: 823–854.

Pradhan, P.S., King, R.L., Youman, N.H., Holcom, D.W., 2006. Estimation of the number of decomposition levels for a wavelet-based multiresolution multisensor image fusion. IEEE Transactions on Geoscience and Remote Sensing 44: 3674–3686.

Pu, R., Gong, P., 2004. Wavelet transform applied to EO-1 hyperspectral data for forest LAI and crown closure mapping. Remote Sensing of Environment 91: 212–224.

Ranchin, T., Wald, L., 2000. Fusion of high spatial and spectral resolution images: the ARSIS concept and its implementation. Photogrammetric Engineering & Remote Sensing 66: 49–61.

Rauste, Y., 2005. Multi-temporal JERS SAR data in boreal forest biomass mapping. Remote Sensing of Environment 97: 263–275.

Ronsenqvist, A., Milne, A., Lucas, R., Imhoff, M., Dobson, C., 2003. A review of remote sensing technology in support of the Kyoto Protocol. Environmental Science & Policy 6: 441–445.

Saatchi, S., Marlier, M., Chazdon, R.L., Clark, D.B., Russell, A.E., 2011. Impact of spatial variability of tropical forest structure on radar estimation of aboveground biomass. Remote Sensing of Environment 115: 2836–2849.

Santos, J.R., Freitas, C.C., Araujo, L.S., Dutra, L.V., Mura, J.C., Gama, F.F., Soler, L.S., Sant'Anna, S.J.S., 2003. Airborne P-band SAR applied to the aboveground biomass studies in the Brazilian tropical rainforest. Forest Ecology and Management 87: 482–493.

Schimel, D.S. et al., 2001. Recent patterns and mechanisms of carbon exchange by terrestrial ecosystems. Nature 414: 169–172.

Shensa, M. J., 1992. The discrete wavelet transform: wedding the â trous and Mallat algorithms. IEEE transactions and signal processing 40: 2464–2482.

Shi, W., Zhu, C., Zhu, C., Yang, X., 2003. Multi-band wavelet for fusing SPOT panchromatic and multiband images. Photogrammetric Engineering & Remote Sensing 69: 513–520.

Simone, G., Farina, A., Morabito, F.C., Serpico, S.B., and Bruzzone, L., 2002. Image fusion techniques for remote sensing applications. Information Fusion 3: 3–15.

Sist, P., Saridan, A., 1998. Description of the primary lowland forest of Berau. *In*: Bertault, J-G., Kadir, K. (*eds.*), Silvicultural research in a lowland mixed Dipterocarp forest of East Kalimantan, 51 - 73. CIRAD-forêt, FORDA, PT Inhutani I, Jakarta.

Souza, Jr., C.M., Roberts, D. A., Cocrane, M.A., 2005. Combining spectral and spatial information to map canopy damage from selective logging and forest fires. Remote Sensing of Environment 98: 329–343.

Steininger, M.K., 2000. Satellite estimation of tropical secondary forest above-ground biomass data from Brazil and Bolivia. Int. Journal of Remote Sensing 21: 1139–1157.

Strang G., Nguyen, T., 1997. Wavelets and filter banks. Wellesley-Cambridge Press, New York.

Tompkins, S., Mustard, J.F., Pieters, C. M., Forsyth, D.W., 1997. Optimization of endmembers for spectral mixture analysis. Remote sensing of environment 59: 472–489.

Trevett, J.W., 1986. Imaging radar for resources surveys. *In* Remote sensing application, Barret, E. C. and Curtis, L. F. (*Ed*.), p. 17–62. Chapman and Hall Ltd., New York.

Tsolmon, R., Tateishi, R., Tetuko, J. S. S., 2002. A method to estimate forest biomass and its application to monitor Mongolian Taiga using JERS-1 SAR data. Int. Journal of Remote Sensing 23: 4971–4978.

Vega, B., 2005. Image fusion of optical and microwave data to assess criteria and indicator (C&I) related to forest encroachment, for certification process of Sustainable Forest Management (SFM). Unpublished MSc thesis: ITC, Enschede, 79 p.

Wang, C., Qi, J. 2008. Biophysical estimation in tropical forests using JERS-1 SAR and VNIR imagery II. Above-ground woody biomass. Int. Journal of Remote Sensing 29: 6827–6849.

Wang, Z., Ziou, D., Armenakis, C., Deren, L., and Li, Q., 2005. IEEE Transactions on Geoscience and Remote Sensing 43: 1391–1402.

Wald, L., Ranchin, T., Mangoli, M., 1997. Fusion of satellite images of different spatial resolution: Assessing the quality of resulting images. Photogrammetric Engineering & Remote Sensing 63: 691–699.

Yunhao, C., Lei, D., Jing, L., Xiaobing, L., and Peijun, S., 2006. A new wavelet-based image fusion method for remotely sensed data. Int. Journal of Remote Sensing 27: 1465–1476.

CHAPTER 5

CAN A 35 YEAR SELECTIVE LOGGING CYCLE RESTORE CARBON STOCKS OF TREE BIOMASS IN TROPICAL FORESTS?*

* This chapter is based on:
Basuki, T.M., van Duren, I., Skidmore, A.K., Hussin, Y.A. 2011. Can a 35 year selective logging cycle restore carbon stock of tree biomass in tropical forest? Paper under review

Abstract

In this paper we evaluate whether a selective logging and replanting system (*Tebang Pilih Tanam Indonesia*, or TPTI), can maintain or restore carbon stocks in forest biomass. The study was carried out in lowland mixed *Dipterocarp* forests in East Kalimantan, Indonesia. The CO2FIX V 3.1 model was used to simulate carbon stocks on a yearly base as a function of logging cycle and volumes of the harvested timber. In this simulation, trees of species with similar growth characteristics were grouped together. The logging cycle used was 35 years with 30 m^3 of harvested timber per hectare on average. The dynamics in the carbon stock was observed for a period of 5 logging cycles. The results showed that using this management regime, the trees could not sequester carbon to the level present at the start of the logging cycle. To obtain the same amount of carbon as present before logging, a 120 year logging cycle was needed. Lengthening the logging cycle from 35 years to 60, 80, 100, and 120 years increased the carbon stock in the trees' biomass by 9, 14, 18, and 23 %, respectively. The forest soil showed its major role in stocking carbon in this simulation. The percentage of carbon stored in the forest soil accounted for 30 to 65 %.

5.1 Introduction

The role that tropical forests play as CO_2 sources or sinks is under debate. Tropical forests can be sources of CO_2 emission through deforestation (Fearnside *et al*., 2009; Masera *et al*., 2003; Santilli *et al*.; 2005) and forest degradation (Fearnside, *et al*., 2009; Fearnside and Launrance, 2004). However, when photosynthesis of trees exceeds their respiratory losses then these forests can also be carbon sinks, as demonstrated by Grace *et al*. (1995). In addition, tropical forests can act as carbon sinks through accumulation of biomass resulting from the continuous growth of trees, retaining *in situ* debris, soil organic carbon storage, and change in woody density as trees change to mature forests (Lugo and Brown, 1992). Nevertheless, the role of forests as sources or sinks of CO_2 depends on succession stage, specific disturbance, and management activities (Masera *et al*., 2003).

In relation to mitigation of greenhouse gas emission by forestry activities, De Jong *et al*. (2007) reported that the feasibility of tropical forest conservation as a mitigation method for the removal of CO_2 from the atmosphere was introduced in the 11th conference of parties (COP-11) of the United Nation Framework Convention on Climate Change (UNFCCC) in Montreal (2005). This concept is known as Reducing Emissions from Deforestation in Developing Countries (REDD) (Boyd, 2010). REDD is a mechanism which is intended to provide compensation to developing countries reducing their national CO_2 emission from deforestation and forest degradation. In the Copenhagen Accord a new concept, namely REDD-plus was adopted. The REDD-plus is an integration between REDD concept with promoting of sustainable forest management and enhancing of carbon sinks and it is considered as a mitigation method (Sasaki and Yoshimoto, 2010). Therefore, forest management definitely has scope to further optimize the uptake of CO_2 from the atmosphere.

There are a number of management options to enhance carbon sequestration in forest biomass. The requirement of a longer logging cycle to restore biomass carbon stock has been examined by previous researchers (Backéus *et al*., 2005; Baral and Guha, 2004; Galik and Jackson, 2009; Kaipainen *et al*. 2004). Extending the logging cycle by 20 years increases the carbon stock in forest biomass and soil for some species in Finland and the UK (Kaipainen et al., 2004). Other options are optimizing the intensity of thinning operations (Backéus *et al*., 2005; Jandl *et al*., 2007) or increasing the sequestered carbon in soil (Jandl *et al*., 2007; Markewitz, 2006; Mund *et al*., 2002). To plan land use

and develop forest policies, forest management requires information on the current and future projection of potential resource conditions, e.g. sequestered carbon in the forests (Dean, *et al*., 2004; Mohren, 2003; Peng, 2000; Schmid *et al*., 2006; Tiejen and Huth, 2006). The information on distribution of carbon flows and pools in forest ecosystems can be analyzed using different modeling approaches (Backéus *et al*., 2005; Coops *et al*., 1998; Huth and Ditzer, 2000; and Waring *et al*, 2010). The choice of a model should be based on its applicability, as well as the type and number of input parameters.

With respect to rotation length or logging cycle, the silvicultural system of selective logging and replanting (*Tebang Pilih Tanam Indonesia*, or TPTI) has been widely applied in Indonesia. The implementation of the TPTI system is based on the Decree of the Ministry of Forestry No. 485/Kpts/II/1989. In this TPTI system, the logging cycle is 35 years. Commercial timbers can be harvested when their DBH (diameter at breast height) is equal to or greater than 50 cm for areas zoned as full production forests (van Gardingen *et al*., 2003). For limited production forests, which are production forest areas with an average slope of more than 40%, the commercial timber may be harvested when the DBH reaches 60 cm (van Gardingen *et al*., 2003). In this study, the CO2FIX V3.1 model (Jong *et al*., 2007; Masera *et al*., 2003; Schelhaas *et al*., 2004) simulated the dynamics of forest carbon in the study area. This model was selected because of its applicability to mixed species in natural forests, while not being dependent on knowledge about the forest stand age.

The study was conducted in the Labanan concession consisting of lowland mixed *Dipterocarp* forests in East Kalimantan, Indonesia. The concession included seven compartments with different starting times for the timber harvesting. *Dipterocarp* forests are important sources of commercial timber in South East Asia and also known for their species richness and biodiversity. In addition, these forests are also important for CO_2 mitigation, as mentioned previously. For these reasons, a study of the effects of the currently applied logging cycle is required to evaluate whether the TPTI system is sustainable in terms of maintaining or restoring carbon stocks in the forest ecosystem. In the current study, carbon stock simulations were based on the current logging cycle of 35 years. Additional scenarios, with extended logging cycles, were evaluated to ascertain the optimal logging cycle and volume of timber to be harvested within the *Dipterocarp* forests. The simulations of this study were restricted to carbon stock in tree biomass and soil carbon.

The specific aims of this study were: 1) examine the impact of a 35 year logging cycle of the selective logging and replanting system (i.e. TPTI system) on carbon stocks in tree biomass and soil. 2) quantify the effect the length of the logging cycle and the quantity of harvested timber has on carbon stock in tree biomass and soil of *Dipterocarp* forests.

5.2 Methods

5.2.1 Study area

The research was conducted in the Labanan forest concession managed by PT Hutan Sanggam Labanan Lestari, Berau Regency, East Kalimantan, Indonesia. The concession lies between 1°45' - 2°10' N, and 116°55' - 117°20' E (Figure 5.1). The forest type in the study area is called lowland mixed *Dipterocarp* forest, which is dominated by the family *Dipterocarpaceae.*

Based on the data (1995 – 2005) collected by the Meteorological and Geophysical Agency, the mean annual rainfall in the study area is 2300 mm. The temperature ranges from 21 to 34 ºC with a mean temperature of 26 ºC (Berau Forest Management Project/BFMP, 1999). Red Yellow Podzolic or Ultisols form the dominant soil type in the study area, though the soil properties vary according to terrain conditions. Other soil types found are Oxisols, Vertisols and Inceptisols (Mantel, 1999).

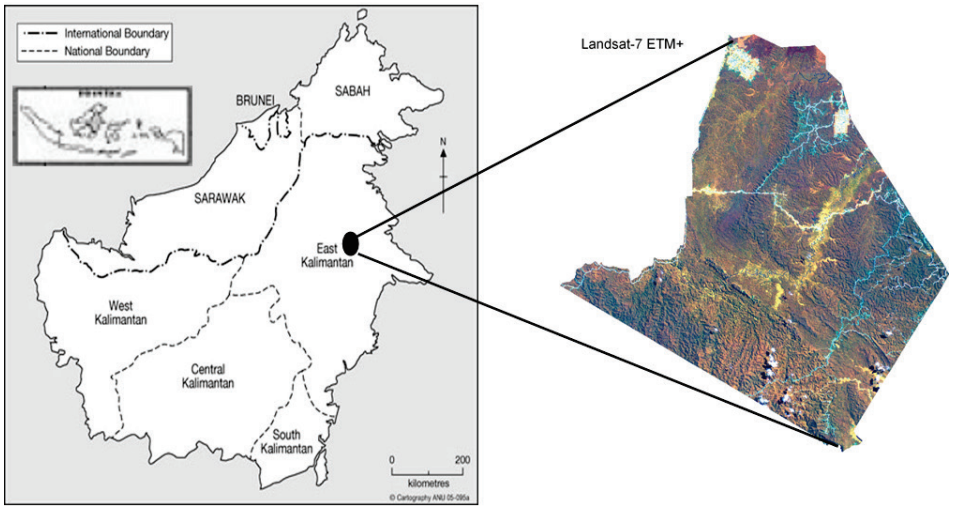

Figure 5.1: Location of the study area

The forest concession was divided into seven units each with a five year working plan known as a RKL (*Rencana Karya Lima Tahun*). Each unit was divided into five logging compartments each with their own annual working plan (*Rencana Karya Tahunan*: RKT). Table 5.1 shows the five year period when logging took place as well as the time elapsed since the last logging event for each RKL. RKL7 can be seen as a reference as this is primary forest that has not been logged yet.

Table 5.1: Five year working plan of the Labanan forest concession area

RKL	Years of logging	Years between logging and the field campaign of 2006 (in years)	Remarks
1	1976-1980	30-26	
2	1981-1985	25-21	
3	1976-1980	30-26	
4	1991-1995	15-11	
5	1996-2000	10-6	
6	2001-2005	5-3	No logging (2004 to June 2007)
7	-	-	Un-logged

5.2.2 Forest inventory and allometric equations

The field campaign to collect primary and secondary data was carried out from March to June 2006. The development of local allometric equations to estimate the above-ground biomass (AGB) is explained by Basuki *et al*. (2009). Seventy seven plots were randomly allocated. The coordinates of the plots in the field were navigated using GPS.

The size of the circular plots was 500 m^2, corrected for the slope of the terrain. The radius ranged from 12.62 m to 15.78 m. Within each of the 77 plots, tree species were recorded and tree diameters equal to or greater than 10 cm were measured at breast height. The diameter at breast height (DBH) data from the forest inventory were converted into biomass of leaves, branches, stem, and total above-ground biomass of a tree (AGB) using local allometric equations. The allometric equation to estimate the AGB in mixed *Dipterocarp* forest is (Basuki *et al*., 2009):

$$\ln(AGB) = -1.201 + 2.196*\ln(DBH),\ n = 122,\ R^2 = 0.963 \quad (5.1)$$

The allometric equations for the partitioned trees were derived from the data which were used to develop the allometric equation for AGB (Basuki *et al*., 2009), and the equations are:

ln stem = -1.472 + 2.180*ln(DBH), n = 122, R^2 = 0.955 (5.2)

ln branches = -0.907 + 1.361*ln(DBH), n = 122, R^2 = 0.813 (5.3)

ln leaves = -1.392+1.250*ln (DBH), n = 120, R^2 = 0.772 (5.4)

where: AGB is the dry weight of the above-ground biomass (kg/tree) and DBH is in cm.

5.2.3 Parameterization of the model

5.2.3.1 Biomass parameters

Species richness is high in the study area. Bertault and Kadir (1998) reported that on average, 182 tree species (DBH≥ 10 cm) were found per hectare in undisturbed forests. It is difficult to put such a large number of individual tree species into a model. For this reason Phillips *et al*. (2002) and Vanclay (1989) suggested grouping species. Applying CO2FIX V 3.1 to mixed *Dipterocarp* forests meant trees were grouped into cohorts. A cohort is a group of individual trees or species with similar growth characteristics (Alder, 1995). The trees on the forest inventory were classified into cohorts based on De Bruijn *et al*. (2005), Gunawan and Rathert (1999), Lemmens *et al*. (1995), Phillips *et al*. (2002), Soerianegara *et al*. (1993) and Sosej *et al*. (1998). The grouped species included cohorts of *Dipterocarps*, large non-commercial trees, medium and small sized trees, pioneers, large- fast growing *Dipterocarps* and rest.

The local allometric equations presented above were applied to estimate the biomass of the leaves, branches, and stem, as well as the total above-ground biomass for each cohort. These biomass values were converted into carbon stock by assuming that 50% of the biomass was made up from carbon (IPCC, 2003). The carbon stock values were used as initial carbon content for every cohort as presented in Appendix 5.1. It was assumed that maximum AGB of the stand could be estimated from mature primary forest (Masera *et al*., 2003). Therefore, these parameters were calculated from the plot located in the primary

(unlogged) forest. The unlogged forest was considered to be the reference forest.

The wood density for each cohort was the weighted mean value of the wood densities of all species within the cohort. The values of the wood densities were obtained from the website http://www.worldagroforestry.org/sea/node/109 and from samples collected in the study area (Basuki *et al*., 2009). The mean wood density per cohort and the carbon content in the biomass were used to convert volume (m^3) into carbon weight.

De Bruijn *et al*. (2005) ran CO2FIX V 3.1 to evaluate carbon stocks in *Dipterocarp* forest in Bulungan East Kalimantan using different scenarios of land cover change. The forest types included: *Dipterocarp* primary protected forest, *Dipterocarp* primary logged forest, and secondary *Diperocarp* forests. Since our study area also consisted of low land mixed *Dipterocarp* forest with similar characteristics to the forest studied by De Bruijn *et al*. (2005), the following parameters from de Bruijn's study were used in the current simulation: current annual increment (CAI), relative growth, a growth modifier, and root biomass. The values of the turnover rates of branches and roots were based on Nabuurs and Mohren (1995). Parameters used in the simulation are presented in Appendix 5.1.

5.2.3.2 Climate and soil parameters

Climatic data were required to simulate decomposition of coarse and fine woody debris and non-woody litter in the soil module. These data were collected from the nearest climate station. The soil module was initialized with annual rainfall, in growing season of 2300 mm, mean monthly temperature 26^0C, and the number of days the temperature rose above 0^0C in a year of 9490. Based on these climatic data, the potential evapotranspiration in growing season was 1500 mm. Annual carbon from each of the partitioned trees (leaves, branches, stem, and root) of each cohort entered in the soil was assumed to be constant and the values were derived from turnover and mortality rate, and logging slash. In this simulation, we used default values of the various soil carbon components.

5.2.3.3 Model simulations

For the simulations, we assumed the following: (1) growth was a function of the total above-ground biomass, (2) the competition between cohorts was relative to

the total above-ground biomass in the stand, and (3) tree mortality was dependent on the total volume harvested as explained in the manual of CO2FIX V 3.1 (Schelhaas *et al*., 2004). The model was run for each compartment using different harvesting times as presented in Table 5.1. The model was operated on an annual time step. This simulation focused only on carbon stock in tree biomass and soil.

Carbon stock was simulated as a function of two management variables: logging cycle and volume of harvested timber. For every compartment, the dynamics in the carbon stock was observed for a period of 5 logging cycles. In the unlogged forests, the model was run for a period 175 years (similar to 5 logging cycles in logged forests). For logged forests, it was known when the last logging took place and how many years were left until the next logging event. This was simulated as well as the next 3 logging periods of 35 years. Besides running the model with the actual logging periods of 35 years, logging cycles of different lengths were also simulated.

The simulation was conducted for the maximum (55 m^3/ha) and the average (30 m^3/ha) net volumes of harvested timber applied by the concessioner. Generally, the net volume of the harvested timber was 70% of the gross volume of the harvested timber. In addition, simulations were made of different volumes of harvested timber for the primary forest that had not been logged previously. In the following section the volume of harvested timber refers to the net volume. A paired t-test was conducted to examine differences in carbon stocks between different logging cycles and different volumes of harvested timber.

5.3 Results

5.3.1 Carbon stock simulation for a 35 year logging cycle with different volumes of harvested timber

The carbon stock simulations for every compartment are illustrated in Figure 5.2. Comparing the above ground carbon stocks in the different logging compartments under the current logging cycle and harvesting volumes showed that in all compartments the above ground carbon stocks decreased. The amounts, however, differed between the compartments, as shown in Figure 5.2.

Forests in RKL 2, 6, and the unlogged forest (Figure 5.2 c, d, g, h, i, and j) had an average carbon stock in the tree biomass of more than 160 ton C/ha. RKL 4

and 5, which were logged from 1991 to 2000, had the lowest carbon stock (Figure 5.2 e and f). The carbon stock in the tree biomass decreased faster in the forests with harvested timber volumes of 55 m^3/ha (Figure 5.2 on the left hand side) than in the forests with harvested timber volumes of 30 m^3/ha (Figure 5.2 on the right hand side). The carbon stock in the compartments varied. Some of the RKLs had more than 160 ton C /ha (or 320 ton biomass/ha).

The carbon stock in the soil tended to increase in all forest compartments. However, the soil carbon in the forests where the simulated timber harvest was 55 m^3/ha was lower than where 30 m^3/ha was harvested. Although the carbon stock in the soil increased, the total carbon in the forests tended to decline.

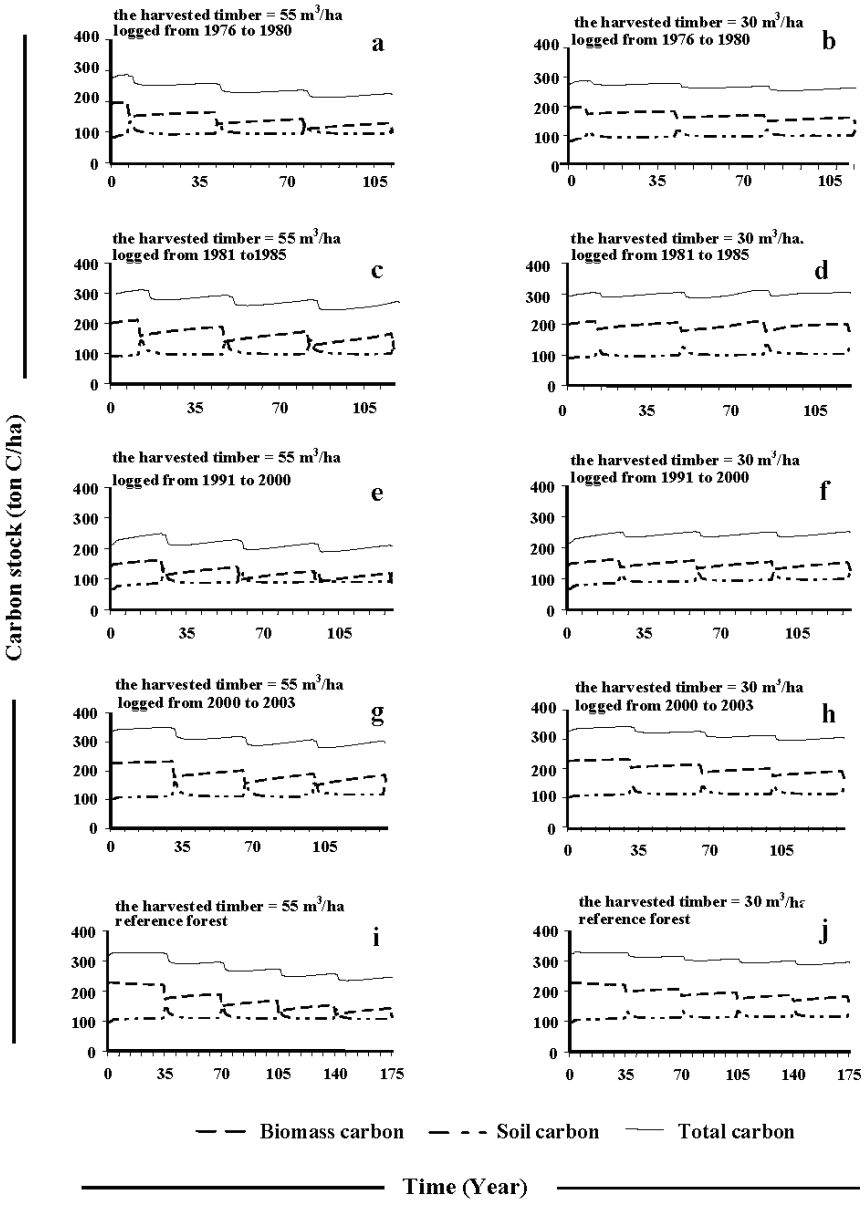

Figure 5.2: Carbon stock simulation for a 35 year logging cycle for every RKL within the study area. The starting point for the simulations is 2006. The left hand side graphs show the model simulations using a net harvesting volume of 55 m^3/ha, while on the right hand side graphs the simulations using 30 m^3 /ha.

5.3.2 Carbon stock as a function of logging cycle length

Figure 5.3 presents forest carbon stock as a result of varying the logging cycle for a harvested timber volume of 30 m^3/ha. The simulation was conducted for

the reference (unlogged) forest. It was observed that the tree growth did not restore the original carbon stock. Only when applying a logging cycle of 120 years was the carbon stock restored through tree biomass. This occurred after the fourth period in the logging cycle (Figure 5.3). This simulation confirmed that the longer the logging cycle, the higher the carbon stock that is restored in the trees.

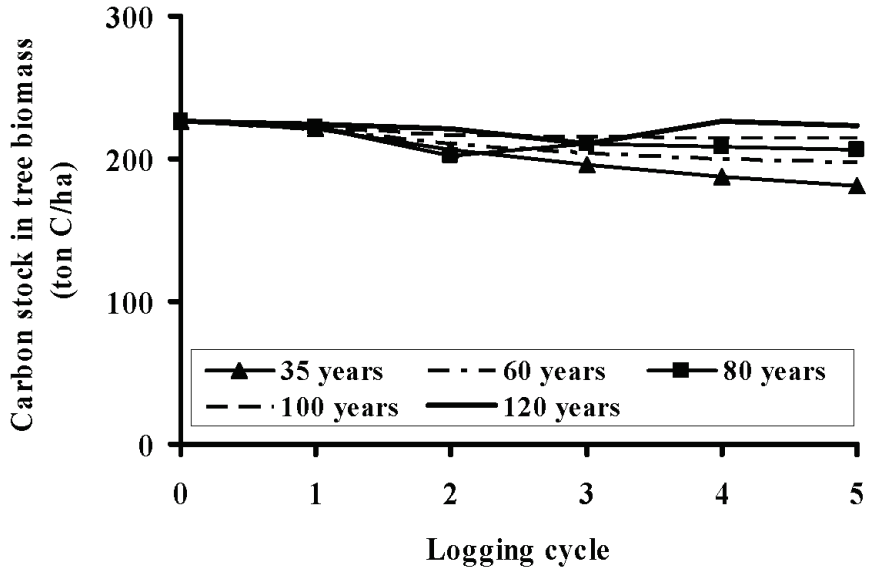

Figure 5.3: Carbon stock in tree biomass as a function of the length of the logging cycle. During each logging event 30 m^3/ha was harvested. The simulation included 5 logging cycles for lowland *Dipterocarp* forest that had not been logged before.

The increment of soil carbon stock as a function of the length of the logging cycle is shown in Table 5.2. It can be seen that for all logging cycles, the soil carbon content increased over time. In addition, the longer the logging cycle was, the higher the increment in soil carbon. An elongation 15 or 10 years of a logging cycle increases carbon stock in tree biomass and soil as presented in the paired t-test in Table 5.3.

Table 5.2: The increment in soil carbon stock (%) as a function of the length of the logging cycle in *Dipterocarp* forest (the harvested timber volume was 30 m^3/ha). The simulation was run for five logging cycles for the unlogged forest. The presented values in the table are the percentages of soil carbon stock just before logging.

Logging period	The increment of soil carbon stock (%) from a 35 year to 50, 60, 70, 80, 90, 100, 110, and 120 year of logging cycle							
	50 years	60 years	70 years	80 years	90 years	100 years	110 years	120 years
1	1.5	2.5	3.4	4.2	5.0	5.8	6.6	7.3
2	2.2	3.7	5.1	7.0	7.4	8.3	9.0	9.5
3	3.1	4.8	6.4	7.4	8.1	8.7	9.3	10.0
4	3.7	5.5	6.8	6.8	8.0	8.8	9.9	11.4
5	3.9	5.6	6.3	6.3	7.9	9.1	10.7	11.9

Table 5.3: Paired t-test at 95 % confidence interval between two logging cycles for carbon stock in the tree biomass and the soil.

A pair of logging cycle	Tree biomass		Soil	
	t-statistic	p	t-statistic	P
35 and 50 years	-8.48	0.000	-5.62	0.000
50 and 60 years	-5.23	0.000	-3.33	0.000
60 and 70 years	-4.67	0.000	-2.13	0.018
70 and 80 years	-3.67	0.000	-1.29	0.100
80 and 90 years	-2.79	0.003	-1.55	0.061
90 and 100 years	-1.34	0.090	-2.01	0.023
100 and 110 years	-5.43	0.000	-3.00	0.002
110 and 120 years	-7.87	0.000	-5.80	0.000

Restoration of carbon stock may be achieved by changing the length of the logging cycle or by adjusting the volume of harvested timber. Figure 5.4 illustrates the carbon stock in tree biomass and soil for different volumes of harvested timber in a 35 year logging cycle. When 30 m^3/ha of timber was removed, tree carbon stock was gradually reduced over time but the soil carbon content gradually increased. This pattern remained when 20 m^3/ha of timber was removed. The decrease in tree carbon stock was less when only 10 m^3/ha was logged.

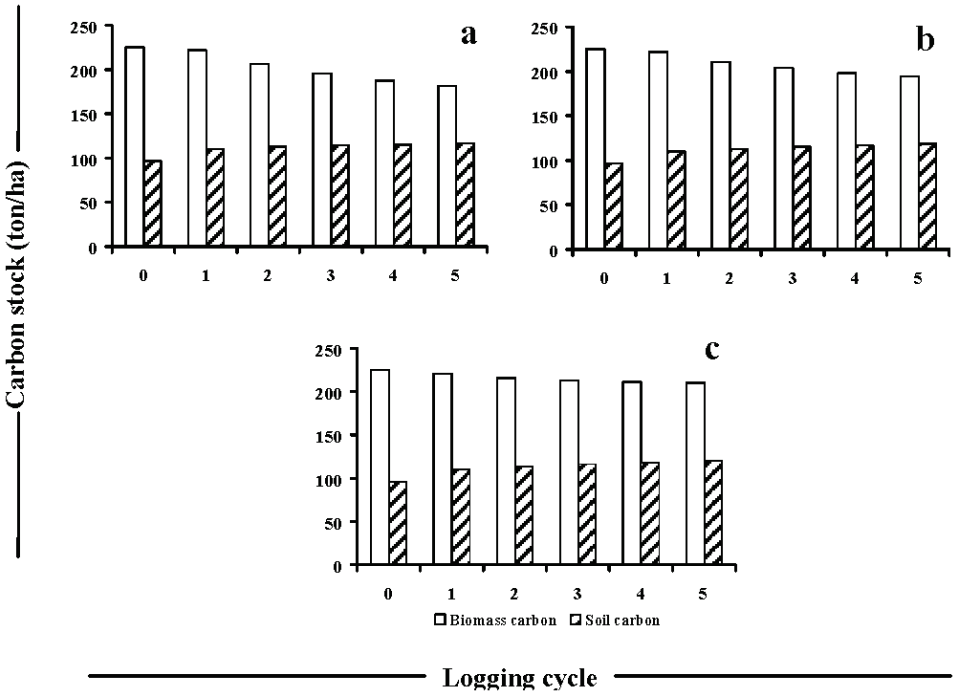

Figure 5.4: Carbon stock in tree biomass and soil simulated for a 35 year logging cycle and a harvested timber volume of 30 m^3/ha (a), 20 m^3/ha (b), and 10 m3/ha (c). The initial carbon stock in the simulation is indicated by 0.

Based on the paired t-test presented in Table 5.4, there were significant differences between carbon stocks in the tree biomass and the soil between the 30 and 20 m^3/ha and between the 20 and 10 m^3/ha of timber harvested.

Table 5.4: Paired t-test at 95 % confidence interval between the volumes of harvested timber for carbon stock in the trees and soil

A pair of volume	Trees biomass		Soil	
	t-statistic	p	t-statistic	P
30 and 20 m^3/ha	-42.0	0.000	-28.2	0.000
20 and 10 m^3/ha	-2.0	0.026	-2.4	0.009

5.4 Discussion

The simulation shows that the trees in the lowland *Dipterocarp* forests cannot restore the above ground forest carbon stock when the logging cycle is 35 years, neither for 55 m^3/ha nor for 30 m^3/ha of harvested timber. As expected, a longer logging cycle increases the carbon stock. However to restore the above ground forest carbon stock to the level of unlogged forest, a 120 year logging cycle is

needed combined with a harvested timber volume of less than 30 m^3/ha. The reason for this could that most of the trees are slow growing species and the logging cycle of the TPTI system is too short.

Our results suggest that lengthening the logging cycle from 35 years to 60, 80, 100, and 120 years would increase the carbon stock in the trees by 9, 14, 18, and 23 %, respectively, by the fifth logging cycle. As a comparison, Kaipainen *et al*. (2004) observed that extending the logging cycle 20 years, from 80, 90, 100, and 120 years to 100, 110, 120, and 140 years, respectively, increased the mean carbon stock 6 to 13% for pine forests (in Finland, Germany, and Spain) and 14 to 67 % for spruce forests (in Finland and Germany). The significant results from the paired t-test of carbon stocks between different logging cycles indicate the important role of extending the logging cycle to restore forest carbon stock.

The mean soil carbon stock in our simulations ranged from 115 to 123 ton C/ha (for logging cycles between 35 and 120 years). In the same study area Triwilaida and Pramono (2000) measured soil carbon concentrations of 1.3 to 3.0 %, which is comparable to 40.4 to 91.5 ton C/ha (for soil samples taken up to 30 cm depth). This is somewhat lower than reported by Power and Schlesinger (2002), who measured soil carbon using 35 plots in the tropical rainforests in Northeastern Costa Rica. They found soil carbon stock values ranged from 51.1 to 139 ton C/ha in soil depths of up to 30 cm. Meanwhile, Sierra *et al*. (2007) established soil carbon stock under primary forest and secondary forest in Colombia and found 96.6 ±2.5 ton C/ha and 72.2 ± 2.5 ton C/ha, respectively also for a soil depth of up to 30 cm. The differences in soil carbon under these tropical forests may be caused by differences in forest type and density, soil properties such as texture, climate, and landscape (Desjardens *et al*., 2004; Jandl *et al*., 2005; Lal, 2005).

Regulating the logging cycle is an effective method for managing the carbon budget of forests (Liski *et al*., 2001). Forests with similar harvested timber volumes and the same logging cycle produce different carbon stocks in biomass and soil because of differences in the initial carbon input. The species composition of a cohort not only influences growth competition within and between cohort trees, it also affects the weight of the carbon content in the biomass since each species has a different wood density. According to Nabuurs *et al*., (2008) wood density is one of the most sensitive parameters in carbon

stock simulations for Norway spruce in central Europe and for secondary tropical forest in Central America. Liski *et al*. (2001) found that at a culmination age of forest growth, shortening the logging cycle will decrease the carbon stock in trees but increase the carbon stock in soils. This is likely caused by accumulation of litter and harvest residues.

Restoring carbon stock can also be achieved by reducing the harvested timber volume as shown in Figure 5.4. Reduction in the volume of timber harvested reduces logging damages and maintains standing stock.

The high carbon stock in the recently logged forests, such as in part of RKL 6 was caused by protected species, such as *Koompasia* sp and *Durio* sp, being left unlogged. Field measurements confirmed that some of the protected trees had a DBH of more than 100 cm. The biomass of these large trees contributed to the accumulation of carbon stock. The carbon stock in the compartments varied. Some of the RKLs had more than 160 ton C/ha or 320 ton AGB/ha. This amount of biomass was similar to the amount of biomass found by Brown (1997) in Sarawak-Malaysia. In dense *Dipterocarp* forests in flat to undulating areas, the tree biomass was around 325 to 385 ton/ha (Brown, 1997).

In conclusion, simulation using the CO2FIX model shows that a 35 year logging cycle cannot restore the amount of sequestered carbon in the forest biomass to the original level of carbon stock present before logging. Restoring carbon in the tree biomass in the Labanan concession may be achieved by lengthening the logging cycle to 120 years. The potential role of forest soil in CO_2 mitigation is demonstrated in the simulation with forest soil storing carbon to a level of 30 to 65 percent of the total carbon present in the forest ecosystem.

Acknowledgements

We would like to thank to Dr. M.J. Schelhaas and Dr. Arjan de Bruijn, Wageningen University, The Netherlands and M. Kanninen, Center for International Forestry Research (CIFOR) for their assistance and discussion of the CO2FIX simulation. This research was supported by a grant from the Netherlands Fellowship Programme (NFP).

References

Alder, D. 1995. Growth modeling for mixed tropical forests. Tropical Forestry Papers 30. Oxford Forestry Institute, Univeristy of Oxford.

Backe´us, S., P. Wikstro¨m, and T. La¨mås. 2005. A model for regional analysis of carbon sequestration and timber production. Forest Ecology and Management 216: 28-40.

Baral, A. and G. S. Guha. 2004. Trees for carbon sequestration or fossil fuel substitution: the issue of cost vs. carbon benefit. Biomass and Bioenergy 27: 41-55.

Basuki, T.M., P.E. van Laake, A.K., Skidmore, and Y.A. Hussin. 2009. Allometric equations for estimating the above-ground biomass in tropical lowland *Dipterocarp* forests. Forest Ecology and Management 257: 1684-1694.

Berau Forest Management Project (BFMP). 1999. The climatic and hydrology of Labanan concession. Ministry of Forestry, Jakarta.

Brown, S. 1997. Estimating biomass and biomass change of tropical forests: a primer. FAO. Forestry Paper 134. Rome.

Coops, N.C., R.H. Waring, and J.J. Landsberg. 1998. Assessing forest productivity in Australia and New Zealand using a physiologically-based model driven with averaged monthly weather data and satellite-derived estimates of canopy photosynthetic capacity. Forest Ecology and Management 104: 113-127.

Dahal, P.P., 2002. Determination of forest status using selected criteria and indicators of sustainable forest management. M.Sc. Thesis, ITC, Enschede, the Netherlands.

Dean, C., S., Roxburgh, and B.G. Mackey. 2004. Forecasting landscape-level carbon sequestration using gridded spatially adjusted tree growth. Forest Ecology and Management 194: 109-129.

De Bruijn, A., M., Kanninen, M.J., Schelhaas, G.J., Nabuurs. 2005. Carbon dynamics simulation in Malinau research forest, Borneo, Indonesia. MSc. summary thesis, Forest ecology and management group. Wageningen University, The Netherlands.

De Jong, B.H., O., Masera, M., Olguín, R., Martínez. 2007. Greenhouse gas mitigation potential of combining forest management and bioenergy substitution: A case study from Central Highlands of Michoacan, Mexico. Forest Ecology and Management 242: 398-411.

Desjardins, T., E. Barros, M. Sarrazin, C. Giradin, A. Mariotti. 2004. Effects of forests conversion to pasture on soil carbon content and dynamics in

Brazilians Amazonia. Agriculture. Ecosystems and Environment 103: 365-373.

Fearnside, P.M. and W.F. Laurance. 2004. Tropical deforestation and greenhouse-gas emissions. Ecological Applications 14(4): 982-986.

Fearnside, P.M., C.A., Righi, P.M.L., De Alencastro Graça, E.W.H. Keizer, C.C. Cerri, E.M. Nogueira, and R.I. Barbosa. 2009. Biomass and greenhouse-gas emissions from land-use change in Brazil's Amazonian "arc of deforestation": The states of Mato Grosso an Rondônia. Forest Ecology and Management 258: 1968-1978.

Galik, C.S. and R.B. Jackson. 2009. Risks to forest carbon offset projects in a changing climate. Forest Ecology and Management 257: 2209-2216.

Grace, J., J. Lloyd, J. Mclntyre, A.C., Miranda, P. Meir, H.S. Miranda, C. Nobre, J. Moncrieff, J. Massheder, Y. Malhi, I. Wright, and J. Gash. 1995. Carbon dioxide uptake by an undisturbed tropical rain forest in southwest Amazon, 1992 to 1993. Science 270: 778-780.

Gunawan, A. and G. Rathert. 1999. Monitoring, data management and analysis of the BFMP permanent sample plots (STREK plots) at Berau. Berau Forest Management Project. European Union- Ministry of Forestry and Estate Crops, Jakarta.

Huth, A. and T. Ditzer. 2000. Simulation of the growth of a lowland Dipterocarp rainforest with FORMIX3. Ecological Modelling 134: 1-25.

Intergovernmental Panel on Climate Change (IPCC). 2003. Good practice guidance for land use, land-use change and forestry (GPG-LULUCF). Edited by Penman, J., M. Gystarsky, T, Hiraishi, T. Krug, D. Kruger, R. Pipatti, L. Buendia, K. Miwa, T. Ngara, K. Tanabe, and F. Wagner. IPCC National Greenhouse Gas Inventories Programme.

Jandl, R., M. Lindner, L. Vesterdal, B. Bauwens, R. Baritz, F. Hagedorn, D.W. Johnson, K. Minkkinen, and K.A. Byrne. 2007. How strongly can forest management influence soil carbon sequestration? Review. Geoderma 137: 253-268.

Kaipainen, T., J. Liski, A. Pussinen, and T. Karjalainen. 2004. Managing carbon sinks by changing rotation length in European forests. Environmental Science & Policy 7: 205-219.

Lal, R. 2005. Forest soils and carbon sequestration. Forest Ecology and Management 220: 242-258.

Lemmens, R.H.M.J., I. Soerianegara, W.C. Wong, W.C. (eds.). 1995. Plant Resources of South-East Asia (PROSEA). Timber trees: Minor commercial timbers 5 (2). Pudoc Scientific Pub. Wageningen. 655p.

Liski, J., A. Pussinen, K. Pingoud, R. Mäkipää, and T. Karjalainen. 2001. Which rotation length is favourable to carbon sequestration? Canadian Journal of Forest Research 31: 2004-2013.

Liski, J., D. Perruchoud, and T. Karjalainen. 2002. Increasing carbon stocks in the forest soils of western Europe. Forest Ecology and Management 169: 159-175.

Lugo, A. and S. Brown. 1992. Tropical forests as sinks of atmospheric carbon. Forest Ecology and management 54: 239-255.

Mantel, S. 1999. Development of environmental framework: Soils and terrain conditions of Labanan. Summary Report. Berau Forest Management Project. European Union- Ministry of Forestry and Estate Crops. Jakarta.

Markewitz, D. 2006. Fossil fuel carbon emissions from silviculture: Impacts on net carbon sequestration in forests. Forest Ecology and Management 236: 153-161

Masera, O., J.F. Garza-Caligaris, M. Kanninen, T. Karjalainen, J. Liski, G.J. Nabuurs, A. Pussinen, and B.J. De Jong. 2003. Modelling carbon sequestration in afforestation, agroforestry and forest management projects: the CO2FIX V.2 approach. Ecological Modelling 164: 177-199.

Mohren, G.M.J. 2003. Large-scale scenario analysis in forest ecology and forest management. Forest Policy and Economics 5: 103-110.

Mund, M., E. Kummetz, M. Hein, G.A. Bauer, and E.D. Schulz. 2002. Forest Ecology and Management 171: 275-296.

Nabuurs, G.J. and G.M.J. Mohren. 1995. Modelling analysis of potential carbon sequestration in selected forest types. Canadian Journal of Forest Research 25: 1157-1172.

Nabuurs, G.J., B. van Putten, T.S. Knippers, and G.M.J. Mohren. 2008. Comparison of uncertainties in carbon sequestration estimates for a tropical and a temperate forest. Forest Ecology and Management 256: 237-245.

Peng, C. 2000. Growth and yield models for uneven-aged stands: past, present and future. Forest Ecology and Management 132: 259-279.

Phillips, P. D., I. Yasman, T.E. Brash, and P.R. van Gardingen. 2002. Grouping tree species for analysis of forest data in Kalimantan (Indonesian Borneo). Forest Ecology and Management 157: 205-216.

Power, J.S. and W.H. Schlesinger. 2002. Relationships among soil carbon distributions and biophysical factors at nested spatial scales in rain forests of northeastern Costa Rica. Geoderma 109: 165-190.

Santilli, M., P. Mountiho, S. Schwartzman, D. Nepstad, L. Curran, and C. Nobre. 2005. Tropical deforestation and the Kyoto Protocol. Climatic Change 71: 267-276. DOI: 10.1007/s 10584- 005-8074-6.

Sasaki, N., Yoshimoto, A. 2010. Benefits of tropical forest management under the new climate change agreement - a case study in Cambodia. Environmental Science & Policy 13: 384–392.

Schelhaas, M.J., P.W. van Esch, T.A. Groen, B.H.J. de Jong, M. Kanninen, J. Liski, O. Masera, G.M.J. Mohren, G.J. Nabuurs, T. Palosuo, L. Pedroni, A. Vallejo, and T. Vilén, 2004. CO2FIX V 3.1 - description of a model for quantifying carbon sequestration in forest ecosystems and wood products. ALTERRA Report 1068. Wageningen, The Netherlands.

Schmid, S., E. Thu¨rig, E. Kaufmann, H. Lischke, and H. Bugmann. 2006. Effect of forest management on future carbon pools and fluxes: A model comparison. Forest Ecology and Management 237:65-82.

Sierra, C.A., J.I. del Valle, S.A. Orrego, F.H. Moreno, M.E. Harmon, M. Zapata,G.J. Colorado, M.A. Herrera, W. Lara, D.E. Restrepo, L.M. Berrouet, L.M. Loaiza, and J.F. Benjumea. 2007. Total carbon stocks in a tropical forest landscape of the Porce region, Colombia. Forest Ecology and Management 243: 299-309.

Sist, P., Saridan, A., 1998. Description of the primary lowland forest of Berau. *In*: Bertault, J-G., Kadir, K. (*eds.*), Silvicultural research in a lowland mixed Dipterocarp forest of East Kalimantan, 51 - 73. CIRAD-forêt, FORDA, PT Inhutani I, Jakarta.

Soerianegara, I. and R.H.M.J. Lemmens (eds.). 1993. Plant Resources of South-East Asia (PROSEA). Timber trees: Major commercial timbers, 5 (1). Pudoc Scientific Publisher, Wageningen, The Netherlands, 610p.

Sosej, M.S.M., L.T. Hong, and S. Prawirohatmodjo. 1998. Plant resources of South-East Asia (PROSEA). Timber trees: Lesser - known timbers, 5(3). Backhuys Publishers, Leiden, The Netherlands.

Tiejen, B. and A. Huth. 2006. Modelling dynamics of managed tropical rainforests—An aggregated approach. Ecological Modelling 199: 421-432.

Triwilaida and I.B. Pramono. 2001. Impact of logging systems on soil properties: A case study on the PT Ihutani concession area, Labanan, East Kalimantan. Prosiding ekspose hasil penelitian dan pengembangan teknologi pengelolaan DAS: 111-123. BTPDAS Surakarta, Indonesia.

Van Gardingen, P.R., M.J. McLeish, P.D. Phillips, D. Fadilah, G. Tyrie, and I. Yasman. 2003. Financial and ecological analysis of management options

for logged-over *Dipterocarp* forests in Indonesian Borneo. Forest Ecology and Management 183: 1- 29.

Vanclay, J.K. 1989. A growth model for north Queensland rainforests. Forest Ecology and Management 27: 245- 271.

Waring, .H., N.C. Coops, and J.J. Landsberg. 2010. Improving predictions of forest growth using the 3-PGS model with observations made by remote sensing. Forest Ecology and Management 259: 1722-1729.

Wijaya, A., S. Kusnadi, R. Gloaguen, and H. Heilmeier. 2010. Improved strategy for estimating stem volume and forest biomass using moderate resolution remote sensing data and GIS. Journal of Forestry Research 21(1): 1-12.

Appendix 5.1: Biomass parameters for every cohort and compartment

Cohort	Partitioned tree	Parameter	Compartment (RKL)				
			1-3	2	4-5	6	7
Dipterocarp	Stem	Carbon content (ton C/ton DM)	0.5	0.5	0.5	0.5	0.5
		Average wood density (ton DM/m^3)	0.649	0.747	0.631	0.7	0.64
		Initial carbon (ton C/ha)	45.98	82.01	21.24	51.95	55.15
	Foliage	Carbon content (ton C/ton DM)	0.5	0.5	0.5	0.5	0.5
		Initial carbon (ton C/ha)	1.07	1.56	0.71	1.3	1.23
		Growth correction factor	5	5	5	5	5
		Turnover rate (per year)	1	1	1	1	1
	Branches	Carbon content (ton C/ton DM)	0.5	0.5	0.5	0.5	0.5
		Initial carbon (ton C/ha)	19.23	35.44	8.22	21.27	23.03
		Growth correction factor	1	1	1	1	1
		Turnover rate (per year)	0.05	0.05	0.05	0.05	0.05
	Roots	Carbon content (ton C/ton DM)	0.5	0.5	0.5	0.5	0.5
		Initial carbon (ton C/ha)	14.00	25.04	6.42	15.78	16.78
		Growth correction factor	0.9	0.9	0.9	0.9	0.9
		Turnover rate (per year)	0.06	0.06	0.06	0.06	0.06
Large non-commercial	Stem	Carbon content (ton C/ton DM)	0.5	-	0.5	0.5	0.5
		Average wood density (ton DM/m^3)	0.854	-	0.786	0.803	0.83
		Initial carbon (ton C/ha)	25.63	-	10.29	7.56	17.31

Note: DM: Dry Matter

Appendix 5.1: (*Continued*)

Cohort	Partitioned tree	Parameter	Compartment (RKL)				
			1-3	2	4-5	6	7
Large non-commercial	Foliage	Carbon content (ton C/ton DM)	0.5	-	0.5	0.5	0.5
		Initial carbon (ton C/ha)	0.4	-	0.25	0.23	0.30
		Growth correction factor	6	-	6	6	6
		Turnover rate (per year)	1	-	1	1	1
	Branches	Carbon content (ton C/ton DM)	0.5	-	0.5	0.5	0.5
		Initial carbon (ton C/ha)	11.77	-	4.18	2.97	11.91
		Growth correction factor	0.8	-	0.8	0.8	0.8
		Turnover rate (per year)	0.05	-	0.05	0.05	0.05
	Roots	Carbon content (ton C/ton DM)	0.5	0.5	0.5	0.5	0.5
		Initial carbon (ton C/ha)	10.05	9.06	11.21	20.10	14.82
		Growth correction factor	1	1	1	1	1
		Turnover rate (per year)	0.06	0.06	0.06	0.06	0.06
Medium and small trees	Stem	Carbon content (ton C/ton DM)	0.5	0.5	0.5	0.5	0.5
		Average wood density (ton DM/m^3)	0.635	0.632	0.631	0.626	0.64
		Initial carbon (ton C/ha)	33.37	30.17	37.25	66.37	56.40
	Foliage	Carbon content (ton C/ton DM)	0.5	0.5	0.5	0.5	0.5
		Initial carbon (ton C/ha)	1.38	1.40	1.59	2.10	1.95
		Growth correction factor	3	3	3	3	3
		Turnover rate (per year)	1	1	1	1	1

Appendix 5.1: (*Continued*)

Cohort	Partitioned tree	Parameter	Compartment (RKL)				
			1-3	2	4-5	6	7
Medium and small trees	Branches	Carbon content (ton C/ton DM)	0.5	0.5	0.5	0.5	0.5
		Initial carbon (ton C/ha)	12.48	10.86	13.82	26.24	21.88
		Growth correction factor	0.7	0.7	0.7	0.7	0.7
		Turnover rate (per year)	0.05	0.05	0.05	0.05	0.05
	Roots	Carbon content (ton C/ton DM)	0.5	0.5	0.5	0.5	0.5
		Initial carbon (ton C/ha)	10.05	9.06	11.21	20.10	17.05
		Growth correction factor	1	1	1	1	1
		Turnover rate (per year)	0.06	0.06	0.06	0.06	0.06
Pioneers	Stem	Carbon content (ton C/ton DM)	0.5	0.5	0.5	0.5	0.5
		Average wood density (ton DM/m^3)	0.684	0.616	0.594	0.646	0.66
		Initial carbon (ton C/ha)	3.15	1.94	5.73	1.76	2.67
	Foliage	Carbon content (ton C/ton DM)	0.5	0.5	0.5	0.5	0.5
		Initial carbon (ton C/ha)	0.12	0.11	0.25	0.08	0.13
		Growth correction factor	2	2	2	2	2
		Turnover rate (per year)	1	1	1	1	1
	Branches	Carbon content (ton C/ton DM)	0.5	0.5	0.5	0.5	0.5
		Initial carbon (ton C/ha)	1.19	0.67	2.11	0.64	0.96
		Growth correction factor	0.6	0.6	0.6	0.6	0.6
		Turnover rate (per year)	0.05	0.05	0.05	0.05	0.05

Appendix 5.1: (*Continued*)

Cohort	Partitioned tree	Parameter	Compartment (RKL)				
			1-3	2	4-5	6	7
Pioneers	Roots	Carbon content (ton C/ton DM)	0.5	0.5	0.5	0.5	0.5
		Initial carbon (ton C/ha)	0.95	0.58	1.72	0.53	0.80
		Growth correction factor	1.2	1.2	1.2	1.2	1.2
		Turnover rate (per year)	0.06	0.06	0.06	0.06	0.06
Rest	Stem	Carbon content (ton C/ton DM)	0.5	0.5	0.5	0.5	0.5
		Average wood density (ton DM/m^3)	0.449	1.08	0.49	0.445	0.53
		Initial carbon (ton C/ha)	2.55	0.7	4.43	1.55	3.25
	Foliage	Carbon content (ton C/ton DM)	0.5	0.5	0.5	0.5	0.5
		Initial carbon (ton C/ha)	0.11	0.05	0.15	0.07	0.11
		Growth correction factor	1	1	1	1	1
		Turnover rate (per year)	1	1	1	1	1
	Branches	Carbon content (ton C/ton DM)	0.5	0.5	0.5	0.5	0.5
		Initial carbon (ton C/ha)	0.94	0.23	1.72	0.64	1.24
		Growth correction factor	0.9	0.9	0.9	0.9	0.9
		Turnover rate (per year)	0.05	0.05	0.05	0.05	0.05
	Roots	Carbon content (ton C/ton DM)	0.5	0.5	0.5	0.5	0.5
		Initial carbon (ton C/ha)	0.77	0.21	1.34	0.47	0.98
		Growth correction factor	1.5	1.5	1.5	1.5	1.5
		Turnover rate (per year)	0.06	0.06	0.06	0.06	0.06

Appendix 5.1: (*Continued*)

Cohort	Partitioned tree	Parameter	Compartment (RKL)				
			1-3	2	4-5	6	7
Large fast growing Dipterocarp	Stem	Carbon content (ton C/ton DM)	0.5	-	0.5	0.5	0.5
		Average wood density (ton DM/m^3)	0.46	-	0.469	0.520	0.46
		Initial carbon (ton C/ha)	0.02	-	3.72	0.05	2.28
	Foliage	Carbon content (ton C/ton DM)	0.5	-	0.5	0.5	0.5
		Initial carbon (ton C/ha)	0.002	-	0.11	0.004	0.079
		Growth correction factor	3		3	3	3
		Turnover rate (per year)	1	-	1	1	1
	Branches	Carbon content (ton C/ton DM)	0.5	-	0.5	0.5	0.5
		Initial carbon (ton C/ha)	0.006	-	1.48	0.02	0.873
		Growth correction factor	0.75	-	0.75	0.75	0.75
		Turnover rate (per year)	0.05	-	0.05	0.05	0.05
	Roots	Carbon content (ton C/ton DM)	0.5	-	0.5	0.5	0.5
		Initial carbon (ton C/ha)	0.006	-	1.13	0.01	0.688
		Growth correction factor	0.8	-	0.8	0.8	0.8
		Turnover rate (per year)	0.06	-	0.06	0.06	0.06

CHAPTER 6

SYNTHESIS

6.1 Introduction

Tropical forests have increasingly come into focus since avoiding deforestation, forest degradation, promoting sustainable forest management, and enhancing carbon sinks have been proposed as mitigation measures in the 15th Conference of the Parties (COP-15) of the United Nation Framework Convention on Climate Change (UNFCCC) in 2009. Accurate measurement of the carbon stored in the forest biomass has become important. Estimating carbon in the forest may be accomplished by measuring tree biomass and assuming that 50% of the dry weight of the tree biomass is composed of carbon (IPCC, 2003).

Quantifying carbon in tree biomass can be conducted directly by felling and weighing the trees. Recently, estimating carbon in the tree biomass has been attempted using remote sensing based models. Remotely sensed data, which provide spatial information over large areas as well as continuous temporal information, provide major benefits over direct measurement. However, due to the geographical position of the tropical forests in the equatorial zone, optical remote sensors have problems collecting cloud free images. Therefore, a sensor that collects data independent of weather conditions must be considered. In relation to understanding the carbon cycle and the implementation of REDD or REDD plus, information is needed about existing and future projections of carbon. A simulation model may provide information about future carbon stock.

The main objectives of the thesis were to improve the accuracy of above-ground biomass (AGB) estimation and to study current and future carbon stock in conjunction with the management of the logging cycle and the amount of harvested timber in *Dipterocarp* forests. In order to achieve these objectives, a series of research activities from the development of local allometric equations to the integration of field measurements and remote sensing data were undertaken to quantify AGB. Carbon stock simulations were run to understand the projection of the future carbon stock under different forest management.

Details of the research activities have been presented in the chapters 2 to 5. In this chapter, the research findings and their application as well as their benefits to society and management are synthesized.

6.2 Do we need local allometric equations?

Allometric equations, constructed from direct measurement of trees biomasses and forest stand parameters, can be used to estimate AGB. The primary reason for developing allometric equations for *Dipterocarp* forests was that local allometric equations could perhaps improve the accuracy of the AGB estimations. Although Chave *et al*. (2005) and Gibson *et al*. (2007) argued that local allometric equations would not increase the accuracy of AGB estimations, our study suggests that the local allometric equations provide a major improvement over the general equations by Brown in the IPCC (2003) as well as over the pan-tropic equation (Chave's *et al*. 2005). The local equations reduced the average deviation by 21 to 28 % compared to the equations by Brown and Chave's (see Chapter 2). Specific or local equations were necessary (Chairns *et al*., 2003; Nelson *et al.*, 1999; Ketterings *et al.*, 2001) as every forest has its own characteristics, e.g. wood density, shape of the canopy, branches, and stems which influence tree volume and biomass.

In this thesis, the allometric equations were employed to estimate AGB for each sample plot. Some of the sample plots were used for developing the equations based on parameters derived from the remote sensing data, as explained in Chapter 3 and 4. The other sample plots were used for validation. In other words, the equations were applied for model development and for validation purposes. The allometric equations are not only useful for estimating the above-ground of the whole tree biomass, but also for quantifying separate parts of the tree biomass such as in the stem, branches or foliage. The above-ground of tree biomass, as well as the biomass of the separate parts of the trees, is needed for parameterization in modelling carbon stock and flux, as was applied in the CO2FIX V 3.1 model.

The allometric equations developed in this thesis produced high coefficients of determination. These equations may also be applied to other forests with similar characteristics. The equations developed in this study complement the lack of equations for tropical forests in the Good Practice Guidance for Land Use and Land Use Change and Forestry (IPCC, 2003). In this guide only two broad categories of allometric equations for tropical forests have been presented.

6.3 Integration of remote sensing and field measurement to estimate above-ground biomass:

-Decomposing the mixed spectral components in selectively logged forests

The mixed spectral reflectance within a pixel is one of the problems in assessing AGB based on medium or coarse resolution remotely sensed data in tropical forests. An area represented by a pixel of medium resolution, such as Landsat-7 ETM+, can contain a mixture of components, e.g. vegetation, soil, and shade. Having knowledge of the proportion of each pure spectral component, as endmembers within the mixed reflectance, is essential before conducting further analysis. Decomposing this mixed spectral response can be carried out using spectral mixture analysis, producing fraction images as discussed in Chapter 3. The retrieval values of the fraction images were integrated with the data from field measurements to develop regression models for estimating the AGB.

The research findings demonstrated the potential of the proposed models to improve the accuracy of the AGB estimation over the conventional methods using spectral reflectance band 4 or band 5, Moisture Vegetation Index derived from band 4 and 5, and Moisture Vegetation Index derived from band 4 and 7, multiple bands 4, 5, and 7, as well as all non-thermal bands of Landsat 7 ETM+. The proposed regression models produced higher coefficients of determination than those in previous studies conducted by Nssoko (2007) and Wijaya *et al*. (2010) in the same study area. In the current study, the fraction images explained 63 % of the variation in AGB. In contrast, Nssoko (2007) found that only less than 10% of the variation in AGB could be explained by common spectral indices, e.g. NDVI, Enhanced Vegetation Index, Advanced Vegetation Index, Soil Adjusted Vegetation Index, Modified Soil Adjusted Vegetation Index, and Simple Ratio. The application of spectral mixture analysis also highlighted the heterogeneity of the forests as the impacts of the selective logging system. It differentiated between the recently logged forest and the mature forest.

Spectral mixture analysis can be applied for forest management purposes, where high spatial remote sensing images are costly or unavailable. However,

information on the proportion of vegetation in the mixed spectral components in the medium or coarse resolution must be obtained for calculating AGB. In a selective logging system timber harvesting damages the canopy structure, thus creating gaps. Such gaps are smaller than the pixel size of medium or coarse spatial resolution images, resulting in mixed spectral components.
The application of the research findings in forest management needs to be supported by remotely sensed data. Since Landsat archive and MODIS images are freely available, implementation of the research findings stands a good chance. In the Global Observation of Forest and Land Cover Dynamics (GOFC-GOLD, 2009) spectral mixture analysis is mentioned as one of the methods for detecting and mapping forest degradation. It has not been used for quantitative purposes, such as estimating biomass. The research findings form a useful contribution to the GOFC GOLD (2009), as the proposed methods improve the accuracy of the AGB estimation in mixed tropical forests.

- ***Does an integration of multi-sensors data improve the accuracy of the estimation of above-ground biomass?***

Realizing the advantages and disadvantages of the information derived from optical sensors and active sensors, novel equations were generated by integrating multi-sensor data and field measurements. The integration of fraction images with other image sources is believed to be a novel fusion technique. In Chapter 4, the fusion between fraction images derived from spectral mixture analysis of the Landsat-7 ETM+ and Phase Arrayed L-band Synthetic Aperture Radar (PALSAR) was explored using the Brovey transform and the Discrete Wavelet Transform. After integrating the optical and SAR data, the retrieval values obtained from the fused images were used together with the field measurements to develop the equations. The aim of this fusion was to improve the accuracy of AGB estimation in lowland mixed *Dipterocarp* forest.

The proposed models integrating the fraction images resulting from the spectral mixture analysis and PALSAR data provide a contribution to the existing methods for estimating the AGB in tropical forests. The regression models significantly improved the accuracy of the AGB estimation compared with the methods mentioned in the previous section. The proposed models highlighted the potential use of PALSAR data fused with the fraction images and the spectral reflectance of the Landsat-7 ETM+.

The applied method of integrating the remotely sensed data also determined the accuracy of the estimation. The use of the Discrete Wavelet Transform produced a better fusion image than the Brovey transform, because the spectral characteristics of the fused images from the Discrete Wavelet Transform were similar to the original multi spectral data. It also improved the accuracy of the AGB estimation as high and low frequency features were preserved during the spectral decomposition. In other words, variation in AGB directly causes change in the spectral characteristics (Pu and Gong, 2004).

The proposed models significantly improved the accuracy of the AGB estimation. The proposed model by integrating vegetation and soil fraction with PALSAR HH or HV polarizations improved the R^2 of the model by 17 and 28% compared to the model based on vegetation fraction and all non-thermal reflectance of Landsat-7 ETM+, respectively. Therefore, these research findings contribute to the mapping, monitoring, and quantifying of carbon stock in mixed tropical forests. These methods complement the existing methods described in Global Observation of Forest and Land Cover Dynamics (GOFC-GOLD) (2009), IPCC (2003), and the other documents of the UNFCCC.

6.4 Capturing and releasing carbon?

Whether tropical forests sequester or emit carbon dioxide to the atmosphere is influenced by effect of the length of the logging cycle on the carbon stock in the forest ecosystem. Therefore, different logging cycles and volumes of harvested timber were simulated using the CO2FIX V 3.1 model (Schelhaas *et al*., 2004). The aim was to ascertain a suitable logging cycle and volume of harvested timber to restore, long term, the loss of carbon caused by the removal of harvested timber from the forest ecosystem, as presented in Chapter 5.

Although the volume of the timber harvested was only 30 m^3/ha, a 35 year logging cycle was not long enough to restore the carbon stock in the forest biomass. The results from the simulations showed that a 120 year logging cycle would restore the carbon stock in the trees to its original pre-logging level. Based on the simulations, elongation of the logging cycle significantly increased the carbon stock in the trees and soil. The increase or decrease of carbon stock in the tree biomass did not simply depend on the length of the logging cycle, but was also affected by the wood density, the initial carbon

content in the trees, the ratio of the existing biomass to the maximum biomass, and the composition of species within cohorts.

The increase in carbon stock in trees and soil as a result of the lengthening of the logging cycle was also observed by Kaipainen *et al*. (2004). However, Liski *et al*. (2001) showed that at the culmination age of forest growth, shortening of the logging cycle would decrease the carbon stock in trees but increase the carbon stock in soil as a result of the accumulation of litter and harvest residues. In production forests, efforts to restore the carbon stock in the forest ecosystem can be conducted either by changing the length of the logging cycle or by managing the volume of harvested timber. The simulation using the CO2FIX V 3.1 model showed that a reduction of the volume of harvested timber from 30 m^3/ha to 10 m^3/ha increased the carbon stock in the trees from 81 % to 94 % by the fifth year of a 35 year logging cycle.

From a practical point of view, the simulation of carbon stock for different logging cycles is an effective method to manage the carbon stock and flux in forest ecosystem. Forest management can regulate the length of the logging cycle or the volume of harvested timber to protect the future carbon stock in the forest ecosystem. For the global framework, the choice of logging cycle is also important for countries if they want to implement sustainable forest management for reduction of greenhouse gas emissions as stated in the REDD-plus. However, regulating the logging cycle or the volume of harvested timber is also dependent on the demand for wood products and the economic viability since forests are one of the main sources of national income in Indonesia.

6.5 General conclusions

The main objectives of the thesis were to improve the accuracy of the AGB estimation and to predict future carbon stock in conjunction with the management of the logging cycle and the volume of harvested timber in the lowland mixed *Dipterocarp* forests. The research findings confirm that improving the accuracy of AGB estimation can be achieved through developing local allometric equations. Over larger areas, for example at landscape scale, remote sensing data combined with field measurements (using spectral mixture analysis and Discrete Wavelet Transform) provide significant improvements (on the average 55%) in the accuracy of AGB estimation compared with more convenstional methods such as vegetation indices, moisture vegetation indices, single and multiple band combinations of Landsat-7 ETM+.

Obtaining the proportion of components within a mixed pixel response in a medium resolution image, e.g. Landsat-7 ETM+, is crucial before integrating the image with PALSAR to improve the accuracy of the AGB estimation. The fusion using Discrete Wavelet Transform provides a better visual interpretation and a higher accuracy for AGB estimation than Brovey transform does. Therefore, the utility of the remotely sensed data to improve the accuracy of AGB estimation does not only depend on the advancement of data type or the cost of remote sensing images, but also on the techniques applied in its processing and analysis of the data.

For society, the improvements in the accuracy of the AGB estimations using allometric equations and remote sensing approaches may improve forest management. An accurate AGB estimation is useful for mapping and monitoring forest biomass as well as to better understand forest carbon dynamics in relation to the global carbon cycle. The research findings may contribute to carbon trading. The accuracy of carbon estimation is a key factor for sellers and buyers to achieve an agreement. The research findings will be especially useful for the implementation of REDD-plus as focused on tropical forests. The major goal of REDD-plus is to reduce carbon emission resulting from deforestation and forest degradation. Although generally selective logging system are applied in timber harvesting, logging activities in production forests are considered to be the main source of forest degradation. However, mapping, monitoring, and quantifying carbon change is considered to be more difficult in degraded forests than in areas subject to deforestation, as in degraded forest the decrement and increment of forest biomass are not homogeneous and an area represented by a pixel may be covered by more than one component. In such cases applying spectral mixture analysis will be necessary.

A 35 year logging cycle with a net volume of harvested timber of 30 m^3/ha needs to be lengthened to a 120 year cycle to restore the carbon stock in the forest ecosystem. A reduction of the harvested timber volume from 30 m^3/ha to 10 m^3/ha cannot restore carbon stock in the trees to the condition before logging. A simulation to evaluate the length of the logging cycle and the volume of harvested timber is not only useful for understanding carbon budget, but it also guides forest managers and policy makers towards optimizing the uptake of CO_2 from the atmosphere. Optimizing the logging cycle to increase the carbon stock in forests can be considered a mitigation measure for forestry activities under the Kyoto Protocol to UNFCCC (Liski *et al.*, 2001).

The benefit of extending the logging cycle may not only be to increase carbon stock in the forest ecosystem, but also to contribute to the conservation of biodiversity. Conserving biodiversity in the study area is important because the *Dipterocarp* forest in Labanan has the richest species composition of all the *Dipterocarp* forests (Sist and Saridan, 1998).

6.6 Future work and recommendations

In this work, the combination of mixed spectral components was considered to be linear. In a natural condition, the relationships between the pure spectral components may be not linear. Hence, to gain a better understanding of the interaction between the components, a non linear spectral un-mixing analysis is necessary.

The current and future carbon budget needs spatial and temporal information. The proposed models generated from the field and remotely sensed data are empirical models and provide only spatial information. On the other hand, the current model of the CO2FIX V 3.1 only produces temporal carbon stock without having spatial information. Integrating remotely sensed data with the CO2FIX V 3.1 model will provide better information for understanding the carbon budget in the forest ecosystem.

Further simulations considering the effects of climatic factors, especially air temperature and rainfall on the forest growth, the decomposition rate of harvest residues, and soil respiration are required. This information is needed to anticipate the effect on the carbon cycle of future changes in the global climate.

Further research is needed to determine an optimal length of the logging cycle and to understand the entire forest carbon cycle, as well as the economic impact changes made to the logging cycle have. The optimal cycle should also safeguard the continuity of forest products. In other words, any recommendation must consider the sustainability of the ecosystem, the wood demand, and economic viability.

References

Baral, A., Guha, G.S., 2004. Trees for carbon sequestration or fossil fuel substitution: the issue of cost vs. carbon benefit. Biomass and Bioenergy 27: 41 – 55.

Cairns, M.A., Olmsted, I., Granados, J., Argaez, J., 2003. Composition and aboveground tree biomass of a dry semi-evergreen forest on Mexico's Yucatan Peninsula. Forest Ecology and Management 186: 125-132.

Chave, J., Andalo, A., Brown, S., Cairns, M.A., Chambers, J.Q., Eamus, D., Fölster, H., Fromard, F., Higuchi, N., Kira, T., Lescure, J.P., Nelson, B.W., Ogawa, H., Puig, H., Riéra, B., Yamakura, T., 2005. Tree allometry and improved estimation of carbon stocks and balance in tropical forests. Oceologia 145: 87-99.

Gibbs, H.K., Brown, S., Niles, J.O., Foley, J.A., 2007. Monitoring and estimating tropical forest carbon stocks: making REDD a reality. Environ.Res.Lett.2. doi:10.1088/1748-9326/4/045023.

Global Observation of Forest and Land Cover Dynamics (GOFC-GOLD), 2009. A sourcebook of methods and procedures for monitoring and reporting anthropogenic greenhouse gas emissions and removals caused by deforestation, gains and losses of carbon stocks in forests remaining forests, and reforestation.

Intergovernmental Panel on Climate Change (IPCC). 2003. Good practice guidance for land use, land-use change and forestry (GPG-LULUCF). Edited by Penman, J., Gystarsky, M., Hiraishi, T., Krug, T., Kruger, D., Pipatti, R., Buendia, L., Miwa, K., Ngara, T., Tanabe, K., Wagner, F. IPCC National Greenhouse Gas Inventories Programme.

Kaipainen, T., Liski, J., Pussinen, A., Karjalainen, T., 2004. Managing carbon sinks by changing rotation length in European forests. Environmental Science & Policy 7: 205-219.

Summary

Greenhouse effects and the carbon cycle, in particular carbon emissions and carbon sequestration, are at the heart of climate change. This is one of the most pressing problems that the earth is facing. Quantifying biomass/carbon and understanding its dynamics in tropical forests are essential because these forests sequestrate CO_2 from the atmosphere. Carbon stock in forests can be estimated from above-ground biomass (AGB) since approximately 50% of the dry AGB is carbon. The AGB can be estimated directly by destructive methods e.g., cutting down and weighing trees, or non-destructive methods such as allometric equations and models based on remote sensing. However, accuracy of the AGB estimation still forms a problem for tropical forests, especially for *Dipterocarp* forests. Therefore, research was conducted to improve the accuracy of AGB estimations and to predict future carbon stock based on the length of a logging cycle and the volume of harvested timber in *Dipterocarp* forests. The research focused on *Dipterocarp* forests because these forests cover extensive areas and harbour some of the most commercialized timber species in South-East Asia. The research proposed a local allometric equation, which proved more suited to predicting the AGB of *Dipterocarp* forests than global or generalized equations. The proposed model, which integrated fraction images resulting from the spectral mixture analysis and Phased Arrayed L-band Synthetic Aperture Radar (PALSAR), significantly improved the accuracy of the AGB estimation. In addition, the findings suggested that the trees could not restore carbon levels to those found at the start of the logging cycle. However, the significant increase in accuracy of the AGB estimation should certainly be useful in the implementation of Reducing Emissions from Deforestation in Developing Countries (REDD) or REDD plus.

Under the United Nations Framework Convention on Climate Change (UNFCCC) countries have to update their reports on the increments and decrements in carbon stock of their forests by implementing emerging mechanisms, such as REDD. Accurate AGB estimation forms a key factor here. Direct measurement to quantify AGB may be suitable at plot level. At landscape level or for larger areas, AGB could be estimated by integrating field measurements and remotely sensed data. Conventional methods for estimating AGB using remote sensing link the measured AGB with spectral reflectance or spectral indices derived from an optical sensor. It is also possible to use backscatter from active sensors of SAR.

As a tool remote sensing can provide reasonable estimates of forest biomass/carbon, however, some problems arise with the use of optical sensors in tropical forests. Estimating AGB using common methods such as spectral indices produces inconsistent results in tropical forests. Another problem may be the mixture of spectral components such as trees, soil, and shade in a pixel of an image. Cloud cover also forms an obstacle for biomass/carbon estimation when using optical sensors. Image processing such as spectral mixture analysis and fusion between data from optical and SAR sensors has the potential to improve the accuracy of the AGB estimation.

Besides improving the accuracy of AGB estimation, research was undertaken to try and understand the dynamics of AGB and carbon stock in the *Dipterocarp* forests. In tropical forests managed for production, the dynamics of these forests are determined by management decisions such as the length of the logging cycle and the volume of harvested timber. For sustainable forest management, knowledge of the forest growth dynamics in relation to carbon stock is essential. In *Dipterocarp* forests, the effects on carbon stock of the length of the logging cycle and the volume of harvested timber had not been explored in sufficient detail to date, especially not for the Indonesian selective cutting and replanting system (TPTI).

In this thesis, quantification of carbon stock was carried out by cutting down and weighing trees, followed by developing allometric equations for a specific local area. The proposed equations were used to convert diameter at breast height (DBH) to AGB at a sampling plot level (500 m^2). Integration of the plot measurements with remotely sensed data was used to develop regression models for estimating AGB over the whole study area. The remotely sensed data were derived from Landsat-7 ETM+ and included reflectance of band 1, 2, 3, 4, 5, and 7, spectral indices, and fraction images resulting from spectral mixture analysis. These data were used for developing regression models. The spectral mixture analysis decomposed the mixed spectral components within a pixel. In addition, fusion was carried out between fraction images resulting from the spectral mixture analysis of Landsat-7 ETM+ and PALSAR. Two fusion techniques were used, namely Brovey and Discrete Wavelet Transforms. The purpose of the fusion was to obtain benefits from the integration of different data sources, namely optical and SAR data. The algorithm of the Brovey transform was intended to enhance the visual interpretation of the red, green and blue combination. Fusion using Discrete Wavelet Transform

decomposed a high spatial resolution and a multispectral resolution into one. Detailed information on the high spatial resolution of PALSAR data was injected into a multispectral image of Landsat-7 ETM+.

To analyse the sustainability of long term forest management, carbon stock simulation was performed using the CO2FIX V 3.1 model. The purpose of the simulation was to know if the harvested amount of carbon did not exceed the amount of carbon that could potentially be stored during the period between two harvests.
The results showed that direct ground measurement of AGB followed by the development of local allometric equations for *Dipterocarp* forests can significantly improve the accuracy of the AGB estimation compared to the general allometric equations developed for global application. Estimating the AGB using Landsat 7 ETM+ underlined the importance of decomposing mixed spectral components into fraction images, e.g. vegetation, soil, and shade. The proposed models based on fraction images improved the R^2 of the model by 107 % and 8 % compared to the model based on the reflectance of Middle Infrared band 5 and all non-thermal spectral bands of Landsat-7 ETM+, respectively.

A marked improvement in the accuracy of the AGB estimation was provided by the model developed from the integration of field measurements and fused fraction images with a PALSAR image using Discrete Wavelet Transform. Using Discrete Wavelet Transform, the R^2 of the models ranged from 0.69 (for fusion between reflectance in the near infrared band 4 and PALSAR horizontal-horizontal (HH) polarizations) to 0.74 (for fusion between vegetation and soil fractions and PALSAR HH or HV (horizontal vertical) polarizations).

The simulation using CO2FIX V 3.1 highlighted that a 35 year logging cycle with harvested timber volumes of 55 or 30 m^3/ha was not suitable for restoring carbon stock. To sequester carbon in the trees to the level present in unlogged forests, a 120 year logging cycle would be needed with a timber harvest of 30 m^3/ha.

The research provides a major contribution to the development of allometric equations and AGB estimation using remote sensing, especially for *Dipterocarp* forests. The research findings can be used to complement the existing methods for biomass/carbon estimation in the Good Practice Guidance for Land Use and Land Use Change and Forestry (GPG-LULUCF) and Global Observation of

Forest and Land Cover Dynamics (GOFC-GOLD). We are now able to make more accurate estimates of biomass/carbon stored in tropical *Dipterocarp* forests. This equips us better for the implementation of REDD, with the aim to reduce greenhouse gases in the atmosphere.

Samenvatting

Tropische bossen spelen een belangrijke rol in de globale koolstofcyclus. Daarom dienen we goed inzicht te krijgen in de dynamiek van deze bossen en de bijdrage van tropische bossen aan de koolstofcyclus. Als we hogere CO_2 concentraties in de atmosfeer willen terugdringen is het van groot belang om nauwkeurige schattingen te kunnen maken van de koolstofvoorraad die is vastgelegd in tropische bosgebieden. Dit is ook van belang voor rapportages die landen moeten verzorgen in het kader van internationale klimaatconventies zoals UNFCCC. Deze klimaatconventies werken met mechanismen zoals REDD (Reduced Emissions from Deforestation and Forest Degradation) en zijn afhankelijk van de nauwkeurigheid waarmee schattingen van biomassa en koolstof in bossen kunnen worden uitgevoerd.

De koolstofvoorraad in bossen kan worden afgeleid van de bovengrondse biomassa omdat ongeveer 50% van droge bovengrondse biomassa bestaat uit koolstof. Voor het bepalen van de bovengrondse biomassa in bossen zijn verschillende technieken mogelijk. Voor heel lokale metingen is het mogelijk om een aantal bomen om te zagen en te wegen. Vervolgens moet dan nog het koolstofgehalte van het hout gemeten worden om precies de totale hoeveelheid koolstof in het bos te kunnen uitrekenen. Voor grotere gebieden is dit geen haalbare methode. Op landschapsniveau en voor grotere gebieden biedt een combinatie van veldmetingen en aardobservatie met behulp van satellieten goede mogelijkheden. Maar hoewel aardobservatie al vele malen haar nut heeft bewezen zijn er ook uitdagingen die nog om een oplossing vragen. Schattingen van de bovengrondse biomassa in tropische bossen met behulp van spectrale indices levert inconsistente resultaten op. Een van de problemen is dat de reflectiewaarden van elke pixel in een satellietbeeld het resultaat is van reflectie afkomstig van een mix van objecten op het aardoppervlak. Dit kan een combinatie zijn van vegetatie, bodem, schaduw, water etc. Daarnaast vormen wolken (vaak aanwezig boven tropische bosgebieden) een obstakel waardoor het gebruik van optische sensoren bemoeilijkt wordt. Daarom moeten methoden ontwikkeld worden om meer informatie uit satellietbeelden te kunnen halen. In dit onderzoek is gekeken in hoeverre het analyseren van de mix waar het spectrale signaal van afkomstig is helpt in het verbeteren van de biomassa schattingen. Ook is er gebruik gemaakt van fusie van beelden afkomstig van verschillende sensoren. Hierbij werden beelden samengevoegd van optische sensoren en radar. Radar is een actieve sensor waarbij de reflectie van een zelf-

uitgezonden signaal wordt opgevangen. Deze techniek heeft als voordeel dat bewolking geen obstakel vormt.

In dit onderzoek is in detail gekeken naar *Dipterocarp* bossen. Dit is een veelvoorkomend bostype in Zuidoost Azië wat zich uitstrekt over grote gebieden. *Dipterocarp* bossen zijn erg interessant voor de commerciële houtindustrie. De dynamiek van deze bossen hangt onder andere af van de lengte van de periode tussen de oogsten en de hoeveelheid hout die uit het bos gehaald wordt. Duurzaam bosbeheer is dan ook alleen mogelijk als we voldoende kennis hebben van de groei of herstel van het bos in relatie tot het management van de bossen. Dit was nog onvoldoende bekend. Het in dit proefschrift beschreven studie werd uitgevoerd in *Dipterocarp* bossen op Kalimantan in Indonesië. Daarbij werd onderzocht wat het effect is van het selectief kap- en plantbeheer (TPTI) op de koolstofvoorraad in het bos. De eerste stap was om de nauwkeurigheid waarmee de biomassa (en daarmee de koolstofvoorraad) bepaald kan worden te verbeteren. Daarna is berekend of het management in de vorm van kapcyclus gecombineerd met hoeveelheid gekapt hout in overeenstemming is met de herstelsnelheid van het bos. In andere woorden: is de hoeveelheid koolstof die uit het bos gehaald in balans met de hoeveelheid koolstof die tussen twee kapbeurten vastgelegd kan worden?

Als eerste stap in deze studie werd de koolstofvoorraad eerst rechtstreekst gemeten op plotniveau. Een plot is een klein gebiedje, in dit geval 500 m^2. Daarbinnen werden alle bomen geïdentificeerd en gemeten. Daarna werden allometrische vergelijkingen ontwikkeld. Dit zijn wiskundige formules waarmee op basis van biofysische kenmerken van bomen uitgerekend kan worden wat de biomassa van deze bomen is. In dit onderzoek werd dit gedaan op basis van de dikte van bomen op borsthoogte (DBH). Na bepaling van de biomassa en hoeveelheid koolstof per vierkante meter werd gekeken naar de relatie hiervan met gegevens afkomstig van satellietbeelden. Integratie van plotmetingen met gegevens uit aardobservatie leverde regressiemodellen op. Hiermee kon de biomassa geschat worden van bossen over grotere gebieden.

Satellietbeelden afkomstig van Landsat-7 ETM+ vormden de input voor het schatten van biomassa in bosgebied. Hiervoor werden spectrale indexwaarden gebruikt. Ook werd een spectrale analyse uitgevoerd om te bepalen van welke mix van componenten op het aardoppervlak de reflectie in pixels van Landsat-7 ETM+ beelden afkomstig was. Daarna werden de digitale kaarten met de

uitgerekende fracties van deze Landsat-7 ETM+ beelden gefuseerd met radarbeelden. Deze radarbeelden waren afkomstig van de PALSAR sensor (PALSAR staat voor Phased Array type L-band Synthetic Aperture Radar) aan boord van de ALOS satelliet. Twee technieken, "Brovey transformatie" en "Discrete Wavelet Transform (DWT), werden toegepast om de spectrale beelden te fuseren met de SAR data. De Brovey transformatie zorgde voor een beter contrast in de rood/groen/blauw combinatie van het gefuseerde beeld wat interpretatie verbeterde. De DWT transformatie was nodig om de verschillende ruimtelijke resoluties van de spectrale beelden en SAR data op elkaar af te stemmen.

Tenslotte werd bestudeerd of de manier waarop hout geoogst wordt in de *Dipterocarp* bossen van Kalimantan duurzaam is of niet. Dit werd berekend met behulp van het CO2FIX V 3.1 model. De hoeveelheid koolstof in bovengrondse biomassa werd berekend voor verschillende scenario's. Deze scenario's bestonden uit combinaties van verschillende tijdspannes tussen oogsten en verschillende hoeveelheden hout (55 or 30 m^3/ha) die uit het bos gekapt kunnen worden.

De resultaten van het onderzoek laten zien dat de schattingen van biomassa en koolstof in *Dipterocarp* bossen met behulp van de nieuw ontwikkelde technieken een significante verbetering opleveren ten opzichte van de bestaande algemene rekentechnieken. Het blijkt van groot belang om de reflectie van het aardoppervlak, zoals dat door de sensor ontvangen wordt, op te delen in fracties. Daarbij ontstaan fractiekaarten die weergeven hoeveel procent van het gebied, gedekt door een pixel, bedekt is met vegetatie, kale bodem en schaduw. De regressiemodellen die deze fractiekaarten als input gebruiken verbeterden de R^2 met 107 % en 8 % vergeleken met modellen gebaseerd op reflectie van midden-infrarood band 5 of alle niet thermale spectrale banden van Landsat-7 ETM+.

De schatting van bovengrondse biomassa werd nog nauwkeuriger door de integratie van veldmetingen met de gefuseerde beelden afkomstig van PALSAR en fractiekaarten. Door gebruik te maken van DWT techniek bij het fuseren van beelden was de R^2 van het model 0.69 na fusie van nabij-infrarood band 4 en PALSAR (met een horizontaal-horizontaal polarisatie). De R^2 van het model verhoogde tot 0.74 na fusie van de vegetatie en bodem fractiekaarten met PALSAR (met een horizontaal-verticaal polarisatie).

De simulatie met CO2FIX V 3.1 liet zien dat een kapcyclus van 35 jaar, waarbij 55 of 30 m^3/ha hout uit het bos gehaald wordt, in beide gevallen geen duurzame situatie oplevert. Gedurende deze periode is het bos niet in staat de koolstofvoorraad voldoende te herstellen. Bij een geoogst volume van 30 m^3/ha wordt pas bij een periode van 120 jaar tussen de kapbeurten een balans bereikt tussen extractie van koolstof en aanmaak van koolstof in de vorm van bovengrondse biomassa in bos. De simulaties lieten wel zien dat ondanks dat er een afname was in de hoeveelheid koolstof in bovengrondse biomassa, de hoeveelheid koolstof in de bodem juist toenam.

Het in dit proefschrift beschreven onderzoek heeft een bijdrage geleverd aan het nauwkeuriger kunnen bepalen van biomassa en koolstofvoorraad in bossen en in het bijzonder de *Dipterocarp* bossen op Kalimantan. De gebruikte technieken zijn een aanvulling op de al bestaande methoden die beschreven zijn in de richtlijnen voor "good practice" in landgebruik en bosbouw. Deze richtlijnen zijn opgesteld door het IPCC (het internationale klimaatpanel van de verenigde naties) en GOF-GOLD (een FAO werkgroep die zich bezig houdt met wereldwijde observatie van bossen en de dynamiek van landgebruik). De belangrijkste verbetering in de schattingen van bovengrondse biomassa in *Dipterocarp* bossen is het resultaat van het ontwikkelen van specifieke allometrische vergelijkingen voor dit bostype. Een verdere verbetering kan worden bereikt door het toepassen van een nieuwe combinatie aardobservatietechnieken. Hierdoor zijn we nu beter in staat nauwkeurige schattingen te maken van hoeveel koolstof er aanwezig is in tropische *Dipterocarp* bossen. En tenslotte levert het ook verbeterde mogelijkheden op voor implementatie van REDD met als doel het terugdringen van broeikasgassen in de atmosfeer.

Curriculum Vitae

Tyas Mutiara Basuki was born in Nganjuk, Indonesia. After finishing her senior high school in Surabaya, Indonesia, she continued to study at Bogor Agriculture University (IPB) in 1978. She graduated from IPB in March 1983 receiving a Bachelor of Soil Science degree. Starting from 1984 to 1994 she worked as a researcher in the Forestry Research and Development Centre in Bogor. In 1988 she was awarded a grant by the Netherlands government to do a Postgraduate Course in Geographical Landscape Analysis for Indonesian Resources specializing in watershed management, at the International Institute for Aerospace Survey and Earth Sciences (ITC), Enschede, The Netherlands. She received her diploma for this course in 1989. In 1991 she was offered a second fellowship, from the World Bank, to continue her studies at Colorado State University (CSU), Colorado, United States of America. At the CSU, she studied in the Department of Earth Resources with as specialization Watershed Management and was awarded a Master of Science in 1993. She continued working in Forestry Research in Bogor until 1994. Then, she moved to North Sumatra and worked in the Forestry Research Institute of Pematang Siantar from 1995 to 2000. From March 2000 up to now she worked as a researcher at the Forestry Research Institute of Solo, Central Java. In 2005 she was awarded a third scholarship, this time through the Netherlands Fellowship Programme, to conduct a Doctoral Programme at the Faculty of Geo-Information Science and Earth Observation, University of Twente, The Netherlands.

ITC Dissertation List

http://www.itc.nl/research/phd/phd_graduates.aspx